

FOREWORD

This report was prepared by Battelle Memorial Institute on Contract No. AF 33(616)-7351, under Project No. 6373, "Equipment for Life Support in Aerospace," and Task No. 637302, "Respiratory Support Equipment." The work was performed under the direction of the 6570th Aerospace Medical Research Laboratories, Aerospace Medical Division, and was administered by Clyde G. Roach, Respiratory Equipment Section, Sustenance Branch, Life Support Systems Laboratory. The work reported here was done between 1 June 1960 and 30 November 1961.

The principal investigators were John E. Clifford, Senior Chemical Engineer, John McCallum, Assistant Chief, Electrochemical Engineering Division, and James T. Gates, Mechanical Engineer. The work was under the direction of Charles L. Faust, Chief, Electrochemical Engineering Division.

Contrails

ABSTRACT

A laboratory-model rotating electrolysis cell was designed for electrolysis of water under zero-gravity conditions. Satisfactory operation was obtained in the three evaluation runs of 3/4, 2, and 2-1/2 hours' duration. Hydrogen and oxygen were evolved with the cell operating at the designed electrolysis current of 254 amperes (corresponding to a 2-man unit for electrolyzing water at the rate of 2.25 pounds of water per day per man). No component of the earth's gravity field was used in effecting the separation of the gas from the electrolyte during electrolysis.

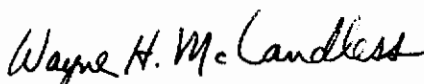
The laboratory model weighs 284 pounds including 30 pounds of electrolyte and occupies a cylindrical space of 4.4 cubic feet (17-1/2 inches' maximum diameter by 31-1/2 inches' height). The electrolysis portion is a drum-shaped unit containing 16 individual cells in parallel electrically. With the unit rotating at about 500 rpm, the lowest measured total power consumption was 637 watts; 457 watts was estimated for extended operation at zero gravity with series-connected cells.

The present laboratory-model design features high reliability, low power consumption, and versatility for use as a 3-, 4-, or 5-man cell.

Appendix II of the report contains a feasibility study of other methods of zero-gravity electrolysis that were considered.

PUBLICATION REVIEW

This technical documentary report has been reviewed and is approved.



WAYNE H. McCANDLESS
Chief, Life Support Systems Laboratory

Contrails

TABLE OF CONTENTS

	<u>Page</u>
INTRODUCTION	1
SUMMARY	2
DISCUSSION OF RESULTS.	9
Cell Design and Operation	9
Design Principles	9
Reliability	9
Electrolysis Pressure	12
Cell Arrangement	12
Detailed Design	12
Cell Weight.	13
Cell Volume	13
Description of Cell and Components	16
Electrolysis Cell	16
Auxiliary Cell Components	19
Control Panel and Circuit	20
Cell Operation.	20
Effect of External Gravity Field in Cell Design and Operation	27
Design Considerations	27
Effect of Cell Rotational Speed on Vortex Shape.	29
Effect of Vortex Shape on Electrode Area.	31
Hydrogen and Oxygen Production	32
Power Requirements	32
Mechanical-Power Consumption	32
Electrical-Power Consumption	42
Voltage Measurement	42
Brush Contact Drop	42
Electrolysis Power Consumption	46
Industrial Cell Comparison	46
Cell Voltage Characteristics	48
Effect of Temperature	50
Estimate of Cell Voltage for Higher Temperature Operation	55
System Optimization.	59
REFERENCES	60
APPENDIX I	
DESIGN AND EXPLANATION OF AUTOMATIC CONTROL CIRCUIT FOR ZERO-GRAVITY ELECTROLYSIS MACHINE	63

TABLE OF CONTENTS
(Continued)

	<u>Page</u>
APPENDIX II	
FEASIBILITY STUDY REPORT ON METHODS FOR ELECTROLYSIS OF WATER UNDER ZERO- GRAVITY CONDITIONS	69

LIST OF FIGURES

<u>Figure</u>	<u>Page</u>
1. Laboratory-Model Rotating Electrolysis Cell Inherently Capable of Operating Under Zero-Gravity Conditions	3
2. Estimated Unit Weight, Volume, and Power Consumption per Man for Operation of Laboratory Model at Higher Power to Supply More Men	8
3. Photograph of Laboratory-Model Rotating Electrolysis Cell	10
4. Detailed Cross Section of Laboratory-Model Rotating Electrolysis Cell	11
5. Dimensional Profile of the Laboratory-Model Rotating Electrolysis Cell	15
6. Control Panel Used for Remote Manual Operation of Laboratory Model	21
7. Control Circuit for Laboratory Model	22
8. Cross Section of Cell Showing Liquid Vortex During Rotation and Liquid-Level Sensors	23
9. Schematic of Auxiliary Equipment Used in Evaluation of Laboratory-Model Rotating Electrolysis Cell	24
10. Liquid-Valve and Pump Arrangement	26
11. Calculated Cell Speed for Various Liquid Level Radii	30
12. Hydrogen and Oxygen Gas-Collection Rate	33

LIST OF FIGURES
(Continued)

<u>Figure</u>		<u>Page</u>
13.	Measured Motor Power Consumption for Rotation of Laboratory Model at Various Speeds	38
14.	Predicted Mechanical Power Consumption at Various Cell Rotational Speeds	41
15.	Brush Contact Drop Voltage Related to Current, Brush Material, and Brush Current Density	43
16.	Comparison of Cell Voltage Obtained With Laboratory Model With Industrial Cells	47
17.	Cell Voltage at Various Current Densities for Operation of Laboratory Model.	49
18.	Laboratory Model Power Consumption at Various Water Electrolysis Rates	51
19.	Decrease in Electrolysis Cell Voltage and Correlation With Increase in Electrolyte Temperature	52
20.	Effect of Electrolyte Concentration on Resistivity	56
21.	Effect of Temperature on Voltage Drop Through Electrolyte at Various Amperes for Laboratory Model	57
22.	Estimated Effect of Electrolyte Temperature on Electrolysis Voltage for Operation of Laboratory Model at 254 Amperes (Two-Man Cell)	58
23.	Automatic Control Circuit for Zero-Gravity Electrolysis Machine	65
24.	High Pressure Cell	71
25.	Bipolar (Series) or Tank (Parallel) Type Cell (Parallel Connection Shown)	74
26.	Vortex Separators	82
27.	Vortex Gas Separator (Pratt & Whitney Design) and Separate Electrolysis Cell (Conventional Design)	84
28.	Section Through Membrane Cell	90

LIST OF FIGURES
(Continued)

<u>Figure</u>		<u>Page</u>
29.	Vapor-Cell Tube Bundle	93
30.	Porous Electrode Cell	96
31.	Rotating Cell With Palladium Cathode	100
32.	Electromagnetic Artificial Gravity Field	106

LIST OF TABLES

<u>Table</u>		<u>Page</u>
1.	Total Power Consumption for the Laboratory-Model Rotating Electrolysis Cell in the Three Evaluation Runs	5
2.	Comparison of Present and Predicted Future Power Consumption of Laboratory-Model Rotating Cell	7
3.	Approximate Component Weight of Laboratory Model	14
4.	Hydrogen and Oxygen Evolution Rates in Evaluation Runs of Laboratory-Model Rotating Electrolysis Cell	34
5.	Cell Rotational Power Consumption, Motor Circuitry and Measurements	36
6.	Zero-Gravity Electrolysis-Machine Summary Table of Automatic Control Functions	66

Contrails

RESEARCH ON THE ELECTROLYSIS OF WATER UNDER WEIGHTLESS CONDITIONS

by

John E. Clifford, James T. Gates,
John McCallum, and Charles L. Faust

INTRODUCTION

The objective of this project was to investigate methods of accomplishing electrolysis of water under weightless* conditions for space missions of extended duration (2 days to 2 years). Consideration of man's respiratory function and water intake-output had indicated that a system should be designed for electrolyzing water at rates from 0.7 to 2.25 lb/man/day. The lower rate is a minimum based on the excess of man's total output of water over his intake. The higher water rate is based on the average requirement of 2.0 lb of oxygen/man/day in a closed ecological system.

Although not a concern of this project, it is generally known that the other product of water electrolysis, namely hydrogen, could be used in the reduction of carbon dioxide to carbon and water, the latter being returned to the electrolysis cell.

Electrolysis of water is a well-established industrial operation for production of hydrogen and oxygen (more so in foreign countries than the United States because of differing economic factors). The problem is to accomplish electrolysis under conditions of weightlessness. On the earth the gravitational acceleration gives weight to the electrolyte, thus creating a hydrostatic pressure differential with depth which causes gas bubbles generated at the normally vertical electrodes to rise to the surface and separate from the liquid.

Thus, there are two problems under zero-gravity conditions. One problem is to remove the hydrogen and oxygen bubbles adhering to the electrodes, otherwise complete polarization would occur (flow of current would become negligible as the gas would prevent the electrolyte from contacting the electrode). The second problem is to separate the evolved hydrogen and oxygen gas bubbles from the electrolyte.

While "zero-gravity electrolysis" is a term descriptive of the problem, any laboratory model must first be developed and demonstrated while under the influence of the earth's gravity field of 1 G. The original system specifications were modified to include capability of operation in the range

*Also termed zero gravity in this report.

Contrails

of 0-1 G. While the equipment should be capable of withstanding accelerations of 15 G, operation of the system during periods of acceleration greater than 1 G was not considered a necessity.

The project was conducted in three steps:

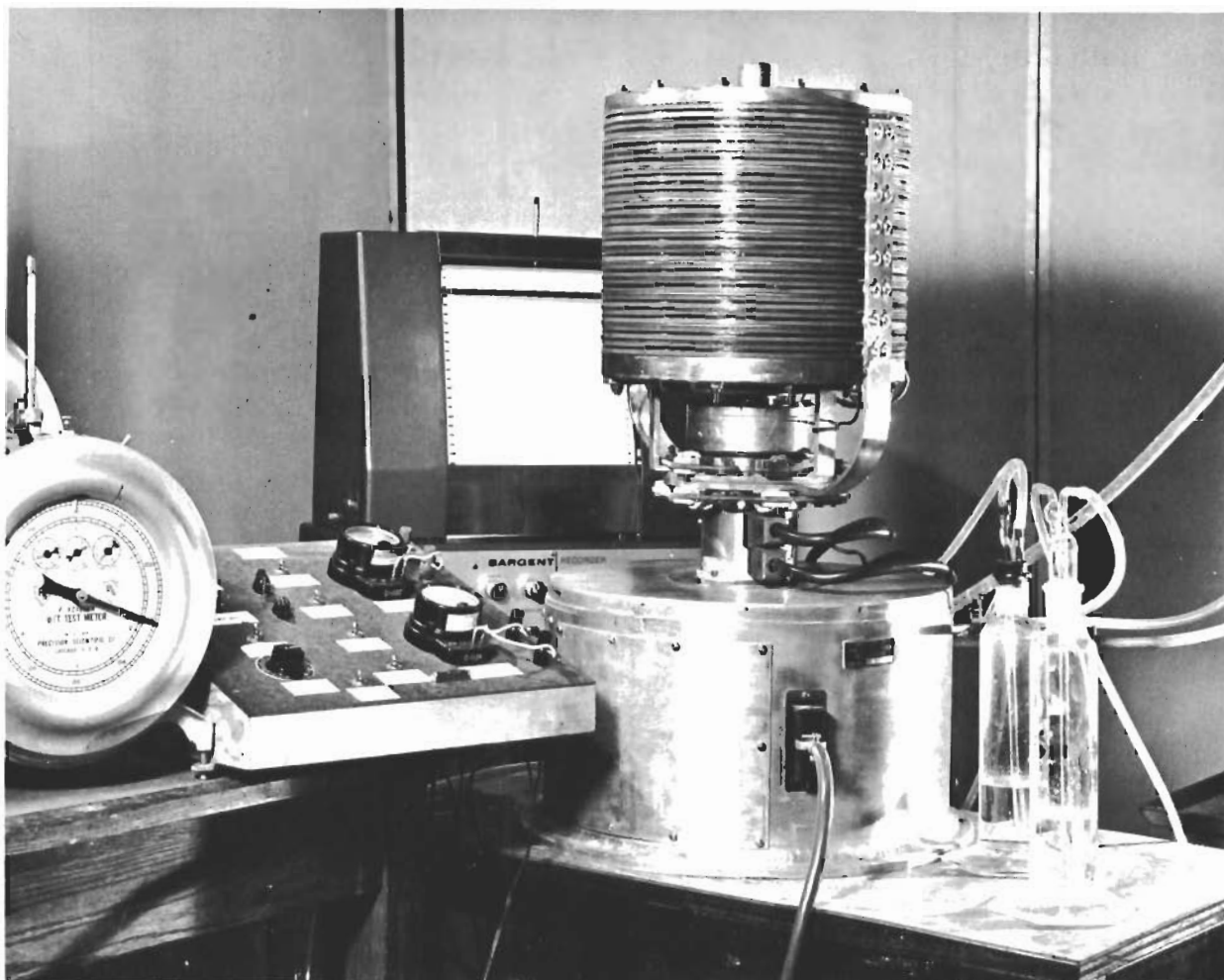
- (1) A "paper study" of methods considered feasible for electrolysis of water under zero-gravity conditions. An informal feasibility study report is included as part of this report in Appendix II.
- (2) Design of a laboratory model of the method of electrolysis selected for further study.
- (3) Construction and evaluation of the laboratory model. This final report is concerned principally with the evaluation of the laboratory model that was constructed.

SUMMARY

The laboratory-model rotating electrolysis cell that was designed and constructed on this project is shown in Figure 1. Satisfactory operation was obtained in three separate runs of 3/4, 2, and 2-1/2 hours' duration. Hydrogen and oxygen gases were evolved with the cell operating at the designed electrolysis current of 254 amperes (corresponding to a 2-man unit for electrolyzing water at the maximum desired rate of 2.25 pounds of water per day per man).

The evidence for capability of zero-gravity operation is inherent in the orientation of the cell relative to the earth's gravitational field during electrolysis. The gas bubbles move in a direction parallel to the plane of the electrodes which is perpendicular to the earth's gravitational field. Thus, no component of the earth's gravitational field is used in effecting the separation of the gas from the liquid.

The important advantage of the cell design is that the electrolysis principle is already well established in industrial cells for electrolytic production of hydrogen and oxygen. The use of steel cathodes, nickel-plated steel anodes, asbestos diaphragms, and 28 per cent potassium



N81249

FIGURE 1. LABORATORY-MODEL ROTATING ELECTROLYSIS CELL
INHERENTLY CAPABLE OF OPERATING UNDER
ZERO-GRAVITY CONDITIONS

Contrails

hydroxide electrolyte is patterned after industrial cells which are known to operate for 5 to 10 years with a minimum of maintenance. Hence, this electrolysis unit has a basis for reliability that would be difficult to match with any other electrolysis system except by extensive operational testing for 2 years.

Reliability for 2-year operation was an important factor in the decision to proceed with a rotating cell. The informal-feasibility-study report in which other methods of zero-gravity electrolysis were considered is included as Appendix II of this report.

The rotating cell designed and constructed on this project emphasized minimum power consumption. The unit weighs about 284 pounds including 30 pounds of electrolyte and occupies a cylindrical space of about 4.4 cubic feet (17-1/2 inches' maximum diameter by 31-1/2 inches' height). It now appears that a 50 per cent reduction in weight and volume might be attained by future optimization of the design without increase in power consumption.

The preliminary data obtained on total power consumption are as good as or better than expected. The data on power consumption for the three consecutive evaluation runs are summarized in Table 1.

After the first run, the graphite brushes supplying current to the cell were replaced with silver-plated brushes to decrease the brush contact resistance and effect a significant reduction in total power consumption.

The lowest total power consumption was obtained at the end of the third evaluation run. The total power of 637 watts is based on actual operation of the cell with electrodes in a parallel electrical scheme. If the 485 watts of electrolysis power were supplied as 30.5 volts (1.91 volts/cell x 16 cells) at 15.9 amperes in a bipolar cell arrangement (series electrical connection), the brush contact drop could be reduced to 0.1 volt or less and the power loss at the brush contact would be less than 2 watts with the lower amperage.

The mechanical power of about 90 watts at 500 rpm could be reduced by a factor of 3 under zero-gravity conditions where a threefold reduction in rotational speed is permissible. Thus, a bipolar cell operated at zero gravity is estimated to require only 520 watts.

The cell voltage of 1.91 volts is 0.1 to 0.2 volt lower than reported for commercial hydrogen-oxygen cells operated at comparable electrode current densities.

The lower cell voltage attained in each run is very probably the result of increased electrolyte temperature for the longer duration runs (111 F at the end of 2-1/2 hours in the third run). While some industrial hydrogen/oxygen cells of similar materials of construction operate at temperatures

TABLE 1. TOTAL POWER CONSUMPTION FOR THE LABORATORY-MODEL ROTATING ELECTROLYSIS CELL IN THE THREE EVALUATION RUNS

Basis: 2-man cell operated at 254 amperes (4.5 lb of water per day or 4.0 lb of oxygen per day).

	Evaluation Run					
	1		2		3	
	Volts	Watts	Volts	Watts	Volts	Watts
Run Duration, hr	1/2		2		2-1/2	
Cell Rotational Speed, rpm	480		510		520	
Final Electrolyte Temperature, F	89		106		111	
Electrolytic Power ^(a)						
Reversible cell potential	1.225	311.3	1.217	308.7	1.214	308.3
Electrolyte voltage drop	0.080	20.3	0.069	17.7	0.066	16.7
Hydrogen overvoltage	0.249	63.4	0.234	59.4	0.229	58.0
Oxygen overvoltage	0.441	112.0	0.410	104.2	0.401	102.0
TOTAL ELECTROLYSIS VOLT-AGE AND POWER	1.995	507	1.93	490	1.91	485
Electrical Power ^(b)						
Brush contact drop	0.875	222.5	0.30	76.2	0.23	58.4
TOTAL APPLIED VOLTAGE AND POWER	2.870	729.5	2.23	566.2	2.14	543.4
Mechanical Power						
Brush drag	51.9		30.1		33.6	
Seals, bearings, etc.	52		57.5		60	
TOTAL CELL POWER CONSUMPTION	833		654		637	

(a) Based on measured value of cell electrolysis voltage at end of run. Reversible cell potential and electrolyte voltage drop were calculated. Total overvoltage determined by difference. Oxygen overvoltage assumed to be 64 % of total overvoltage.

(b) Brush contact voltage drop determined by difference between measured values of applied voltage and electrolysis-cell voltage.

Contrails

up to 170 F, the possibility of 0.1 to 0.2-volt reduction and saving in power must be weighed against possibly shorter cell life and less reliability.

Table 2 gives a comparison of the power consumption of the laboratory model in evaluation Run 3 with that predicted for extended operation at higher temperature (165 F) as a bipolar (series connected) cell in an external zero-gravity field. The basis for the estimates of reduced total power consumption is discussed in greater detail later in this report under sections dealing with mechanical, electrical, and electrolytic power consumption.

In considering more advanced space missions, an interesting feature of the present laboratory-model design is that it might be used as a 3-, 4-, or 5-man cell. The cell has been operated at 410 amperes which is above the amperage required for a 3-man cell. Since there was no indication of electrode polarization at the highest current density used, a straight-line extrapolation of the cell voltage vs. log current density curve over the range of 60 to 90 amperes per square foot appears reasonable. Figure 2 shows that on a unit basis (per man), the present laboratory model requires little change in unit power, while effecting the expected reduction in unit weight and unit volume as the design basis is extended from a 2-man to a 5-man cell. Bipolar operation has been assumed for the higher rates to avoid power loss at the brush contacts.

Alternatively, if size and weight are relatively more important than power consumption, the laboratory model could be redesigned to operate as a 2-man cell at higher current density with a reduction in weight and size.

Conventional industrial electrolytic cells operate at current densities up to 100 amperes per square foot based on apparent electrode area (and higher for special electrode designs). A limiting factor is the compromise required between closer electrode spacing to reduce voltage drop through the electrolyte and the greater electrolyte resistivity caused by the greater volume of gas evolved in a smaller space between the electrodes. There is reason to believe that the effective G-values in the rotating cell would aid gas removal from the interelectrode space and allow higher current density than in the earth's 1-G field.

As the report progresses it will be shown that the laboratory model could have been made smaller by allowing increase in power consumption. A number of factors influence size and weight of the cell which can be regulated at the design stage depending on whether size and weight or power consumption is the more important. The preferred design of the electrolysis cell depends on the weight/power ratio of power-supply system.

TABLE 2. COMPARISON OF PRESENT AND PREDICTED FUTURE
POWER CONSUMPTION OF LABORATORY-MODEL
ROTATING CELL

Basis: 2-man cell operated at 254 amperes (4.5 lb of
water per day or 4.0 lb of oxygen per day).

	Power Consumption, watts	
	Present (measured at end of 2-1/2-hr evaluation run as parallel- connected cell in earths' field of 1 G)	Future (estimated for extended opera- tion at high temperature as bipolar cell at zero gravity)
Electrolytic Power		
1.91 v at 111 F	485	
1.7 v by increase to 165 F		432
Electrical Power (Brush Contact)		
Parallel cell connection	58.4	
Series Bipolar cell		2
Mechanical Power		
Rotation at 520 rpm in 1-G field	93.6	
Rotation at 140 rpm at zero gravity		<u>23</u>
Total Power	637	457

Contrails

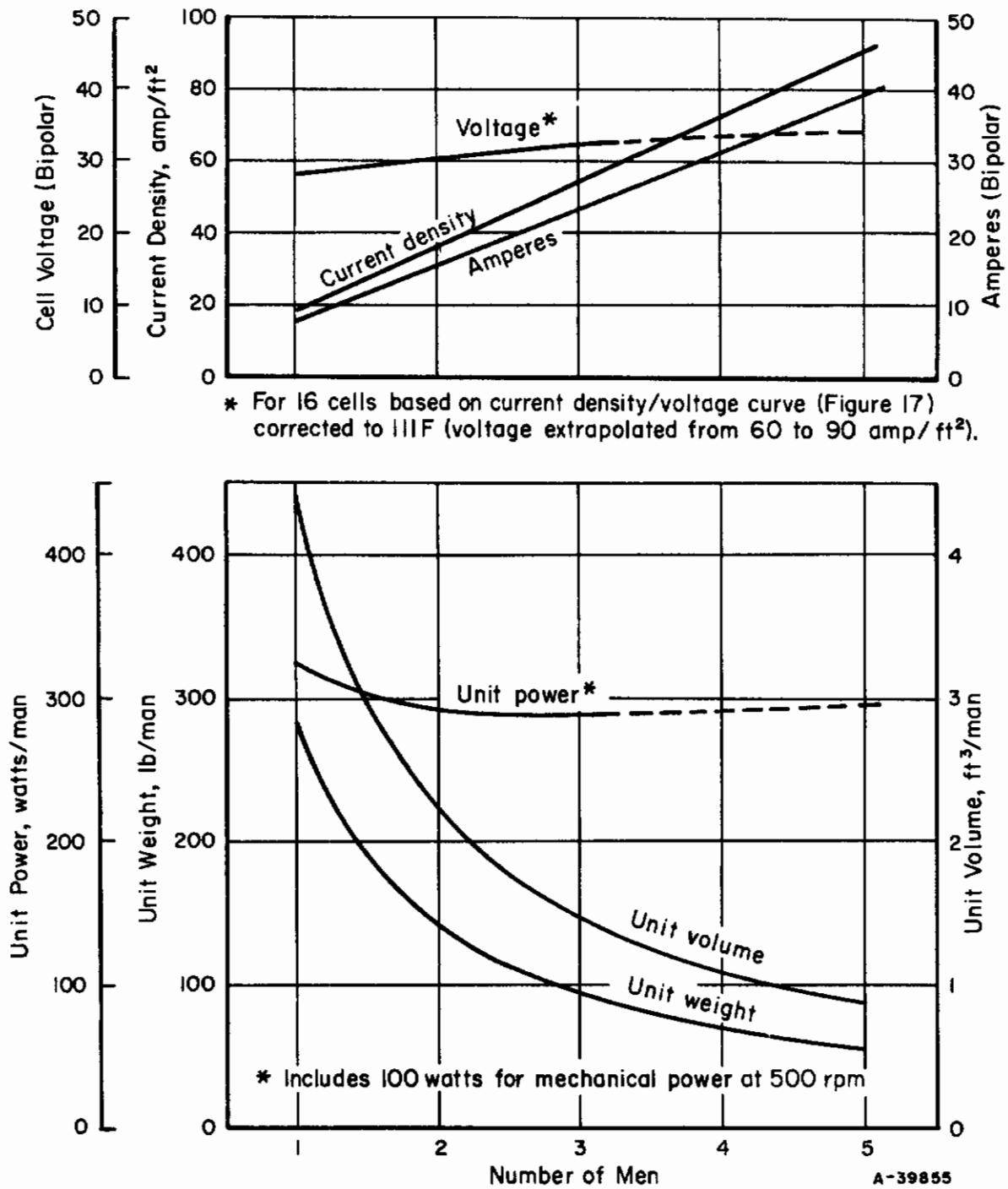


FIGURE 2. ESTIMATED UNIT WEIGHT, VOLUME, AND POWER CONSUMPTION PER MAN FOR OPERATION OF LABORATORY MODEL AT HIGHER POWER TO SUPPLY MORE MEN

Water electrolysis rate - 2.25 lb/day/man; bipolar operation assumed to make brush contact loss negligible.

DISCUSSION OF RESULTS

Cell Design and Operation

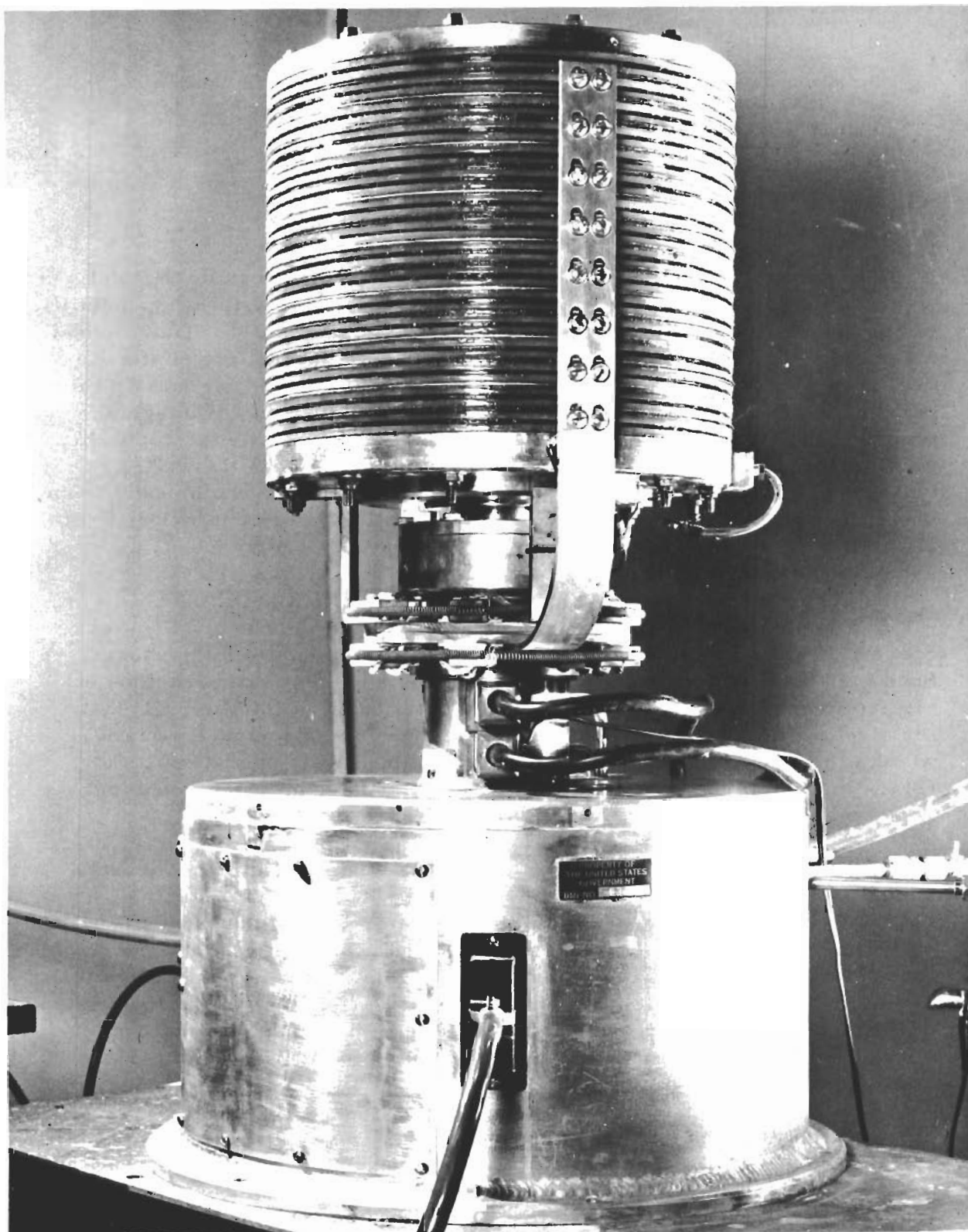
Design Principles

Reliability. Following the feasibility study of various methods of electrolysis of water considered workable at zero gravity (see Appendix II), further study of the rotating-cell method was recommended. This method meant an integral electrolysis and gas-separation unit patterned after industrial electrolytic cells for production of hydrogen and oxygen. An important reason for this choice of method was the apparent advantage of more reliability than other systems considered. The basis for reliability was not considered to be in the mechanical features but in the well-established electrochemical reactions of industrial cells which result from use of potassium hydroxide electrolyte (normally 28 per cent by weight of KOH for good conductance), nickel-plated anodes, steel cathodes, and asbestos diaphragms.

With the above-mentioned materials, industrial cells are known to operate satisfactorily for 5 to 10 years with a minimum of maintenance. Such reliability would be difficult to match by any other known method of electrolysis of water. There are two aspects of the reliability: (1) that the electrode reactions are stable and steady over long periods of time, which is probably unique among industrial electrolysis operations, and (2) the materials in contact with the electrolyte have an established high resistance to corrosion.

Thus, to retain the basis for reliability, the laboratory model was built with similar materials used in the internal parts of the electrolysis cell. Two other materials used in the laboratory model that contact the electrolyte are polyethylene cell spacers, and neoprene (gaskets and molding); both are known to have high chemical resistance to the concentration and temperature of electrolyte used. In considering the project objectives, particularly mission duration of up to 2 years, the emphasis on a conservative electrolysis method seems warranted in view of the importance of reliability in aerospace equipment.

At the time the present study was undertaken, there was no known working model of a zero-gravity electrolysis system. A primary need existed for a workable unit. The size, weight, and power requirement of the first prototype system could then serve as a basis for evaluating proposed improved systems.



N81251

FIGURE 3. PHOTOGRAPH OF LABORATORY-MODEL
ROTATING ELECTROLYSIS CELL

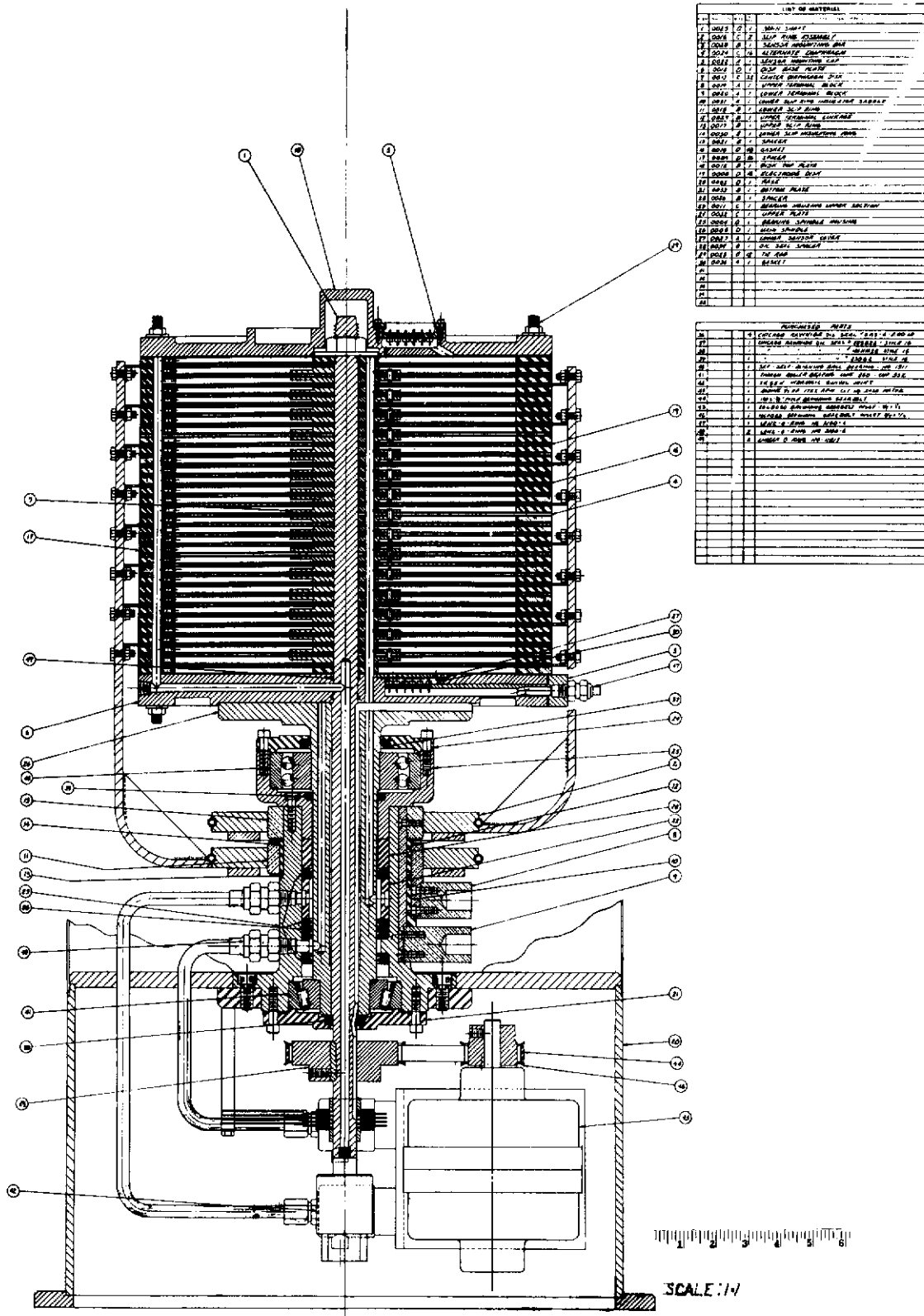


FIGURE 4. DETAIL CROSS SECTION OF LABORATORY-MODEL ROTATING ELECTROLYSIS CELL

Electrolysis Pressure. Industrial electrolytic cells for production of hydrogen and oxygen include both high-pressure and low-pressure systems as well as "bipolar" (series connected) and "tank-type" (parallel connected) cells. The possibility of eventually investigating all variations influenced the design of the laboratory model.

The possible advantages to be gained by a high-pressure system (from 1 to 20 atm) in relation to power reduction did not seem to justify the added complexity of the pressure controls, reduction in over-all reliability of the mechanical system, and added system weight. Thus, attaining satisfactory power requirement for the low-pressure system was the first objective. The favorable power consumption results with the laboratory model obtained in the subsequent evaluation runs on this project (which may be partly due to the rotation) have given added support to the recommendation of a low-pressure cell over a high-pressure cell.

Cell Arrangement. The electrolysis cell was designed for easy conversion from a parallel to a series-connected (bipolar) cell. The contract period did not permit investigation of the bipolar cell according to the original plan. The cell was connected in parallel for the initial evaluation to favor experimental studies, since obtaining data on electrolysis power was important. In a parallel-connected arrangement, the cell voltage can be measured directly. More accurate interpretation of data is possible than if the average cell voltage is calculated from the bipolar cell voltage and the number of cells in series. It is preferable to compare results of bipolar operation against the results previously obtained in the equivalent parallel-connected unit.

The data obtained in a parallel-connected unit can be converted to the equivalent bipolar unit since the electrolytic power consumption should be the same. The number of cells times the cell voltage gives the voltage to be applied to a bipolar unit. The total power divided by the bipolar cell voltage indicates the current that will result. The current density on the electrodes is the same for bipolar operation as for parallel operation.

Detailed Design

Figure 3 is a close-up photograph of the laboratory-model rotating electrolysis cell for comparison with the detailed cross section shown in Figure 4.

The upper drum-shaped unit is the electrolytic cell which is rotated on a central shaft. The remainder of the unit is termed the "superstructure" which includes the bearing assembly, the brush assembly, seals, and the aluminum shell base which houses the drive motor and pulleys, gas lines, and gas valves. Other items in the base relating to the liquid system such as pump, valves, lines, etc., were omitted from Figure 4 for clarity.

Contrails

Selected drawings and sketches are included as figures in this report to supplement the discussion of the important design features which follows.

Appendix I contains a design for an automatic control circuit intended for use with the laboratory model. The automatic control circuit was not built. Instead, a manual control panel was constructed for use in the preliminary evaluation.

Cell Weight

The measured weight of the laboratory model was 254 pounds (empty). The added weight of the electrolyte required was calculated to be 30 pounds based on 10-1/2 liters (28% KOH, sp gr 1.27). Thus, the total cell weight is 284 pounds. An approximate breakdown of the total cell weight is shown in Table 3 to indicate the components that could be reduced in weight in a future design directed toward weight optimization.

It is estimated that the total cell weight could be reduced to about 200 pounds readily in a future design without affecting the electrolysis portion or the power (reduce by 1/2 the weight of the top and bottom plates and by 1/2 the weight of the superstructure).

Cell Volume

The drawing in Figure 5 shows the essential dimensions of the laboratory model that would be of use in estimating the space occupied by the electrolysis cell in an integrated life support system.

The total cylindrical space occupied by the cell is:

$$\frac{\pi}{4} (17.5)^2 (31.5) = 7560 \text{ in.}^3 = 4.4 \text{ ft}^3.$$

The power supply and source of water to be fed to the cell are not considered a part of the electrolysis machine. The electrolyte reservoir is considered a part of the cell since with the present design, the electrolyte would not be retained in the cell during two periods:

- (1) During any period when cell rotation is stopped (i. e. , for maintenance)

TABLE 3. APPROXIMATE COMPONENT WEIGHT OF LABORATORY MODEL

	Weight, pounds	
<u>Electrolysis Portion</u>		
Top plate	18.8	
Negative electrodes + gaskets (8)	19.7	} 108 lb (6-3/4 lb/cell)
Positive electrodes + gaskets (7)	17.3	
Asbestos diaphragms (16)	3.7	
Polyethylene cell spacers (32)	19.1	
Tie rods (12)	2.1	
Bus bars (2)	6.4	
Central shaft	3.0	
Electrolyte (10-1/2 liters)	30.0	
Plastic cover	5.0	
Miscellaneous	1.9	
Bottom plate	35.0	
	<u>162.0</u>	
<u>Superstructure</u>		
Aluminum base shell	37.6	
Rotational motor	17.8	
Pump + motor	28.7	
Valves, strainer, lines, etc.	7.9	
Bearings and seals	20.0	
Brush assembly	10.0	
TOTAL LABORATORY MODEL WEIGHT	<u>284.0</u>	

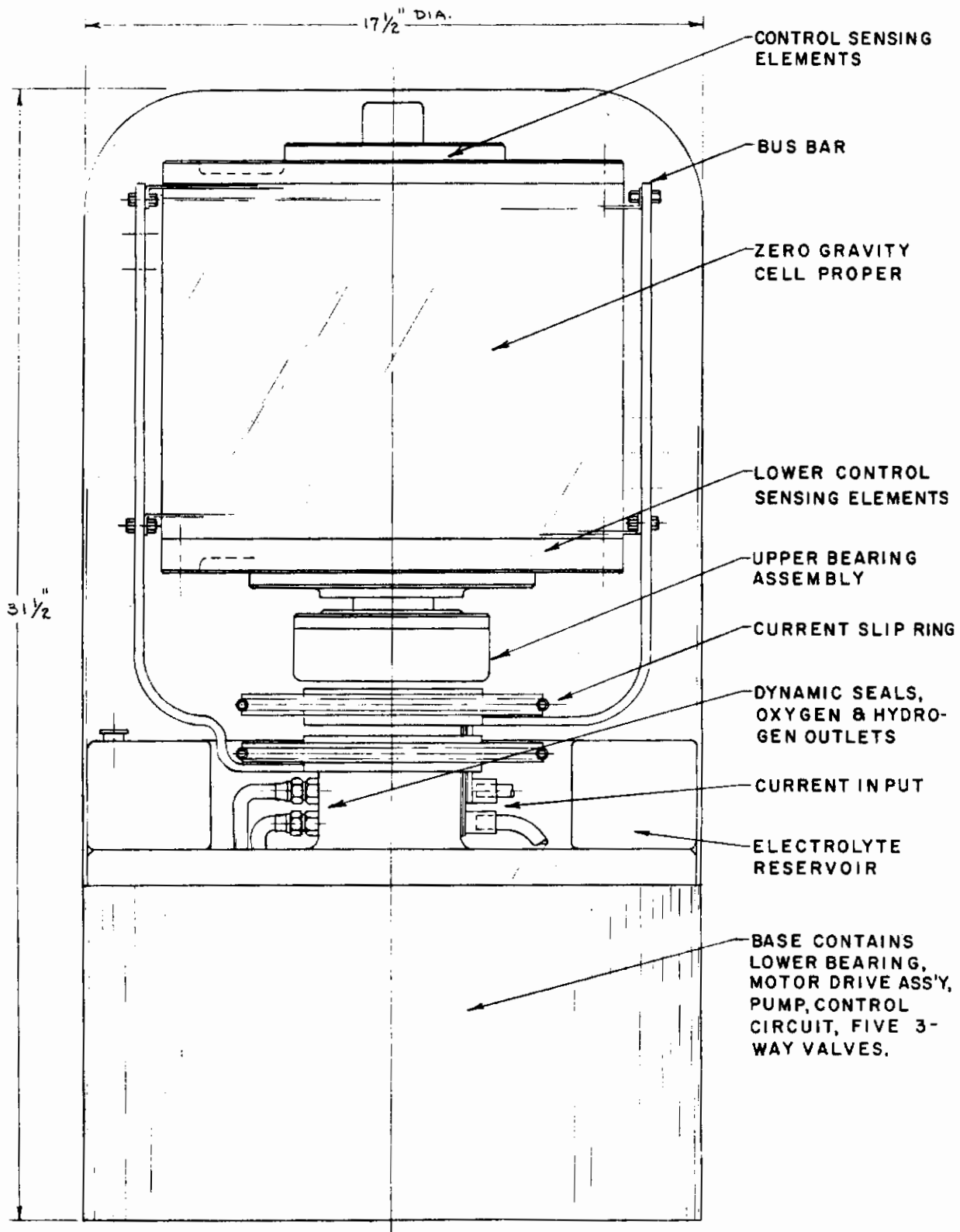


FIGURE 5. DIMENSIONAL PROFILE OF THE LABORATORY-MODEL ROTATING ELECTROLYSIS CELL

- (2) During periods of high acceleration (up to 15 G external field) when the cell would not be in operation for electrolysis.

For the experimental evaluation in the laboratory, the electrolyte was contained in a 5-gallon bottle external to the cell. Experience showed that about 2.8 gallons of electrolyte filled the cell. Thus, 630 in.³ of electrolyte reservoir capacity is needed. In Figure 5, an annular ring-type reservoir located at the top of the base is shown to suggest the best utilization of available space. The reservoir in Figure 5 has a capacity of about 530 in.³; being limited by the bus bars on the present laboratory model. For a bipolar cell, the bus bars would not be used and the annular reservoir could be increased in height to hold over 1000 in.³ of electrolyte. Alternatively, the reservoir could be included in the base in a future design which optimized location of motor, pump, valves, lines, etc.

The total cylindrical volume of 4.4 ft³ is conservative enough to allow for inclusion of 0.37 ft³ of reservoir capacity by future optimization of design.

It is estimated that the volume of the laboratory model could be reduced by about one-half, to 2.2 ft³, without increase in power in a future design of a prototype model which emphasized compactness of the superstructure and miniaturized the auxiliary cell components. The apparent density of the entire laboratory model is 65 lb/ft³ (284 lb/4.4 ft³) compared to the apparent density of 180 lb/ft³ (162 lb/0.9 ft³) for the more compact electrolysis cell portion.

Description of Cell and Components

Electrolysis Cell. The cylindrical electrolysis portion of the laboratory model is made up of 16 individual cells connected in parallel by the copper bus bars along the side. Each cell unit is made up successively of an anode plate, a neoprene gasket, a polyethylene cell spacer, an asbestos diaphragm, a polyethylene cell spacer, a neoprene gasket, and a cathode plate.

The plate electrodes also served to separate the unit cells. Since each side of the separating plate served as an electrode in adjoining cells, there were 8 negative plates and 7 positive plates with the top and bottom end plates each serving as positive electrodes. Figure 4, which was drawn prior to the final cell assembly, does not show the modification in which the top and bottom end plates are used as electrodes. The latter modification, which reduced the cell weight and size a little, became possible after the decision to electroplate the end plates with nickel.

The 15 electrode plates were made of 1/16-inch sheet steel and were designed so that, even though made identical, they could be used either as

Contrails

positive or negative electrodes. The plates to be used as anodes were electroplated with nickel (from a Watts'-type solution) to a minimum thickness of 0.001 inch on both sides. The plates to be used as cathodes were pickled in sulfuric acid solution to remove rust and scale prior to assembly in the cell. [For a bipolar cell, each electrode plate would be nickel plated on only one side. Thus, when assembled to form cells, the nickel-plated side of the electrode would be the anode of one cell and the opposite side of the electrode (unplated steel) would be the cathode of the adjoining cell.]

The asbestos diaphragm between an anode and cathode keeps the oxygen and hydrogen separated below the liquid level. Above the liquid level, the asbestos might "dry out" and then would not be an effective barrier to gas diffusion. To prevent intermixing of hydrogen and oxygen, a gas-impermeable barrier was needed for that portion of the diaphragm that would be above the liquid level (i. e. , in the gas core of the liquid vortex formed with cell rotation).

The cell diaphragms were made from high-grade asbestos cloth* normally used in electrolytic cells. A neoprene rubber coating was applied to both sides of the asbestos as a central 6-inch diameter disk by molding in a specially designed die. At the same time, a rubber layer was applied to the outer radial inch of the asbestos to act as a seal. The rubber was molded completely around the outer periphery of the asbestos so as to prevent electrolyte leakage by permeation through the asbestos under the action of centrifugal force.

Whether or not a series or parallel cell is considered, the asbestos diaphragm always separates hydrogen and oxygen. The centrally located polyethylene spacer on either side of the diaphragm contained an axially aligned hole which served to lead gas to the appropriate central gas port. Two polyethylene spacers were riveted on each side of the asbestos diaphragm; one side aligned to conduct gas to the hydrogen port and the other side aligned to conduct gas to the oxygen port. Thus, each diaphragm assembly was identical but its orientation depended on the electrode arrangement. [The same diaphragms could be used for a bipolar cell by proper alignment with respect to the gas to be evolved from the electrode.]

The gas ports through the cell (aligned during assembly) were formed by six equispaced 1/4-inch holes on a 2-inch diameter in the electrode plates, polyethylene spacer and asbestos diaphragm. Three alternate holes were for hydrogen; the other three for oxygen. The gas ports in the cells aligned with the gas ports in the bottom end plate and shaft to conduct gas to the appropriate place between seals on the shaft for gas takeoff.

Electrolyte was pumped into the cell through the centrally located hole in the shaft as far as the bottom end plate, then radially outward in the bottom plate to the aligned holes on the outer periphery which formed the

*Grade AAAA, Style 12T370, Raybestos-Manhattan, Inc.

Contrails

distributing system by interconnection to each cell. Electrolyte was pumped out of the cell in the same channel, and by suitable valving water could be added to the cell by the same port to replace the water decomposed by electrolysis.

In the top and bottom plate, there was a series of probes for sensing the liquid level during operation. The sensing element and circuitry are discussed later.

The cell was assembled from the bottom plate up by sliding the components down on the 12 tie rods. A polyethylene tube was slipped over each tie rod before assembly. The center hole in the cathode plates was made slightly larger than the center hole in the positive anode plates; so that the cathode plates would not be grounded to the main center shaft. This meant that alternate plates made contact with the center shaft for purpose of good alignment. After the top plate was added, and the tie rods tightened, the individual electrodes were then bolted to the copper bus bars.

The laboratory model was operated with a plastic canopy around the electrolytic-cell portion (see Figure 5). The purpose of the plastic canopy in experimental work was primarily as a shield against any leaking electrolyte which would be thrown away from the rapidly rotating cell. Leakage was not evident until the cell was rotated and the location of fine spray on the shield over a period of time was useful in identifying the source of the leakage. The shield used was made of Plexiglas. It was known that polystyrene would be more compatible with caustic, however, because of molding time and expense the more expendable-type shield was used. By the final evaluation runs, the leakage had been eliminated and recommendations could be made for future minor design changes in cell construction that would remove the cause of leakage.

In general, the cell design appears adequate to prevent leakage. A small amount of leakage occurred in the early check-out runs which was temporarily corrected by sealing the outer surface with plastic. Two minor changes in design would remove the cause. The first small leakage occurred at the tie rods from electrolyte permeating through the asbestos to the tie rod hole. The tie rod holes were cut in the asbestos after molding, thus exposing the asbestos. The preferred procedure would be to cut the tie rod holes slightly oversize in the asbestos first, then mold with rubber to fill the tie rod hole, then cut the tie rod hole to size in the rubber. This would seal the asbestos all around the tie rod hole.

When first assembled, the cell did not leak at the junction of the plate, gasket, and polyethylene spacer. The gasket had not been glued to the metal plate but was found to be stuck fairly tight on disassembly of the cell. However, when the gaskets were removed from the plates and replaced, on reassembly, slight leakage was seen between the gasket and plate. This could be corrected in the future by using an adhesive to bond the gasket to the electrode.

Contrails

Auxiliary Cell Components. Brush Assembly. Direct current for electrolysis was supplied to the cell by way of two copper slip rings. Six Speer Carbon Company, Grade 580 carbon brushes (size 5/8 x 1 inch) made contact with each slip ring providing a brush area of 3.75 square inches (0.625 x 1 x 6) for each conductor. The brushes on each slip ring were contained in a spring-loaded magazine, such that at design speed each brush made contact with the ring with a force of only a few ounces. The brush material rated at 70 amp/in.² gave a safe current capacity of 262 amp.

The brush assembly design had the disadvantage of an added starting torque until such time as the centrifugal force in rotating the cell counteracted some of the spring pressure. In any future rotating cell model, a different design would be recommended that would allow rotation of the slip rings with the brushes stationary so that brush pressure against the slip ring would be independent of the cell rotational speed.

The electrical characteristics and performance of the carbon brushes are discussed in detail in a later section on electrical power consumption.

Bearings and Seals. The main cell spindle rotates on an upper SKF self-aligning bearing, No. 1311, and at a 7-inch center-line distance below is held by a radial Timken bearing, No. 350-352. The cell, being designed for laboratory use did not have a sophisticated bearing system capable of taking thrust in all directions.

The seals used in the cell were a special Chicago Rawhide Mfg. Co. "CRS"-A spring-loaded Buna compound double lip seal for 2-in. shaft. It was found that the seals resulted in too much starting torque for the 1/8-hp drive motor being used. As a temporary expedient, the seals were trimmed, making thin single lip seals and the springs were removed - this still provided a satisfactory seal for laboratory runs and reduced the starting torque to a minimum so that it could be handled by the motor in use. In subsequent models a carbon face seal would be more appropriate.

Drive Motor. It was desirable to drive the cell with a minimum horsepower motor. A Bodine 1/8-hp, 1725 rpm, 110-volt-dc, shunt wound, ball bearing Motor # B-2420-NSH54 was selected. The control of this motor for increased speeds is explained in the body of the report. The motor rotated the cell at 400 rpm (conventionally) through step-down pulleys and a 3/8-in.-pitch x 1/2-in.-width timing belt (Browning # 210-L).

Liquid Pump. An Eastern Industries, Model VW-1, 110-volt-dc, positive pressure, stainless steel pump was used to supply electrolyte and water to and from the cell by way of appropriate valving. This pump has a

Contrails

capacity of 1-1/2 to 2 gal/min at 10 psi. In use with a Y-type strainer and a rheostat speed adjuster, the pump performed satisfactorily.

Valves. Five Skinner, stainless steel, 3-way, No. V54-DA-2-075, 110-volt-dc, type GD mounting valves were employed in the base of the cell housing. Some difficulty in valves sticking was experienced, which would suggest manually operated bypass lines as well as the use of a more foolproof valve.

Control Slip Rings. The liquid-control, sensing-element circuitry (see Figure 7) was provided electrical contact with the rotating cell through a Breeze Corp. No. AJ-8003-4 standard slip-ring assembly. The slip rings performed satisfactorily without incident.

Rotary Hydraulic Swivel Joint. To supply water and electrolyte to the rotating cell, a Chiksan C Model SK55H, 1/4 P. T., Style 30 swivel joint was used. This means of providing a dynamic leak-free liquid passage to the rotating center shaft may be seen at the bottom of Figure 4, Part 42.

Control Panel and Circuit. Figure 6 is a sketch of the control panel used for remote manual operation of the cell. Figure 7 is a wiring diagram of the control circuit used in the laboratory evaluation. The circuitry of the liquid-level sensors is shown in Figure 7 for the preferred method of operation with the power supplied from the auxiliary rectifier. A rheostat reduces the voltage to 10 volts for the sensing-element control. The interpretation of liquid level from the voltmeter readings can be seen with reference to Figure 8. The expected voltmeter readings as each successive probe is wet with electrolyte (the resistance of that probe and any farther out radially are short circuited and removed from the circuit) are tabulated in Figure 8 for an assumed source voltage of 10 volts (separate dry battery). Similar calculations could be made for a different source of voltage. For the preliminary laboratory evaluation, it was preferable to power the sensing elements from a separate dry cell because the auxiliary rectifier voltage was varied to adjust cell speed.

Except for manual operation, the sensing control circuit of Figure 7 is very similar to the automatic sensing control method of Figure 23, Appendix I.

Cell Operation

Figure 9 shows schematically the auxiliary equipment, principal electrical circuits, and measuring instruments used in the evaluation runs

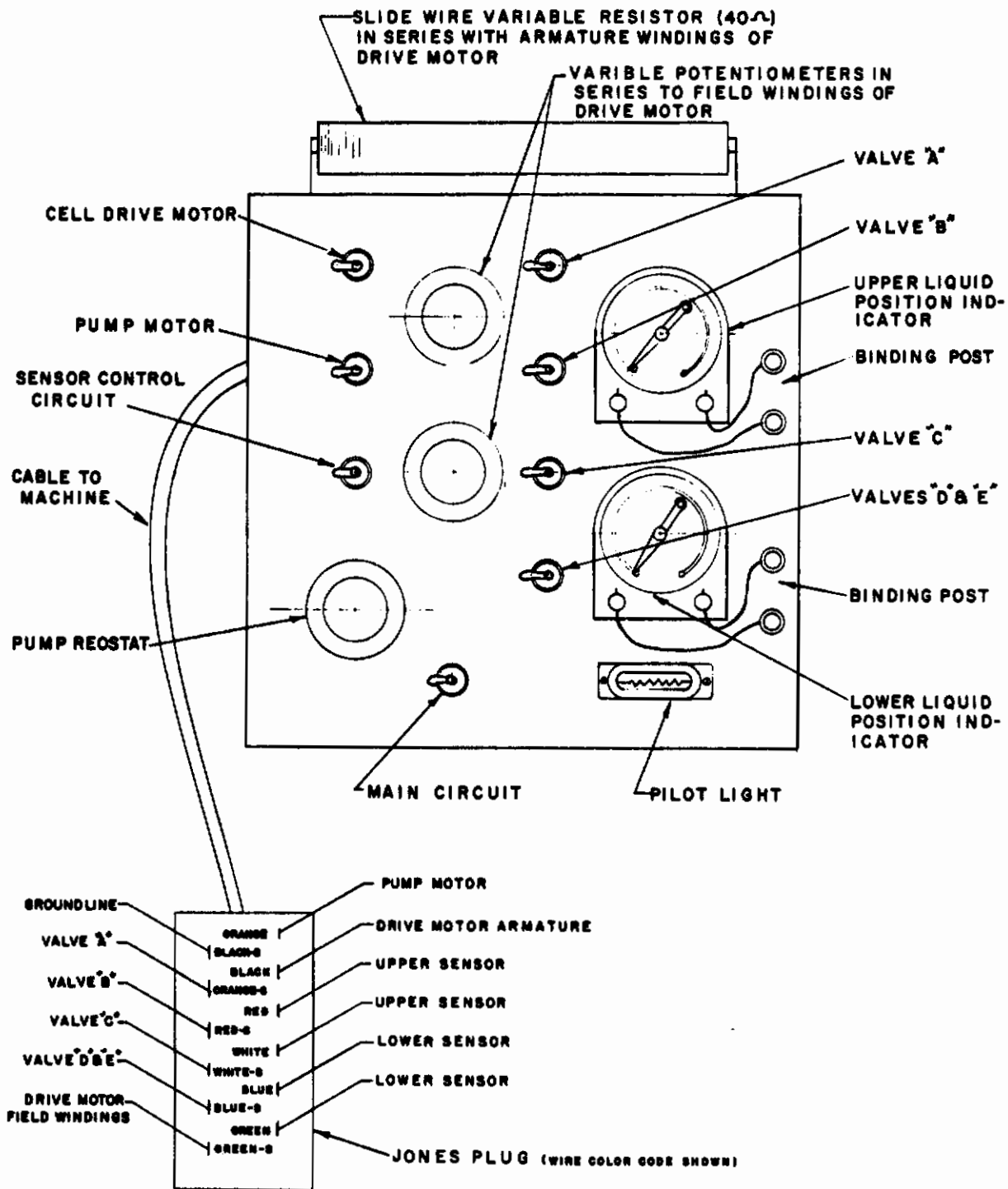


FIGURE 6. CONTROL PANEL USED FOR REMOTE MANUAL OPERATION OF THE LABORATORY MODEL

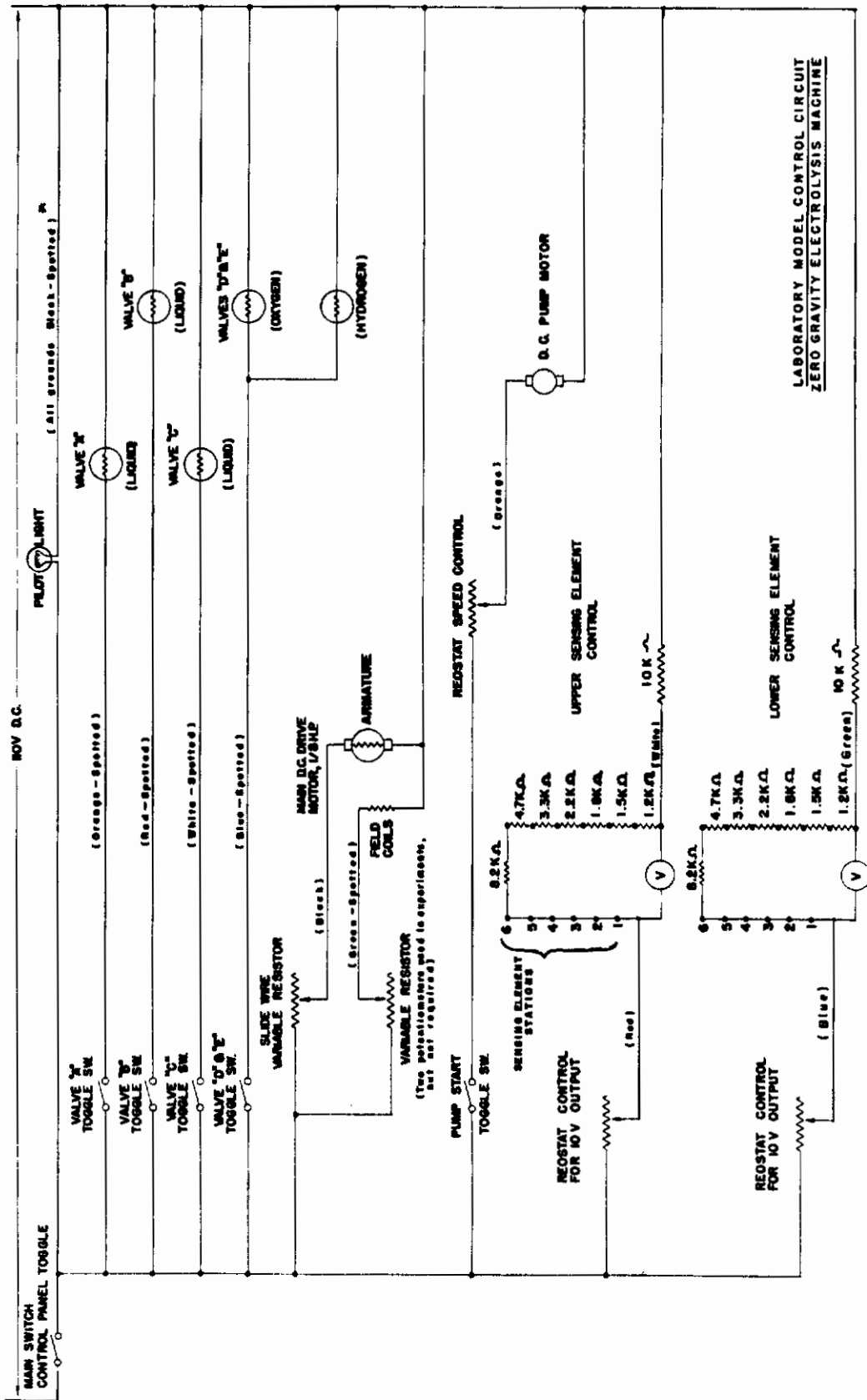


FIGURE 7. CONTROL CIRCUIT FOR LABORATORY MODEL

Contrails

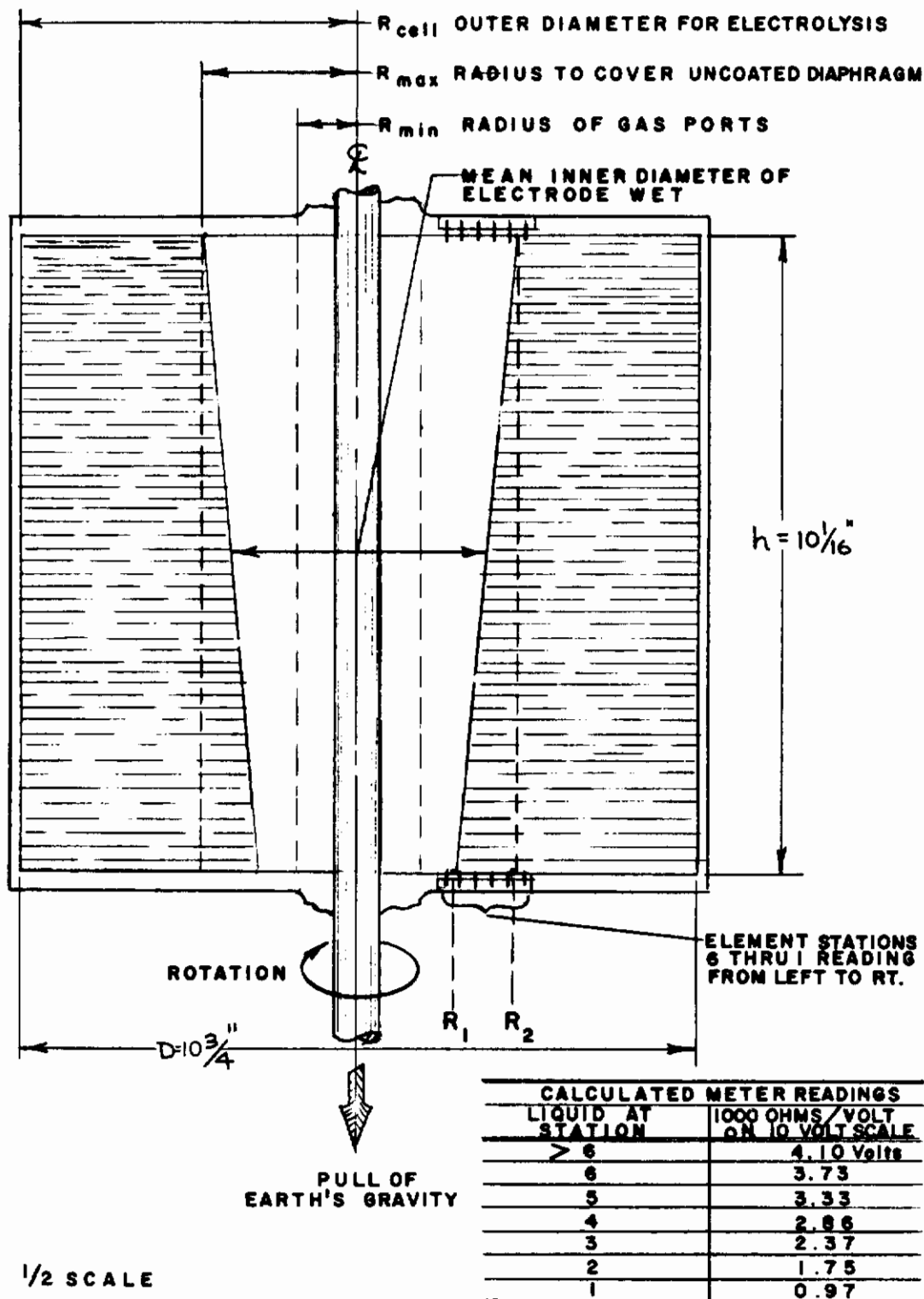


FIGURE 8. CROSS SECTION OF CELL SHOWING LIQUID VORTEX DURING ROTATION AND LIQUID-LEVEL SENSORS

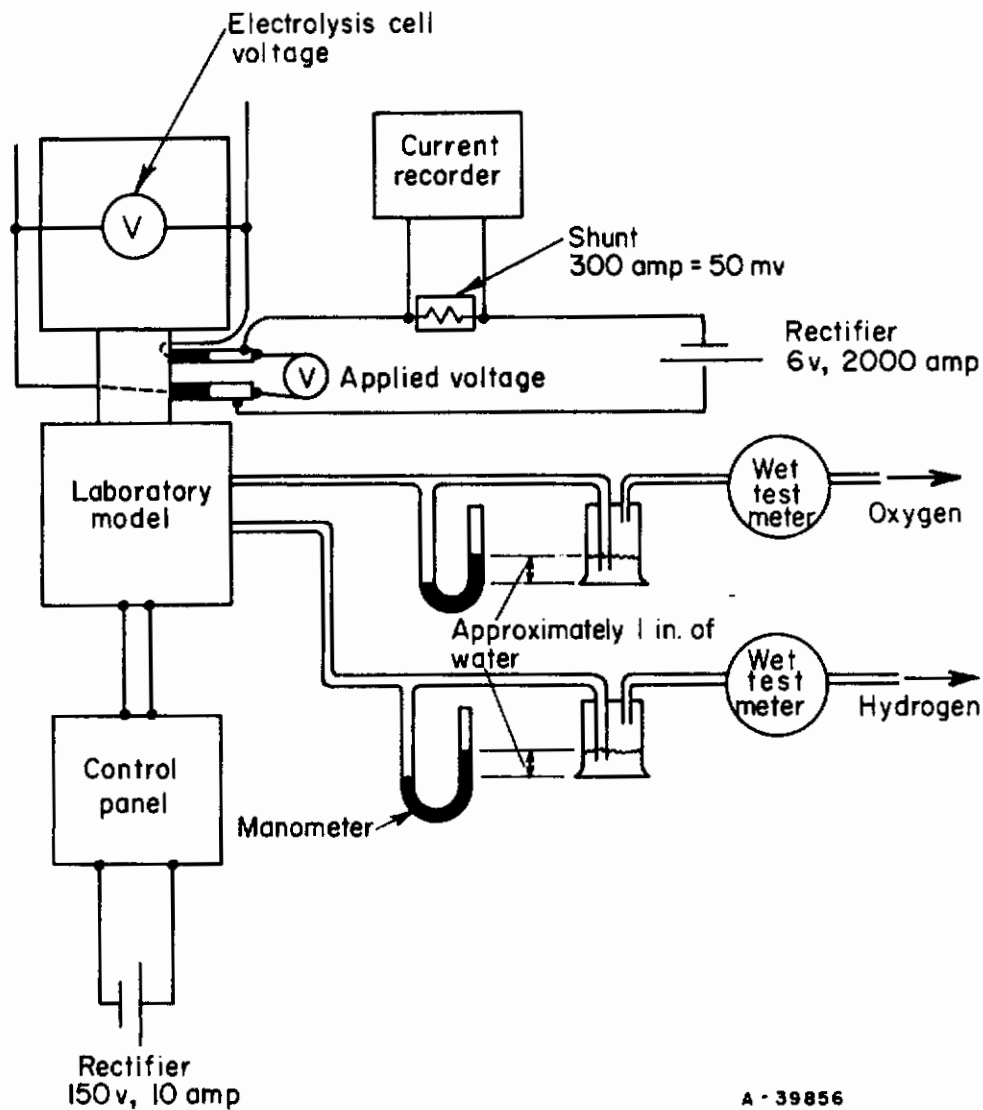


FIGURE 9. SCHEMATIC OF AUXILIARY EQUIPMENT USED IN EVALUATION OF LABORATORY MODEL ROTATING ELECTROLYSIS CELL

Contrails

of the laboratory model. The operation of the cell from startup to shutdown is described below for a typical run with reference to the control panel (Figure 6), control circuit (Figure 7), and Figure 10 showing the liquid valve settings for operational functions.

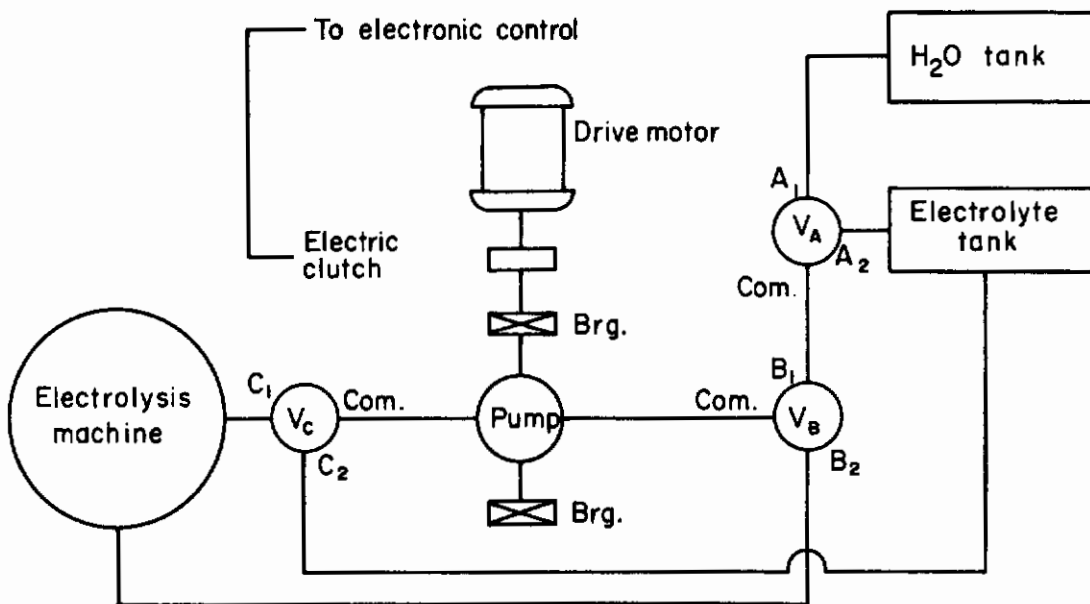
The auxiliary power rectifier was turned on first and set at 120 volts. An indicator light on the control panel indicated power available after the panel control switch was turned on. The motor field rheostats were set for minimum resistance (to allow maximum field current for high motor starting flux). When the motor is turned on the cell slowly rotates and gradually picks up speed. The high overload (about six times normal power) on the motor lasts for a few seconds until the cell speed picks up to 10-20 rpm. A slide-wire resistance in the armature circuit was used to manually increase resistance and prevent high current surge to the armature during startup while maintaining high voltage on the field circuit.

With the motor running at 1700 rpm, the cell rotates at 450 rpm through a belt-and-pulley speed reduction based on the initial design. Although the cell would probably operate satisfactorily at 400 rpm, a speed of 500 rpm was found necessary to obtain a liquid-level indication because of the location of the sensing probes. Higher speed from the motor was obtained by reducing the field current to the motor. Two rheostats added additional resistance and allowed a cell rotational speed of about 500 rpm.

With the cell rotating at 500 rpm and prior to filling with electrolyte, the liquid-level indicators were turned on by a switch. The indicators, which were voltmeters, were powered from a separate battery so that the initial reading was about 6.4 volts. Valve D was turned on so that gas within the cell would be displaced through exhaust lines as electrolyte filled the cell.

To fill the cell with electrolyte, Valve A was turned on (Valves B and C off). The pump was turned on and electrolyte was pumped from the reservoir (5-gallon bottle) to the cell. The pump motor speed was adjusted by a rheostat to control the filling rate. The maximum filling rate was about 1 liter per minute. After about 7 to 7-1/2 liters had entered the cell, the first indication was obtained on the lower level sensor. The voltage on the lower level indicator continued to drop as successive lower contacts were bridged with electrolyte (see Figure 8). At about 10-1/2 liters, the first contact on the upper sensor was bridged which indicated that the liquid-level diameter at the top was small enough to cover the central rubber disk on the asbestos diaphragm (less than 6-inch diameter). Since the liquid-level diameter at the bottom was about 3 inches and close to the gas ports, it was important to stop filling as soon as there was an indication on the top sensor.

After the cell was filled with electrolyte Valve A was turned off (Valves B and C off) in which position the cell would receive distilled water from the water reservoir when the pump was turned on. At the rated



Cycle of 3-Way Valves Used in Zero-Gravity Electrolysis Machine

VALVE FUNCTIONS	VALVE A		VALVE B		VALVE C	
	Port A ₁ Norm. Op.	Port A ₂ Norm. Cl.	Port B ₁ Norm. Op.	Port B ₂ Norm. Cl.	Port C ₁ Norm. Op.	Port C ₂ Norm. Cl.
Pump the electrolyte into electrolysis machine	Closed	Open	Open *	Closed *	Open *	Closed *
Pump H ₂ O into the electrolysis machine	Open *	Closed *	Open *	Closed *	Open *	Closed *
Pump electrolyte out of electrolysis machine	Open *	Closed *	Closed	Open	Closed	Open

* - Valve de-energized

FIGURE 10. LIQUID-VALVE AND PUMP ARRANGEMENT

design current of 254 amperes, the water consumption is only 85 ml per hour. Thus, the evaluation runs of maximum duration, 2-1/2 hours, were too short to need a water addition. In extended operation, the level sensors would indicate the need for water addition. Circuitry was designed to automatically add water on signal from the level sensor. However, the automatic circuitry was not built for the preliminary evaluation since manual addition of water could be made if needed.

At the end of the third evaluation run, 180 ml of water was added to the cell electrolyte to check out the system and verify that the valve and pump system operated satisfactorily for water addition.

At the end of an electrolysis run and prior to stopping the cell rotation, the electrolyte must be emptied from the cell or else electrolyte would enter the gas ports as the cell slowed down. To empty the cell, Valves A, B, and C were turned on and the pump started, thus, pumping electrolyte out of the cell and back to the electrolyte tank. With the cell empty, the rotation could be stopped.

A desirable procedure for stopping the cell rotation is to first reduce the field resistance to reduce the speed from 500 to 400 rpm and then turn off the motor switch. This procedure avoids the possibility of turning the cell off by the motor switch and leaving the high resistance in the field circuit. If the motor switch is turned on with high field resistance, there is insufficient starting flux, and abnormally high currents are drawn by the motor armature when the motor is not turning, which could burn out the motor or other components of the circuit.

Effect of External Gravity Field in Cell Design and Operation

Design Considerations. There are various methods of water electrolysis that can be designed to operate in spite of variations in the external gravity field. However, it would be technically inaccurate to say that they operate independent of gravity (i. e., not influenced by the external gravity field). There is no known or proposed method of electrolysis that is truly independent of gravity since all matter has mass and all mass is influenced by the earth's gravitational field. Therefore, in the design for any method that must operate over the range of 0 to 1 G consideration must be given to the effect of external gravity. It is possible that the effect of gravity on design is less in some electrolysis methods than others. The following discussion relates to the effect of external gravity field on the design and operation of the laboratory-model rotating cell and is generally applicable to any method involving use of rotation of a liquid to establish an artificial gravity field.

Contrails

Figure 8 (shown previously) is a scaled sketch of the electrolysis cell in cross section, showing the liquid vortex and gas core. The slope of the liquid-gas interface forming the gas core of the vortex is a function of the cell rotational speed and orientation in the external gravity field. The slope shown in Figure 8 is for a speed of about 500 rpm in the earth's gravity with the cell vertical (i. e. , axis of rotation parallel to direction that gravity is acting), which was the condition for the cell evaluation runs. Because of the requirement that the laboratory model operate in a 1-G field as well as at zero gravity, there were several cell design factors to be considered.

From reported experience^{(1)*} in industrial electrolytic production of hydrogen and oxygen, it is known that an asbestos diaphragm will effectively prevent mixing of the gas on either side of the diaphragm if the asbestos is maintained wet (i. e. , mixing does not occur below the electrolyte level). Above the electrolyte level, an ordinary asbestos diaphragm could dry out sufficiently to allow mixing of hydrogen and oxygen by diffusion through the asbestos.

The asbestos diaphragms for the laboratory model were made impervious by molding rubber on both sides of the inner 6 inches of diameter to prevent intermixing of gases in the gas-core region. The radial limit of the rubber-covered portion is shown by the dashed line in Figure 8 (at a radius of $R_{\max} = 3$ inches). The inner radial limit is the outer radius of the gas port in each polyethylene cell spacer shown by the dashed line in Figure 8 (at a radius of $R_{\min} = 1$ inch).

For satisfactory operation the liquid/gas interface, forming the gas core of the vortex or "liquid level", must be maintained between R_{\max} and R_{\min} so that the uncoated portion of the asbestos diaphragm is everywhere covered with electrolyte without electrolyte entering the gas port.

The choice of R_{\max} involves several interrelated factors in cell design all affecting the important criteria of weight, volume, and power. An increase in R_{\max} allows a lower speed of rotation in an external gravity field but a decrease in effective electrode area. The loss of central electrode area can be compensated by a larger diameter cell, which increases size and weight. If the electrode area loss is to be compensated by adding more cells, consideration must be given to the increase in cell height (h). An increase in h would require an increase in speed for the same radial limits ($R_{\max} - R_{\min}$).

The many factors involved in a choice of cell design could be related by equations or optimization curves. However, it is necessary to have quantitative data on the relationship between current density and electrolysis voltage, rotational speed and rotational power, etc. , for a particular size and weight of cell. Obtaining the quantitative data was an important objective of the evaluation of the laboratory model. Deriving optimization curves was beyond the scope of the present project.

*References are listed ahead of Appendix I.

Contrails

Effect of Cell Rotational Speed on Vortex Shape. With reference to the radii, R_1 and R_2 , indicated at the bottom of the cell in Figure 8, an equation can be derived for operation in a 1-G field to relate the actual minimum liquid radius (R_1) and the maximum liquid radius (R_2), the cell height (h) and the rotational speed (N) as follows:

Select a point, A, on the bottom cell surface that is at a radius R_2 . Equating vertical and radial forces at A gives:

$$\begin{aligned}h\rho &= \frac{\rho\omega^2}{g} \int_{R_1}^{R_2} R \, dR \\&= \frac{\rho\omega^2}{2g} [(R_2)^2 - (R_1)^2] \\h\rho &= \frac{1\rho}{2} \frac{(2\pi N)^2}{(60)^2} \frac{[(R_2)^2 - (R_1)^2]}{(32.2)(12)}\end{aligned}$$

$$h = 1.415 \times 10^{-5} N^2 [(R_2)^2 - (R_1)^2],$$

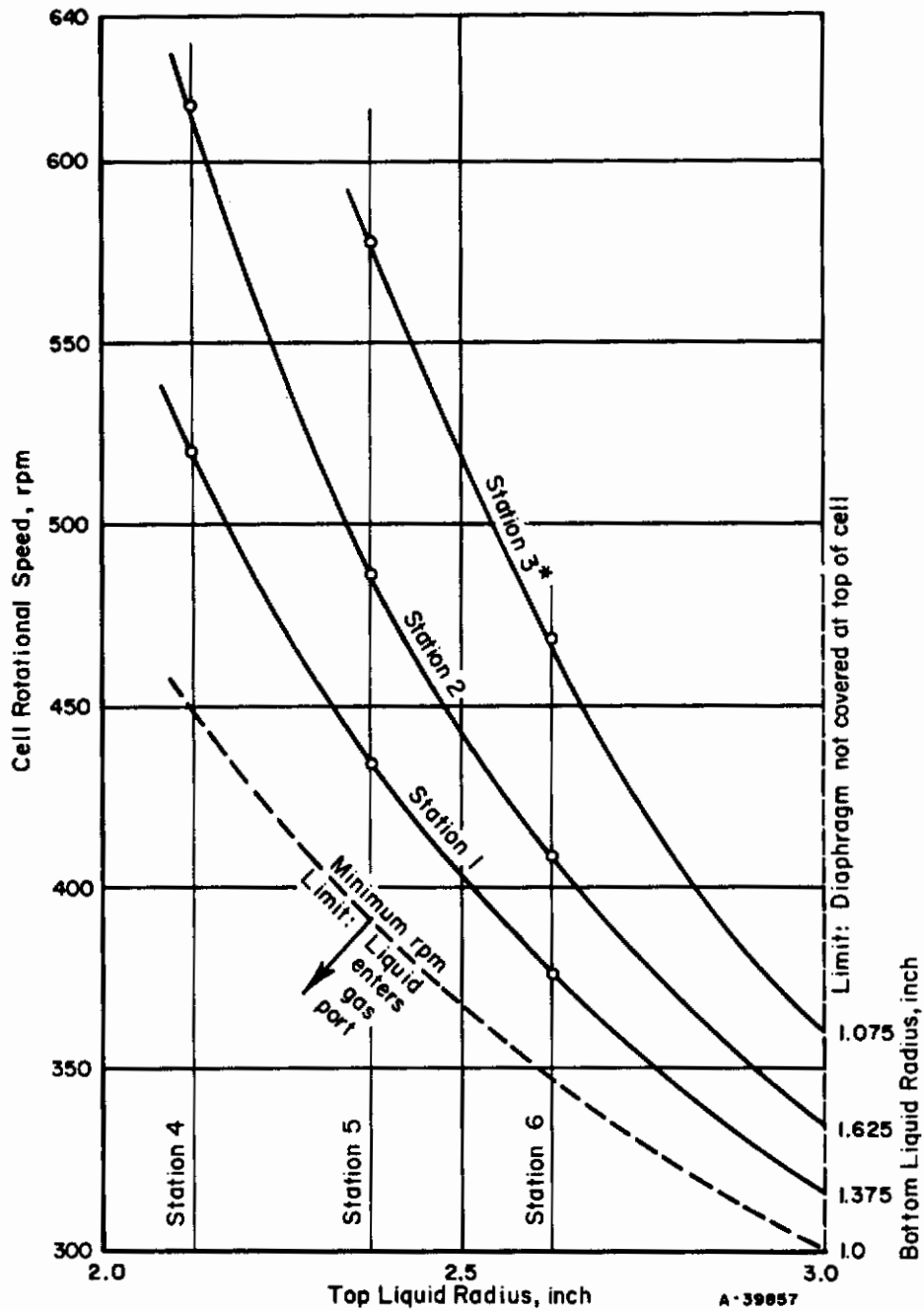
where $h = 10.0625$ inches (R in inches, N in rpm),

$$N = \sqrt{\frac{711000}{[(R_2)^2 - (R_1)^2]}}.$$

The above equation was used to construct the curves in Figure 11 over the range of interest for operating the model in the laboratory.

The circled points on the curve represent the rpm at which the liquid level just contacts both of the indicated probes on the bottom and top sensor which is an ideal situation. At best the sensing device tells only that the liquid level is somewhere between two adjacent probes. Thus, in practice when the cell is being filled with electrolyte, the speed is maintained high enough so that on the bottom sensor the liquid contacts the second probe radially out (Station 2, Figure 8) but not the first probe (Station 1).

Once the required cell speed is known and used, electrolyte is added until the top outer probe (Station 6) is bridged with electrolyte. Experience has indicated that about 500 rpm is required and about 10.5 liters of electrolyte. As the volume of electrolyte pumped in reaches 10.5 liters with no indication on the top sensor, it was found that if the pump was turned off, the liquid level quickly reaches equilibrium and contacts the outermost top sensor probe. Possibly, the pump pressure is sufficient to upset the delicate equilibrium that determines the gas-core shape.



* See Figure 5 for meaning of sensor station number

FIGURE 11. CALCULATED CELL SPEED FOR VARIOUS LIQUID LEVEL RADII

Speed to maintain vortex shape between limits of various combinations of probes on top and bottom sensors (basis: total liquid height in cell is 10-1/16 inches).

On the other hand, the cell rotational speed may increase slightly as the pumping is stopped. While electrolyte is being added to the cell, there is an additional load on the rotating motor because all the electrolyte that enters axially has to be accelerated to the cell rotational velocity.

As can be seen from Figure 11, the calculated minimum speed is 300 rpm for just covering the diaphragm at the top and not letting electrolyte in the gas port at the bottom. At 500 rpm, there is at least a safety factor of 1/2 inch radially at the top and bottom. A cell speed of 400 rpm might have been used if there were a more sensitive measure of liquid level at the top between 2-1/2- and 3-inch radius and at the bottom between 1- and 1-1/2-inch radius (i. e. , a greater number of closer spaced probes in the critical areas). Improvement in the method of detecting the liquid level would be desirable. A continuous radial level indicator rather than the stepwise indication as by probes would be preferred.

For operation of the laboratory model with the axis of rotation horizontal with respect to the earth's gravity field a different set of conditions define the speed at which a stable gas core is maintained. The detailed calculations are not of concern except to know that the rpm required for horizontal operation would be less than for vertical operation.

At zero gravity the gas core would be a cylinder and the shape of the cylinder would be independent of speed once formed. The minimum rotational speed required at zero gravity depends on the amount of artificial G-force needed to cause separation of the gas from the liquid and might be quite small and less than 1-G average. It has been assumed that for zero-gravity operation it would be desirable to have 1 G at the electrolyte/gas core interface (which is an average G-value higher than 1 in a radial direction through the electrolyte) and for the laboratory model 140 rpm would be required.

Effect of Vortex Shape on Electrode Area. Throughout this report, the effective electrode area has been assumed to be equal to the uncoated diaphragm area.

$$A_e = \pi [(5.375)^2 - (3)^2] \frac{16}{144} = 7 \text{ ft}^2.$$

As can be seen in Figure 8, the maximum wetted electrode area is greater on the bottom plate. If the mean inner diameter of wetted electrode were used, the total wetted electrode area would be 8.7 ft². However, with the close electrode spacing used, the rubber-covered portion of the asbestos probably acted as a partial shield at the current densities used. The true electrode area might be between 7 and 8.7 ft², but for simplicity the current densities were calculated on the basis of uncoated diaphragm area and any error involved would be less than normally associated with calculations that do not take into account electrode roughness.

There is one other problem that might be encountered at higher current densities than used thus far which relates to the difference in wetted electrode area from top to the bottom of the cell. The highest current density and highest gas production rate occur in the lowest cell which has the least "freeboard" if there is any tendency toward foaming. Any such problem would be greatly minimized in a bipolar cell. In a bipolar cell arrangement, the current and thus the gas production per cell is the same independent of the true electrode area per cell. There might be variations in cell voltage from cell to cell in a bipolar arrangement but this would not affect operation.

Hydrogen and Oxygen Production

Figure 12 is a record of the hydrogen and oxygen evolution during the first evaluation run at an average current of 255 amperes. The gases as measured with a wet-test meter were assumed to be saturated with water vapor at the temperature of measurement. The corrected rates for dry gas at standard conditions is compared with the expected rate based on the current in Table 4. The indicated per cent efficiency for Run 1 is within the estimated accuracy of measurement ($\pm 2\%$) for current and gas volume.

The steady gas-evolution rate indicated in Figure 12 by the straight line through the measured gas volumes was typical of all runs although the slope of the line was not the expected value for 100 per cent efficiency. Because of the constant slope, it is believed that the inaccuracy of the wet-test meters (which were not calibrated prior to the runs) is the cause of the indicated low efficiency. This is the only explanation available at the present time for the low oxygen efficiency of Runs 2 and 3 as shown in Table 4. Different wet-test meters on the hydrogen and oxygen line were used in Runs 2 and 3 than used in Run 1.

No chemical analysis of gas purity was made in the first three evaluation runs which were primarily concerned with measurements of cell power requirements.

Power Requirements

Mechanical-Power Consumption

The mechanical power required to rotate the cell is an important factor since it is the additional power required to permit electrolysis and effect a liquid-gas separation under zero-gravity conditions. The rotational power is a factor that must be considered in comparing the laboratory model with other proposed methods of zero-gravity electrolysis (see Appendix II). For example, a method which accomplishes liquid-gas

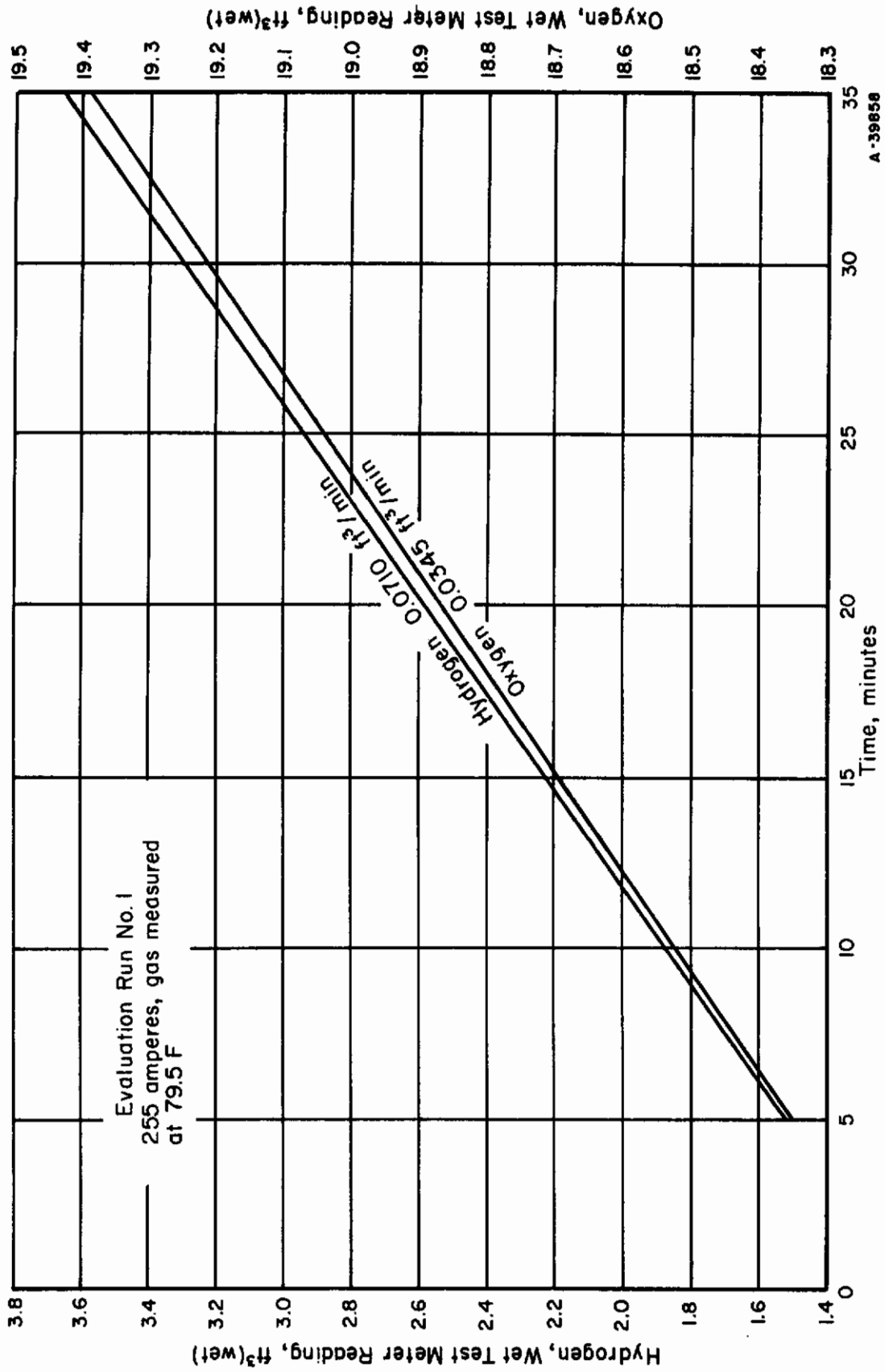


FIGURE 12. HYDROGEN AND OXYGEN GAS-COLLECTION RATE

TABLE 4. HYDROGEN AND OXYGEN EVOLUTION RATES
IN EVALUATION RUNS OF LABORATORY-
MODEL ROTATING ELECTROLYSIS CELL

	Evaluation Run		
	1	2	3
Gas Measurement Temp, F	79.5	83.5	85
Average Current, amp	255	251	259
Measured Rate (Wet)			
H ₂ , ft ³ /min	0.0710	0.0726	0.0713
O ₂ , ft ³ /min	0.0345	0.0317	0.0284
Corrected Rate (Dry at 32 F)			
H ₂ , ft ³ /min	0.0626	0.0633	0.0618
O ₂ , ft ³ /min	0.0304	0.0277	0.0247
Theoretical Rate for Current			
H ₂ , ft ³ /min	0.0629	0.0620	0.0632
O ₂ , ft ³ /min	0.0314	0.0310	0.0316
Efficiency, per cent			
H ₂	99.6	102.1	97.8
O ₂	96.8	89.4	78.2

Contrails

separation in a separate unit would require additional power for pumps to continually recirculate the electrolyte. Other methods which have no moving parts might pay a greater penalty in the form of higher electrolysis power requirements.

Preliminary estimates had indicated a low power consumption to overcome the frictional forces of bearings, seals, windage, etc., to maintain rotational speeds sufficient for operation in an external zero-gravity field. Although, not readily apparent, the mechanical-power consumption increases with the external G-field because of the higher rotational speed needed. As discussed in the preceding section, the rotational speed depends on the electrolysis cell design. Frictional drag of brushes transferring current is difficult to predict.

The quantitative data on mechanical-power consumption obtained with the laboratory model plus the discussion and interpretation of the results which follow are intended to indicate the design factors involved and provide a basis for estimation of optimum design.

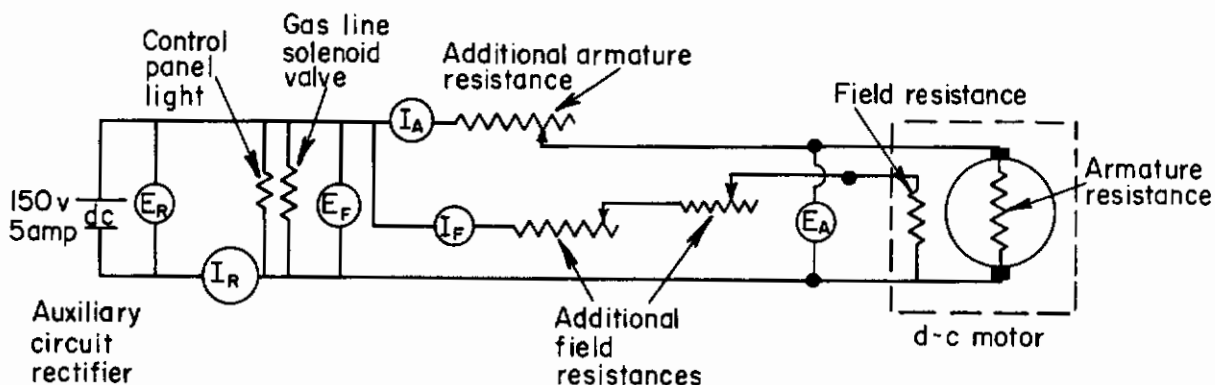
In order to measure the rotational power, the auxiliary equipment was powered by a separate rectifier from that used to supply electrolysis power. The auxiliary rectifier powered the motor, pump, solenoid valves, and control panel. To distinguish the power supplied to the motor to rotate the cell, the voltage and amperage supplied to both the armature and field circuit were measured separately.

In continuous operation the total power output of the rectifier was slightly higher by the amount required to energize the solenoid valves that directed the gas flow. (For long periods of operation and to increase solenoid life, gas should be taken from the valve position that is "normally open" when de-energized; the valve would be energized for gas bypass for only brief periods during startup.)

The total rectifier output was also higher by the power consumed in the slide-wire resistance used in the armature circuit to decrease the armature voltage for lower than rated motor speed. The power consumed in the slide-wire resistance was not included in calculating the total motor power. For the evaluation runs at high rotational speed, no external armature resistance was used.

Table 5 shows the wiring diagram and measurement points for the motor circuit. The tabulated values for the three runs are the values toward the end of the run to correspond with the other power measurements shown previously in Table 1. The total power shown in Table 5 corresponds to the total motor power shown in Table 1 except that in Table 1 an estimate was made of the proportion of the total power consumption due to brush drag and that due to seals, bearings, etc. Table 1 indicates more clearly that the general reduction in mechanical-power consumption in evaluation

**TABLE 5. CELL ROTATIONAL POWER CONSUMPTION,
MOTOR CIRCUITRY AND MEASUREMENTS**



	Evaluation Run		
	1	2	3
Cell Rotational Speed, rpm	480	510	520
Rectifier volts (E_R)	112	120	120
Rectifier amperes (I_R)	1.16	0.9	1.10
Armature Circuit			
Volts (E_A)	113	120	120
Amperes (I_A)	0.85	0.65	0.7
Watts	96	78	84
Field Circuit			
Volts (E_F)	113	120	120
Amperes (I_F)	0.07	0.08	0.08
Watts	7.9	9.6	9.6
Total Mechanical Power	103.9	87.6	93.6

Runs 2 and 3 compared to 1 is the result of reduction in brush drag. The spring tension on the brushes was probably reduced in the course of the work done on the brushes after Run 1.

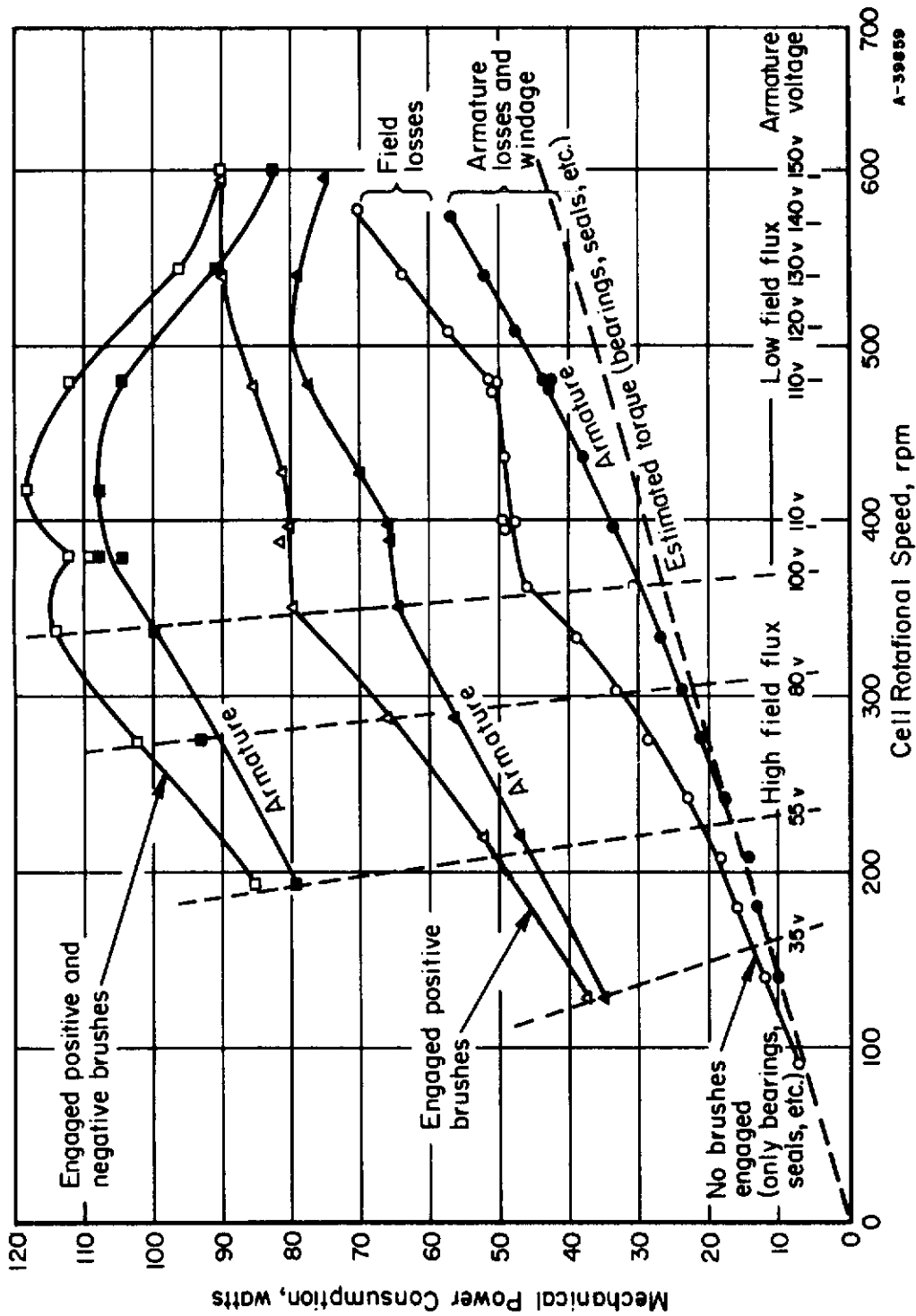
The relation between mechanical-power consumption and rotational speed was desired for forecasts of total power consumption when actual zero-gravity conditions would allow reduction in rotational speed. Since the effect of the earth's gravity field prevented operation at low speed while electrolysis was proceeding, measurements of power consumption were made with the cell empty. The effect of the lighter cell (minus electrolyte) on power requirements for maintaining rotation should be negligible.

Figure 13 shows typical curves of motor power consumption that were obtained shortly after the first evaluation run. The first series of measurements at various cell speeds were made without any of the brushes in contact (by removing the tensioning spring). Thus, with brush drag excluded, power losses were caused by drag of the bearings, seals, rotary swivel joint, belt losses, windage, and electrical losses in the motor and leads. The second series of measurements was made with only the positive set of six brushes engaged. The third series of measurements were made with both positive and negative brushes engaged.

The method of making a series of measurements was as follows:

- (1) Set armature voltage at 110 volts and measure speed of rotation with tachometer and read voltage and amperage for the rectifier, armature, and field circuits
- (2) Increase resistance in armature circuit to reduce armature voltage to 100 volts and make measurements
- (3) Thereafter, reduce rectifier voltage in increments and make measurements down to the lowest stable rotational speed attainable
- (4) Return to 110 volts and conditions of (1) above
- (5) Increase resistance in field circuit with one potentiometer to increase speed
- (6) Further increase field resistance with second potentiometer
- (7) Increase rectifier voltage in increments to obtain higher speeds as mentioned previously.

The readings on the rectifier were not used to calculate the total power shown in Figure 13. Referring to the circuitry in Table 5, the small power loss in the added external armature resistance was not included but the



A-39859

FIGURE 13. MEASURED MOTOR POWER CONSUMPTION FOR ROTATION OF LABORATORY MODEL AT VARIOUS SPEEDS

Absolute values of total power at any speed depend on brush tensioning.

Contrails

minor power loss in the added field resistance was included. The armature power was obtained from the product of armature voltage (E_A) and armature current (I_A). The product of the field voltage (E_F) and field current (I_F) was the power consumed in the field circuit which was added to the armature power to obtain the total power consumed by the motor.

The reduction in power consumption obtained by increasing the field resistance and thus decreasing the field current is evident in Figure 13. High flux is not needed to maintain rotation. However, high flux is desirable for starting the motor although the time required to come up to operating speed does not appear to be important. Since field control is an accepted procedure of speed regulation for d-c motors, it would appear desirable to provide for reduction of flux at operating speed to obtain whatever savings in power can be realized while maintaining stable speed control. Since the total power used at various speeds reflects the more or less efficient use of field power, the armature power reflects better the power required to overcome the frictional forces opposing rotation. For the data obtained with no brushes engaged, the deviation of the armature power data from a straight line at higher speeds is believed to represent essentially the motor inefficiency (i. e., I^2R losses in the armature) and windage (air resistance). The dashed straight line is drawn to represent the estimated torque which is about 0.5 ft-lb* excluding the brushes and is essentially the frictional force opposing rotation resulting from the bearings, seals, swivel joint, and belt.

In the design of the brush and slip ring assembly on the laboratory model, the brushes rotate and are subjected to various centrifugal forces as the speed changes. The tension in the retaining spring was adjusted to hold the brushes in light contact at the designed operating speed. Thus, the tension would be too high at less than design speed and possibly too low at greater than design speed.

The laboratory model was originally designed to operate at 400 rpm. The later increase to 500 rpm required an adjustment of spring tension. This was difficult to do accurately and the force would not be stable as the brushes wear.

As shown in Figure 13, a plot of power versus speed indicates the speed at which the brushes begin to pull away from the slip ring. The data for the particular experiment in Figure 13 indicate that the tension on the negative brushes is less than on the positive brushes. At 500 rpm, both brush assemblies are still contacting the slip ring (although possibly not all brushes in each assembly). At 600 rpm the negative brushes appear to have pulled away. At about 650 rpm it would appear that all brushes would have lost contact with the slip ring.

$$*Torque = \frac{44 \text{ watts}}{746 \text{ watts}} \left| \frac{33,000 \text{ ft-lb}}{600 \text{ rpm } 2\pi} \right| = 0.5 \text{ ft-lb (0.5 lb at 1-ft radius).}$$

Contrails

Figure 13 was used to make estimates of the proportion of the power consumed by brush drag compared to bearings, seals, etc. The total power with no brushes engaged was read from Figure 13 for the particular speed of rotation used in the evaluation run. The power consumption due to brush drag was obtained by difference from the actual mechanical power consumption measured in the evaluation run.

Figure 13 cannot be used directly to estimate power consumption at various rotational speeds since the brush tension was optimum for only one speed. Thus, the total power consumption at lower speeds indicated in Figure 13 is much too high and other means of arriving at estimates were used.

The optimum brush tension for minimum power consumption requires consideration of both brush drag and brush contact drop (to be discussed in a later section). Table 1 showed that the lowest combination of power loss for brush drag and brush contact drop was 92 watts obtained in Run 3. Thus, at least adequate brush pressure was obtained when the brush drag power consumption was no more than 34 watts at 520 rpm.

The curve in Figure 14, which is an estimate of total mechanical-power consumption at various speeds to be expected in an optimum design, indirectly shows the effect of G-field magnitude and orientation with respect to the cell rotational axis. Figure 14 rather than Figure 11 should be used for extrapolation of data obtained in the cell evaluation runs to other cells speeds (i. e. , G-fields).

The assumptions used in constructing Figure 14 are as follows:

- (1) At 520 rpm, the estimated torque to overcome friction (bearings, seal, etc.) and windage is 38 watts.
- (2) The cell drive would have a pulley ratio such that 520 rpm could be obtained at rated motor speed rather than 450 rpm. With the motor at rated speed of 1750 rpm (corresponds to 400 rpm in Figure 13), only 12-1/2 watts would be required in excess of the power indicated by the torque.
- (3) At 520 rpm, as in Evaluation Run 3, the maximum brush drag is 34 watts and would vary linearly with rpm for optimum tensioning.

Thus, the power (P_M) in watts is:

$$P_M = k (\text{rpm}) = \left(\frac{38\text{w} + 12-1/2\text{w} + 34\text{w}}{520 \text{ rpm}} \right) (\text{rpm})$$

$$P_M = 0.16 (\text{rpm}) .$$

The above estimated relationship is shown in Figure 14.

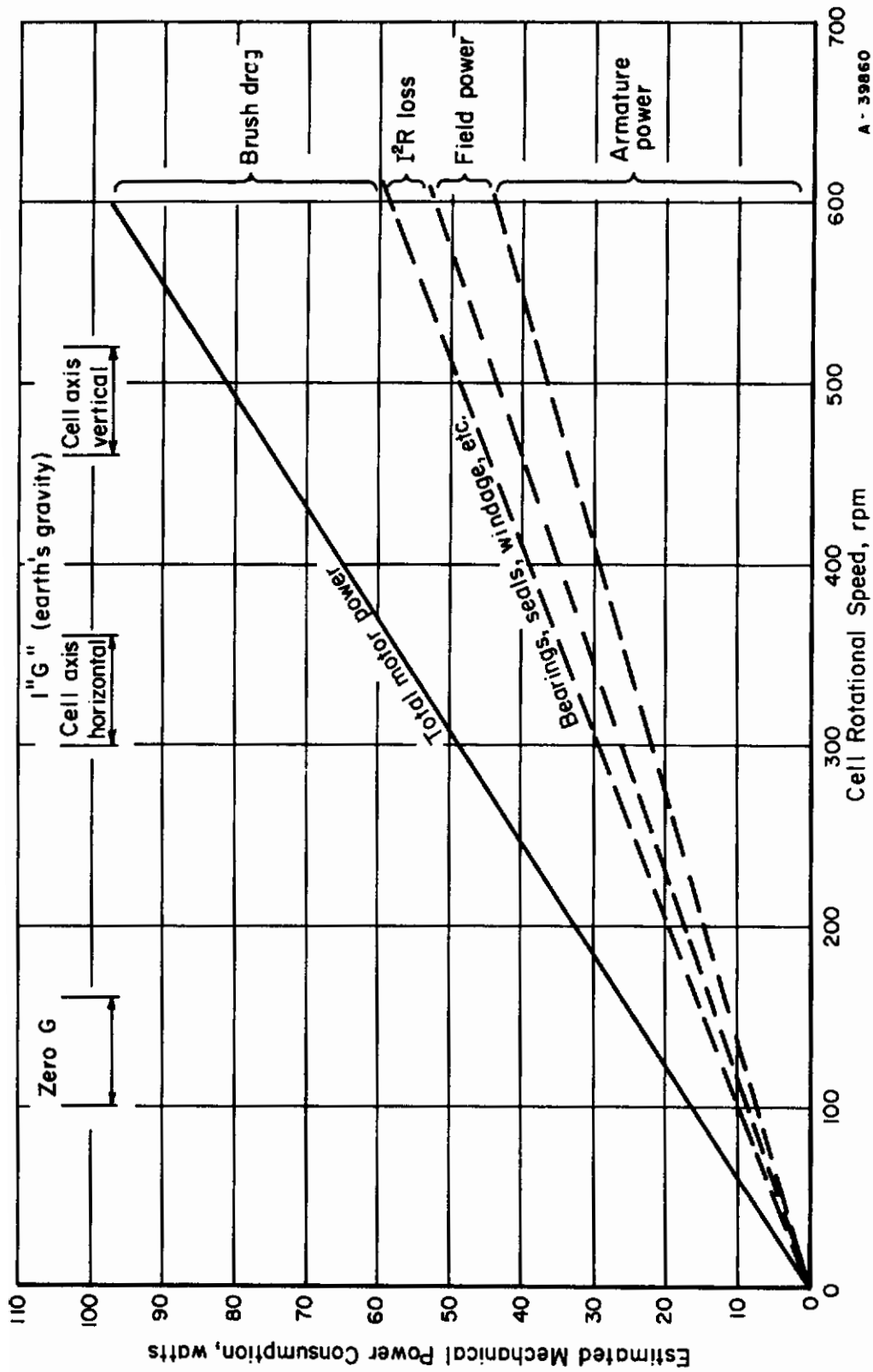


FIGURE 14. PREDICTED MECHANICAL POWER CONSUMPTION AT VARIOUS CELL ROTATIONAL SPEEDS

Assuming constant brush pressure for laboratory model, using 1/8-hp motor, low field flux, and voltage control of speed below 520 rpm.

Electrical Power Consumption

Voltage Measurement. That portion of the total power consumption which is due to electrical contact resistances was measured and treated separately because the power loss relates to design considerations and does not affect the electrolysis results.

Losses in the rectifier and leads supplying power to the laboratory model were not considered a concern of this project and were not measured. The laboratory model is provided with two copper connectors into which are inserted the positive and negative cables from the rectifier. A voltmeter was connected directly to the copper connectors. Any electrical contact loss between the cables and the connector was not measured. Thus, only the potential difference existing between the anode and cathode connectors was measured and is termed the "applied voltage".

The difference between the applied voltage and the electrolysis cell voltage is due to contact losses between the brushes and the copper collector ring on which they ride plus any losses associated with the conduction of current through the brushes. The latter is small compared to the contact losses. For the graphite brushes with a resistivity of 0.00035 ohm-inch, at 254 amperes for the cell (42.2 amp per brush, 5/8 inch x 1 inch x 1-inch long) the voltage drop through each brush is only 0.02 volt compared to the contact drop of about 0.87 volt.

The electrolysis cell voltage was measured across the copper distributor bars which are connected to the collector ring. Any voltage losses through distributor bar and electrodes and their contacts were negligible and are included in the electrolysis cell voltage by nature of the location of the measurement of electrolysis cell voltage.

In order to measure the electrolysis cell voltage while the cell was rotating, the voltmeter leads were connected to the control slip ring leads previously used for the bottom liquid-level probe. [With sufficient rotational speed (about 500 rpm) to assure that liquid would not enter the gas ports, filling of the cell with electrolyte was controlled by the upper liquid-level probe and the bottom probes were not needed.]

Brush Contact Drop

Following Run 1, data for a curve of current versus electrolysis cell voltage was obtained (shown later in Figure 17). The voltage difference between the applied voltage and the electrolysis cell voltage which is essentially the brush contact drop is shown in Figure 15 for various currents. The brush contact drop as normally expressed includes both voltage drop at the positive, plus that at the negative brush. The apparent straight-line

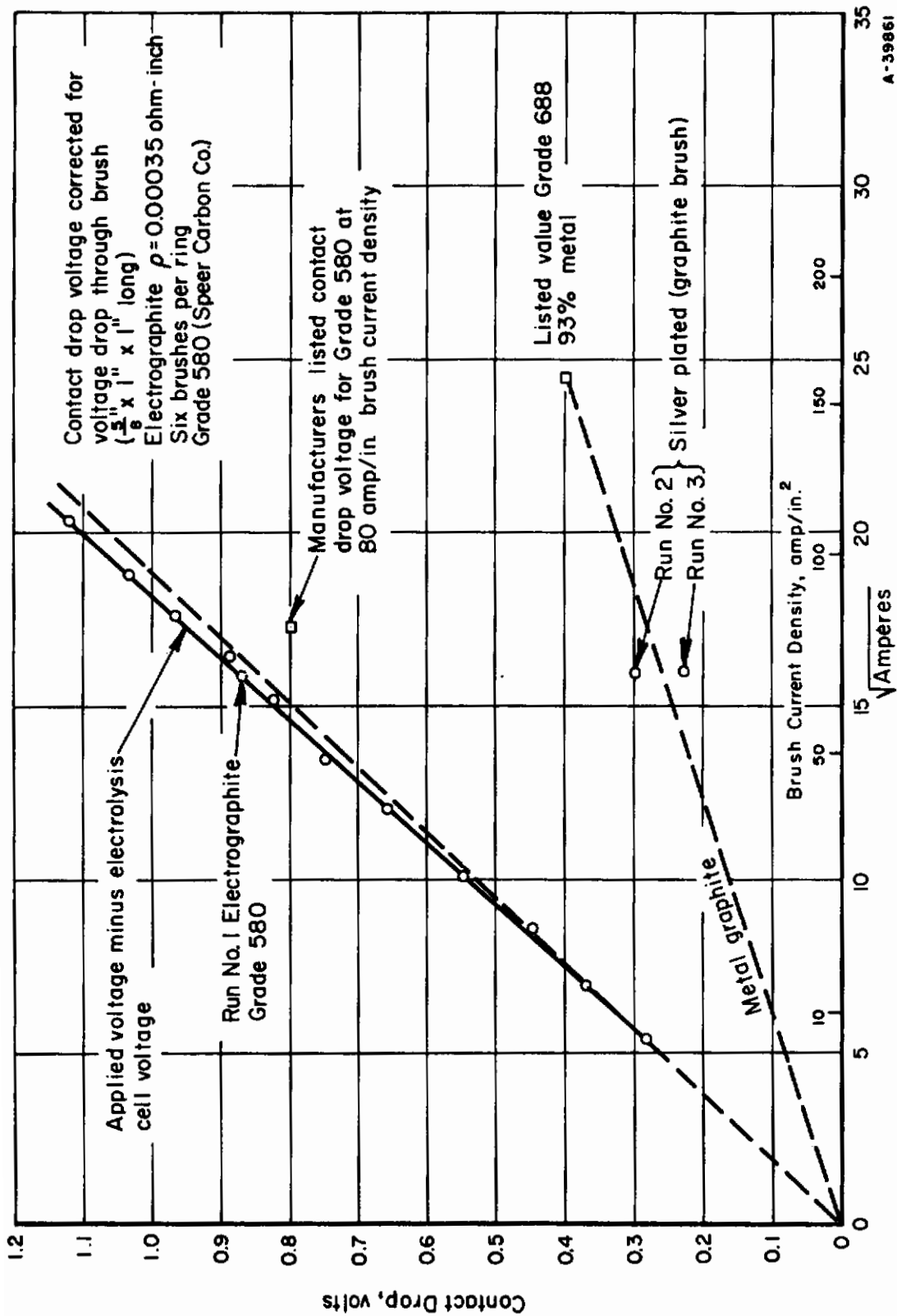


FIGURE 15. BRUSH CONTACT DROP VOLTAGE RELATED TO CURRENT, BRUSH MATERIAL, AND BRUSH CURRENT DENSITY

Contrails

relation between contact-drop voltage and the square root of the current was not expected. The physical significance of the relationship expressed by the following equation is not fully understood:

$$E_E = 0.056\sqrt{I} + k ,$$

where

E_E = applied voltage minus electrolysis cell voltage

I = cell current.

The value of k appears related to the voltage drop through each brush. For example, the following equation could describe the observed values:

$$E_E = 0.056\sqrt{I} - \left(\rho \frac{L}{A}\right)I ,$$

where

ρ = resistivity of brush material, ohm-inch (0.00035 ohm-inch for Grade 580 electrographite used)

L = length of brush, inch

A = cross-sectional area of brush, in.²

The dashed line of Figure 15 through the origin is believed to be the brush contact drop voltage:

$$E_{BC} = 0.053\sqrt{I} .$$

The contact drop voltage can be related to the brush current density by the following relation:

$$E_{BC} = 0.053\sqrt{nAI_B} ,$$

where

I_B = brush current density, amp/in.²

A = cross-sectional area of brush, in.²

n = number of brushes per collector ring.

The observed value of contact drop voltage checks fairly closely with the manufacturers (Speer Carbon Co.) listed value at 80 amp/in.² brush current density for the grade of brush used. The assumption was made that the relationship observed in Figure 15 would hold for other brush materials. Thus, the manufacturer's listed value of contact drop voltage for a metal graphite brush [Grade 688, 93% metal (Cu)] is 0.4 volt at 160 amp/in.² and is plotted in Figure 15 with a straight line (dashed) drawn through the origin.

Contrails

Because there was insufficient time to order new brushes, the graphite brushes were electroplated with silver (about 0.001 inch). The reduced contact voltage drop obtained with the silver-plated brushes in subsequent evaluation runs (Runs 2 and 3) is shown in Figure 15.

As mentioned previously, the physical significance of the relation shown in Figure 15 is not known. The observed relation to brush current density might be questioned since the data with graphite brushes was obtained early in the evaluation when the laboratory model had not run sufficiently long for the brushes to wear in. The actual contact area of the brushes with the collector ring was less than 25 per cent of the brush cross-sectional area (judging from the worn area). The contact area was increased by abrading the brushes with emery paper to fit the contour of the collector ring better. The cell was then rotated continuously for about 8 hours. However, this effort did not appear to decrease the contact drop.

A significant drop in contact voltage was obtained only when the brushes were silver plated. (Only three of the six brushes on each collector ring were silver plated. The points plotted for Runs 2 and 3 in Figure 15 correspond to the cell current used (254 amperes); the brush current density on the silver-plated brushes would be about twice that shown.)

The brush contact voltage drop appears to be an important source of power consumption only when the laboratory model is run with parallel-connected electrolysis cells as in the experimental evaluation. If the laboratory model were converted to a bipolar cell (series electrical connection) the brush contact becomes a negligible source of power consumption. For example, the 485 watts of electrolysis power used in Run 3 (Table 1) was supplied as 254 amperes at 1.91 volts.

For a bipolar cell, the 485 watts would be supplied as 15.85 amperes at 30.6 volts (assuming 16 cells in each case). From Figure 15, it is estimated that the brush contact voltage drop would be less than 0.08 volt (metal-graphite brushes). The power loss at the brushes would be less than 1.3 watts (0.08 volt x 15.85 amp) compared to the 58.4 watts for the parallel-connected cell.

For a bipolar cell arrangement, fewer (or smaller) brushes might be used to achieve an optimum relation between electrical-power consumption from contact drop and mechanical-power consumption from the rotational drag of the brushes. Referring to Table 1, Run 3, it is estimated that 1/6 as many brushes could be used for a bipolar cell (one on each collector ring). This would reduce the brush drag loss from 33 watts to 5.5 watts while increasing the brush contact voltage drop from 0.08 to 0.18 volt (Figure 15) and the contact drop power loss from 1.3 watts to 2.8 watts.

By optimization of the number of brushes for the type of cell to be operated it is estimated that the sum of the brush power losses (brush

contact + brush drag) for a bipolar cell would be 8.3 watts compared to 92 watts measured for the parallel connection of the laboratory model during the experimental evaluation.

Whereas a bipolar cell arrangement appears to be the more economical of power, there may be other considerations in the over-all system integration for space application that would dictate the use of a parallel-connected cell (i. e. , a low-voltage power source).

In a parallel connected cell where brush contact drop is important there are several design considerations. Adding more brushes to reduce the brush current density might be desirable depending on the relation between the cell current and the rotational speed. Silver-graphite brushes could be obtained, probably with any proportion of silver to graphite. However, while the increased metal content would tend to reduce brush contact voltage drop, the life of the brushes would decrease as the metal content is increased. The latter factor might be important for the objective of minimum maintenance and high reliability for long periods of operation. No specific information was readily available on brush life.

Electrolysis Power Consumption

Industrial Cell Comparison. Figure 16 shows that the cell voltage obtained with the laboratory model is 0.1 to 0.2 volt less than reported⁽²⁾ for industrial electrolysis cells for producing hydrogen and oxygen. At a current density of 36.6 amp/ft² (254 amperes design current for a 2-man cell), the cell voltage of 1.91 volts at 111 F represents the lowest value demonstrated at the end of the longest continuous run of 2-1/2 hours.

No temperature was specified for the values of cell voltage reported for industrial cells. However, it is known that such cells operate at temperatures greater than 111 F. Higher temperature can lower the cell voltage considerably as will be shown later.

It is difficult to obtain representative values of cell voltage at a meaningful current density for comparison with the laboratory model. Whereas the current density based on the apparent electrode area might be similar most industrial cells involve special electrode designs of increased true area and lower true current density which gives a lower cell voltage.

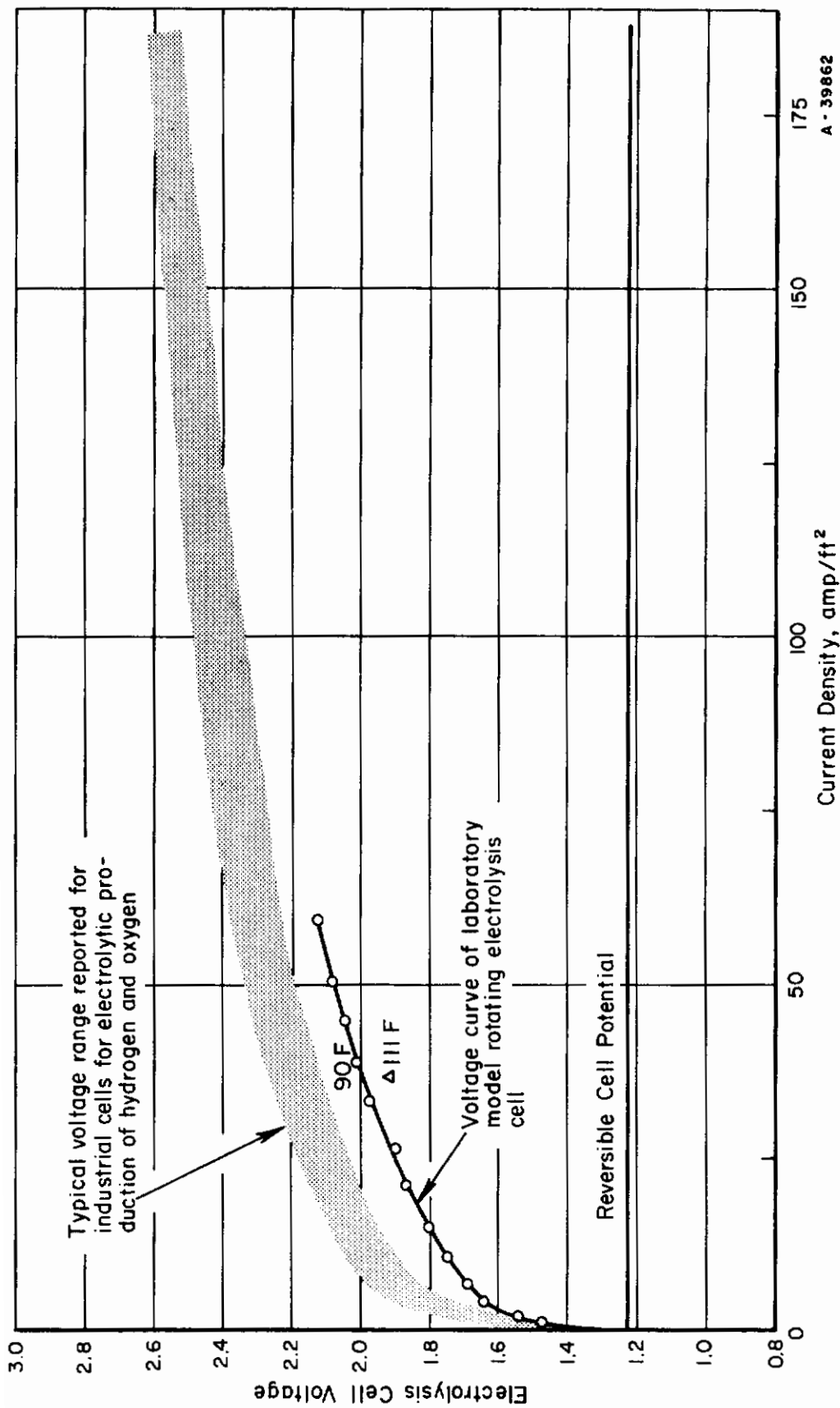


FIGURE 16. COMPARISON OF CELL VOLTAGE OBTAINED WITH LABORATORY MODEL WITH INDUSTRIAL CELLS

Typical voltage range for industrial cells from data of Bowen (see text for reference).

Some examples of industrial cells are:

Levin (or Electrolab) Cell⁽³⁾

2.7 ft³; 145 lb; 250 amperes, about 24 amp/ft²

Trail Cell⁽⁴⁾

28 ft³; 10,000 amperes; apparent current density, 67 amp/ft²;
28% KOH; 167 F; 2.25 volts

Stuart Cell⁽⁵⁾

15 ft³; 3000 amperes; apparent current density, 94 amp/ft²;
28% KOH; 170 F; 2.02 volts

Zdansky-Lonza⁽⁶⁾ (Bipolar pressure cell)

425 psig; 212 F; 1.78 volts, about 50-100 amp/ft² of apparent
area (wire gauze electrodes in front of waffle-shaped plate)

Cell Voltage Characteristics. Figure 17 is a curve of the electrolysis cell voltage versus the log of the current density obtained after Run 1 by starting at 410 amperes and progressively reducing the current at 1-minute intervals. The curve is typical of electrolytic operations wherein the cell voltage follows the general equation:

$$E = E_0 + k \log \left(\frac{I}{A} \right) + \rho L \left(\frac{I}{A} \right) ,$$

where

E = cell voltage

E₀ = reversible cell potential

k = constant (approximately the sum of the Tafel constants for hydrogen overvoltage and oxygen overvoltage at low current density)

I = cell current, amp

A = electrode area, in.²

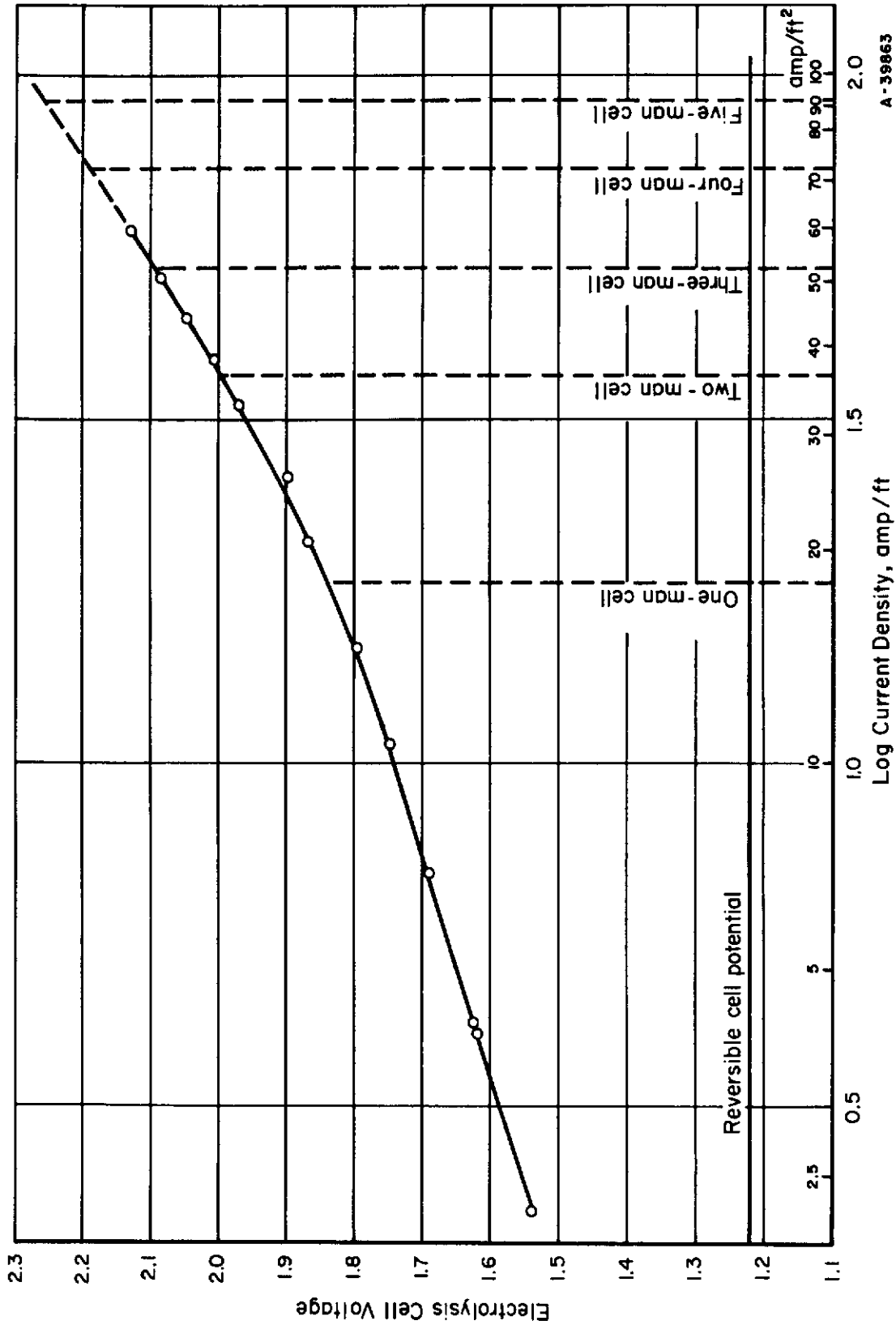


FIGURE 17. CELL VOLTAGE AT VARIOUS CURRENT DENSITIES FOR OPERATION OF LABORATORY MODEL

With electrolyte (28 per cent KOH solution) at 90 F (after Run No. 1).

A-39963

Conclusions

ρ = electrolyte resistivity, ohm-inch

L = distance between electrodes, inch

A' = effective cross-sectional area of electrolytic solution between the electrodes (approximately equal to A at low current but smaller than A at high current because of the blocking effect of the diaphragm and gas bubbles).

In Figure 17, the value of k (slope) is about 0.3 from 1 to 10 amp/ft². The increasing slope of the voltage curve above about 10 amp/ft² can be accounted for mostly by the electrolyte resistance ($\rho = 0.55$ ohm-inch for 28% KOH solution at 90 F and L = 0.57-inch electrode spacing for laboratory model).

From a characteristic voltage curve such as shown in Figure 17, much information can be derived for optimization of cell design for a particular application. As shown on Figure 17, there is little increase in cell voltage for operation at higher than designed capacity (i. e., as a 3-man, 4-man, or 5-man cell). The cell voltages shown in Figure 17 with extrapolation from 60 to 90 amp/ft² and corrected to a temperature of 111 F were used to predict the power consumption for higher rates of operation of the laboratory model as shown previously in Figure 2.

As pointed out in the introduction to this report, there were two water-electrolysis rates of interest; a minimum rate of 0.7 lb/day/man and a maximum of 2.25 lb/day/man. For the design objective of a 2-man cell, the above water-electrolysis rates would be 1.4 to 4.5 lb/day. Using the electrolysis cell voltages of Figure 17, the electrolysis cell power consumption is shown in Figure 18 for various water rates up to the maximum water rate for operation as a 5-man cell. Whereas the relative importance of electrolysis cell weight (and volume) versus power is not known for all space missions, a characteristic voltage curve such as Figure 17 is a basis for estimating optimum design for a specific system integration.

One example shown in Figure 18 is a derived estimate of electrolysis power consumption based on a smaller cell than the laboratory model such as obtained by using 8 cells rather than 16 cells. This would reduce by almost one-half the weight and size of the rotating portion of the cell with only a 10 per cent increase in electrolysis power consumption. The other example shows that a larger cell than the present laboratory model (i. e., 32 cells rather than 16 cells) would nearly double the weight and size of the rotating portion and would reduce the power consumption less than 10 per cent.

Effect of Temperature. Figure 19 shows the decrease in cell voltage with time in the three evaluation runs. As shown in Figure 19, the voltage

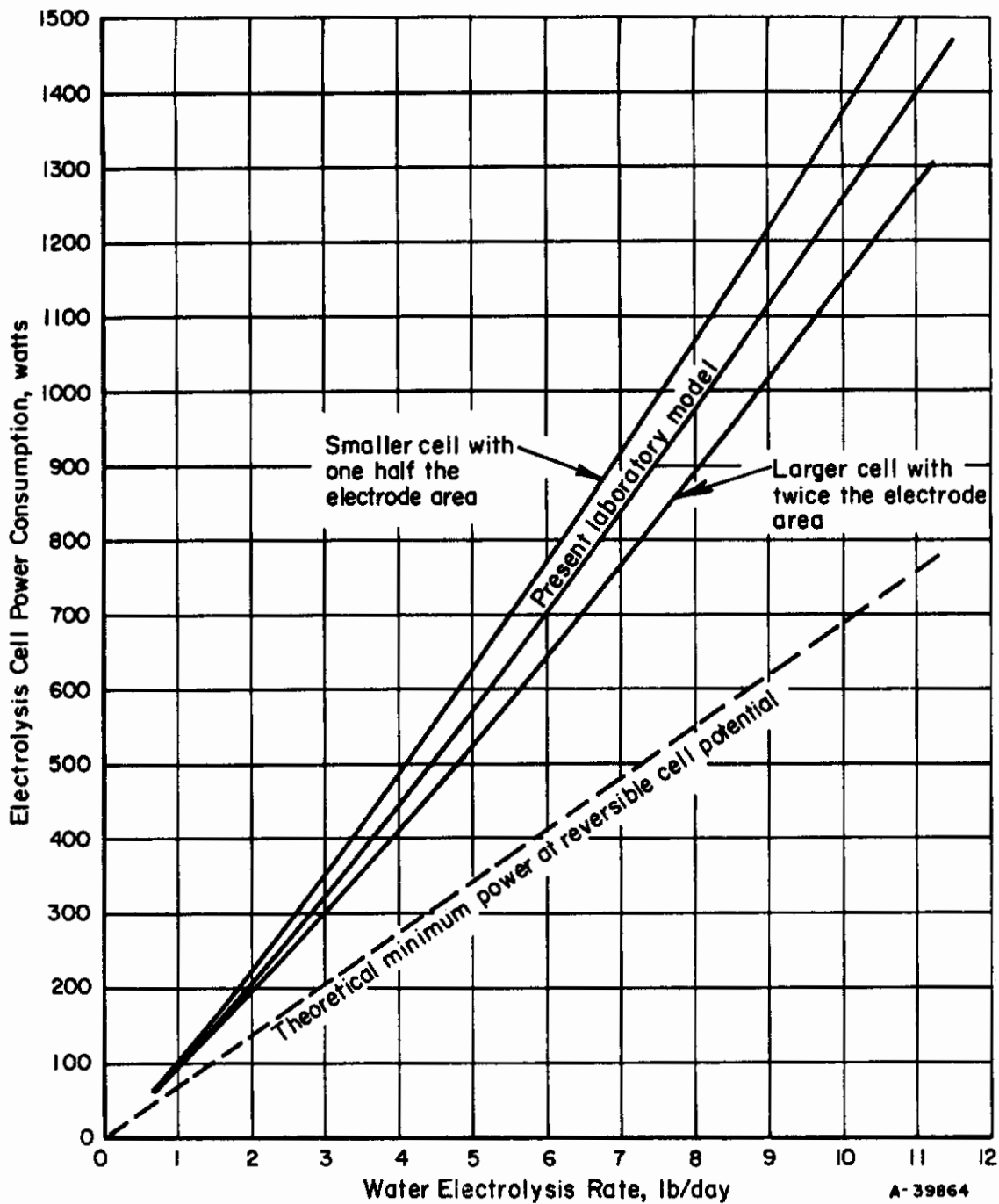


FIGURE 18. LABORATORY MODEL POWER CONSUMPTION AT VARIOUS WATER ELECTROLYSIS RATES

Based on cell voltages for laboratory model operated at 90 F.

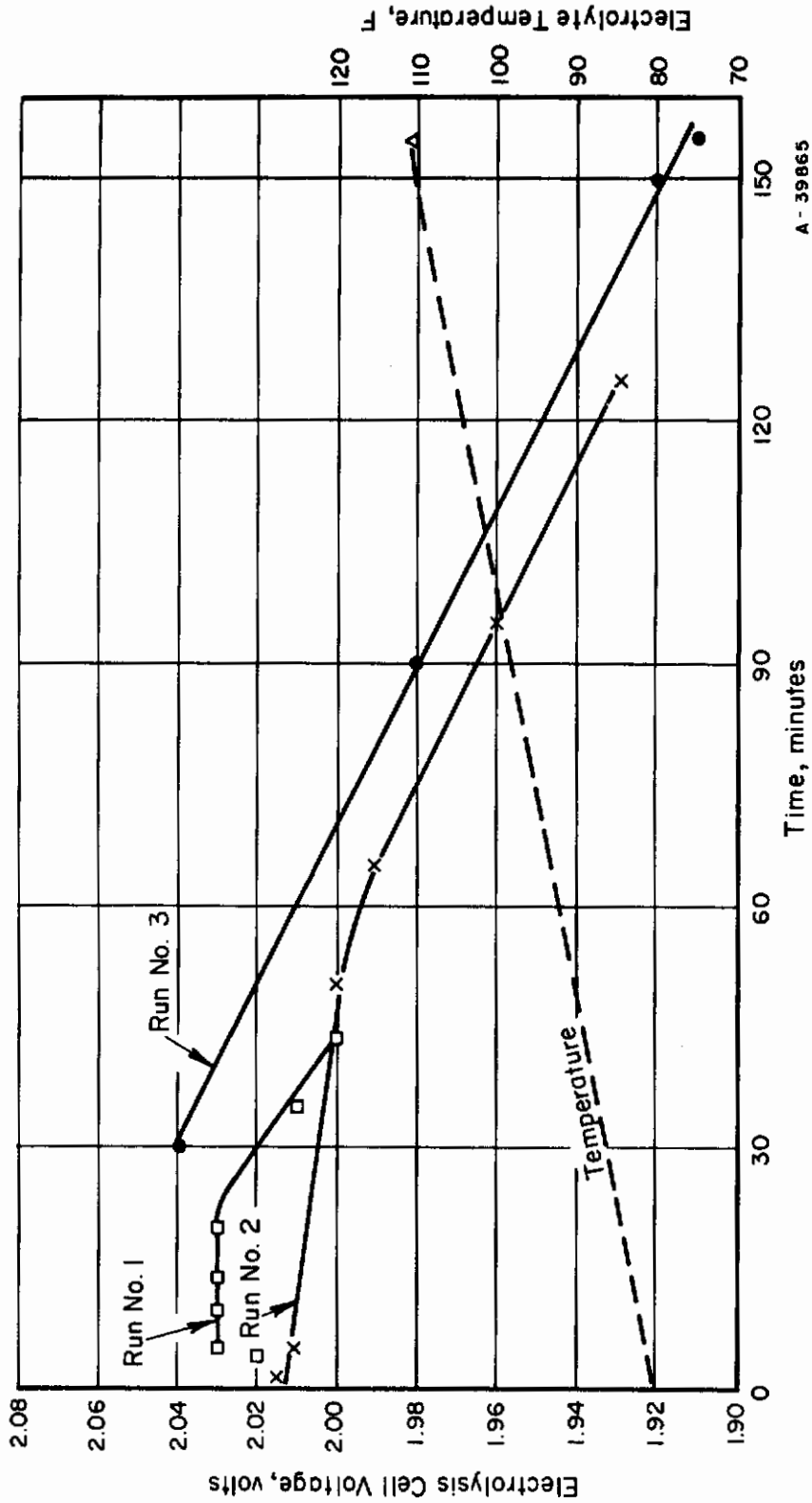


FIGURE 19. DECREASE IN ELECTROLYSIS CELL VOLTAGE AND CORRELATION WITH INCREASE IN ELECTROLYTE TEMPERATURE

During extended electrolysis runs at approximately 254 amperes (4.5 lb water/day).

Conrails

decrease has been correlated with the temperature rise of the electrolyte as being the most logical explanation. If the voltage drop were due to some activation of the electrodes or increase in true electrode area (as by microetching) one would expect a cumulative voltage reduction in consecutive runs rather than approximately the same voltage at the beginning of each run.

There was no provision made for measuring the electrolyte temperature during a run. However, at the end of the third run the electrolyte pumped from the cell was at 111 F which represented a 31 F rise from the initial room temperature value of 80 F. As shown in Figure 19, a constant increase of temperature with time (about 12 F/hour) has been assumed which is logical for a constant current run. A rough approximation of the heat input to the electrolyte can be made from the difference between the reversible cell potential and the observed cell voltage.

$$\begin{aligned} \text{Heat Input} &= (2.03 - 1.23) \text{ volt} \times 254 \text{ amp} \times 3.42 \frac{\text{Btu}}{\text{hr-volt amp}} \times \frac{\text{hr}}{60 \text{ min}} \\ &= 11.5 \text{ Btu/min} \end{aligned}$$

Heat Loss by Radiation and Convection

(assume 1.65 Btu/hr/ft²/F based on combine h_c + h_r for 13-inch-diameter steel pipe and Δ15 F)⁽⁷⁾

$$\begin{aligned} \text{Heat Loss} &= \frac{1.65 \text{ Btu}}{\text{hr-ft}^2\text{-F}} \left| \frac{\text{hr}}{60 \text{ min}} \right| \frac{(13)^2 3.14/4(2) + 3.14(13)(10)\text{in}^2}{144 \text{ in.}^2/\text{ft}^2} \left| 15 \text{ F} \right| \\ &= 1.9 \text{ Btu/min} \end{aligned}$$

Temperature rise of electrolyte (30 lb) + metal (200 lb)

$$\begin{aligned} \Delta T &= \frac{11.5 - 1.9 \text{ Btu}}{\text{min}} \left| \frac{155 \text{ min}}{0.8 \frac{\text{Btu}}{\text{lb-F}} (30 \text{ lb}) + 0.12 \frac{\text{Btu}}{\text{lb-F}} (200 \text{ lb})} \right| \\ &= 31 \text{ F.} \end{aligned}$$

The precise check of estimated and measured temperature rise is considered fortuitous considering the assumptions used in the calculation. However, a comparison of estimated heat input and heat loss from the cell indicates that equilibrium had not been reached at 111 F which is borne out by the indications for further voltage decrease beyond 2-1/2 hours. A "guestimate" is that the cell would have reached a temperature equilibrium with heat input from electrolysis equal to heat loss by convection and radiation at about 150 F after about 6 hours of operation.

Effect of Temperature on Reversible Cell Potential. Based on a free-energy change of -56.69 and -53.85 kcal/mol $H_2O(l)$ at 25 C and 100 C respectively, the reversible cell potential is

$$E_o = \frac{-JQ}{nF} = \frac{-(4.182)(-56.69)}{(2)(96,494)} = 1.23 \text{ volts at } 25 \text{ C}$$

$$E_o = 1.168 \text{ volts at } 100 \text{ C}$$

$$\frac{\Delta E_o}{\Delta t} = \frac{1.23 - 1.168}{100 - 25} = 0.00083 \text{ volt/C} = 0.00046 \text{ volt/F .}$$

The above data were used in Figure 22 (shown later).

Effect of Temperature on Overvoltage. The temperature coefficient of overvoltage is reported⁽²⁾ to be

$$\text{Oxygen at nickel anodes } \frac{\Delta E_{oA}}{\Delta t} = 0.00325 \text{ volt/C} = 0.0018 \text{ volt/F}$$

$$\text{Hydrogen at iron cathodes } \frac{\Delta E_{oC}}{\Delta t} = 0.0025 \text{ volt/C} = 0.00139 \text{ volt/F .}$$

According to the same reference⁽²⁾, of the total overvoltage at 36 amp/ft² approximately 2/3 is oxygen overvoltage and 1/3 is hydrogen overvoltage. The above data were used in Figure 22 (shown later).

Effect of Temperature on Electrolyte Resistance. The effect of electrolyte concentration on electrolyte resistivity was determined from data on equivalent conductivity (Λ) for potassium hydroxide solutions⁽⁸⁾ and the following relationship

$$\rho = \frac{1000}{2.54 \Lambda N} \text{ ohm-inch}$$

where

ρ = specific resistivity of electrolyte, ohm-inch

Λ = equivalent conductivity, ohm⁻¹ cm⁻¹

N = normality of solution.

Conclusions

The equivalent conductivity and specific resistivity at 18 C are plotted in Figure 20 along with a curve of weight per cent potassium hydroxide solution versus normality based on specific-gravity data at 15 C⁽⁹⁾. From Figure 20 it can be seen that the minimum resistivity of the electrolyte is obtained with 28 per cent KOH solution which is why this concentration is often selected for hydrogen and oxygen production in industrial electrolysis cells.

From equivalent conductivity data at various temperatures, the specific resistance as a function of temperature was calculated for a 28 per cent KOH solution as shown in Figure 21.

Also shown in Figure 21 is the calculated voltage drop through the electrolyte for various temperatures and currents based on the specific resistivity and the cell constants for the laboratory model: 6.94 ft² of electrode area and an electrode spacing of 0.57 inch. The effect of reduction in cross-sectional area of electrolyte for current flow caused by the diaphragm and gas bubbles was neglected. A comparison of the voltage drop from Figure 21 at 90 F for various currents with the observed cell voltage in Figure 17 accounts fairly well for the higher rate of increase of cell voltage above about 10 amp/ft².

The electrode spacing used in the laboratory model is smaller than for commercial cells run at comparable current densities. Normally, gas entrained in the electrolyte between the electrodes has a significant effect on the electrolyte resistance. The indication that the gas bubbles have a negligible effect in the laboratory model suggests a beneficial effect of rotation possibly resulting from the higher average G-field than in conventional electrolysis.

The calculated values of voltage drop through the electrolyte from Figure 21 were used in Figure 22. At a current of 254 amperes for the laboratory model, the average temperature coefficient of electrolyte voltage drop was calculated to be

$$\frac{\Delta E_e}{\Delta t} = \frac{0.088 - 0.055}{140 - 80} = 0.00055 \text{ volt/F.}$$

Estimate of Cell Voltage for Higher Temperature Operation. Figure 22 summarizes the previous calculations to show the relative effect of the various components of excess voltage above that theoretically required to decompose water into hydrogen and oxygen.

The final cell voltages and estimated final temperatures for the three evaluation runs from Figure 19 are plotted in Figure 22. The apparent

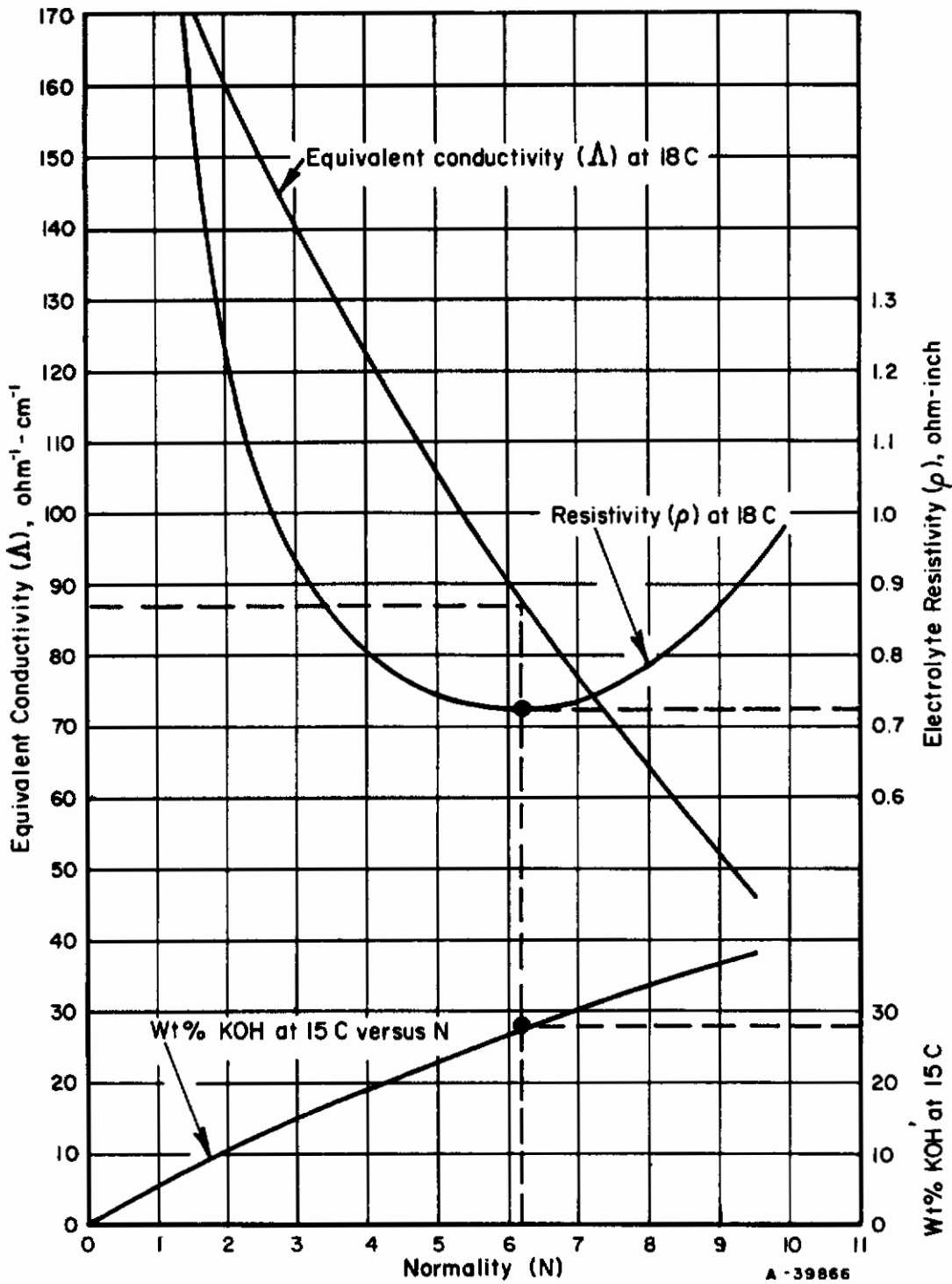


FIGURE 20. EFFECT OF ELECTROLYTE CONCENTRATION ON RESISTIVITY
 Calculated from equivalent conductivity of KOH.

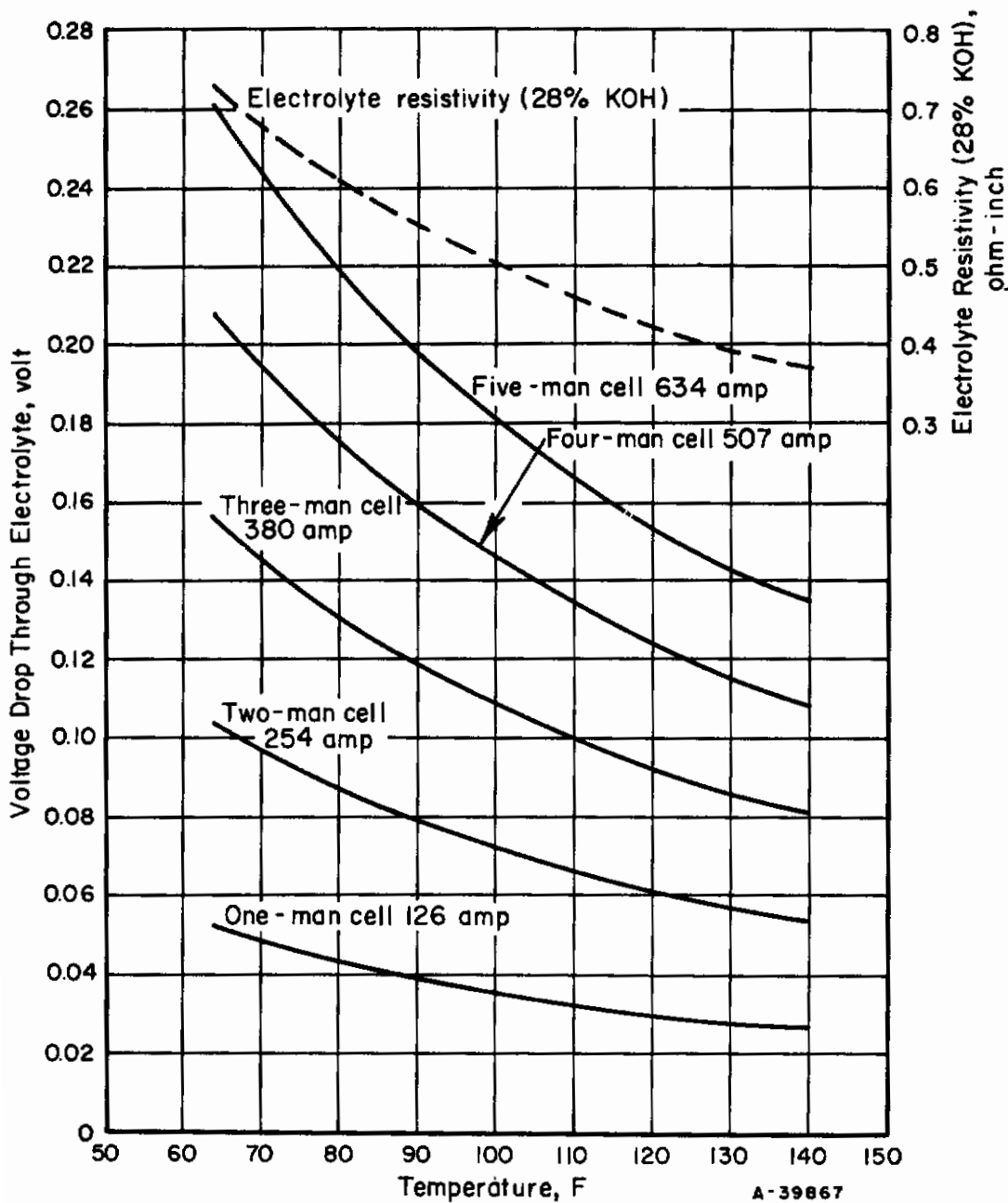


FIGURE 21. EFFECT OF TEMPERATURE ON VOLTAGE DROP THROUGH ELECTROLYTE AT VARIOUS AMPERES FOR LABORATORY MODEL

6.94 ft² of electrode area, 0.57-inch electrode spacing; electrolyte resistivity at various temperatures calculated from equivalent conductivity data for 28 per cent KOH at various temperatures.

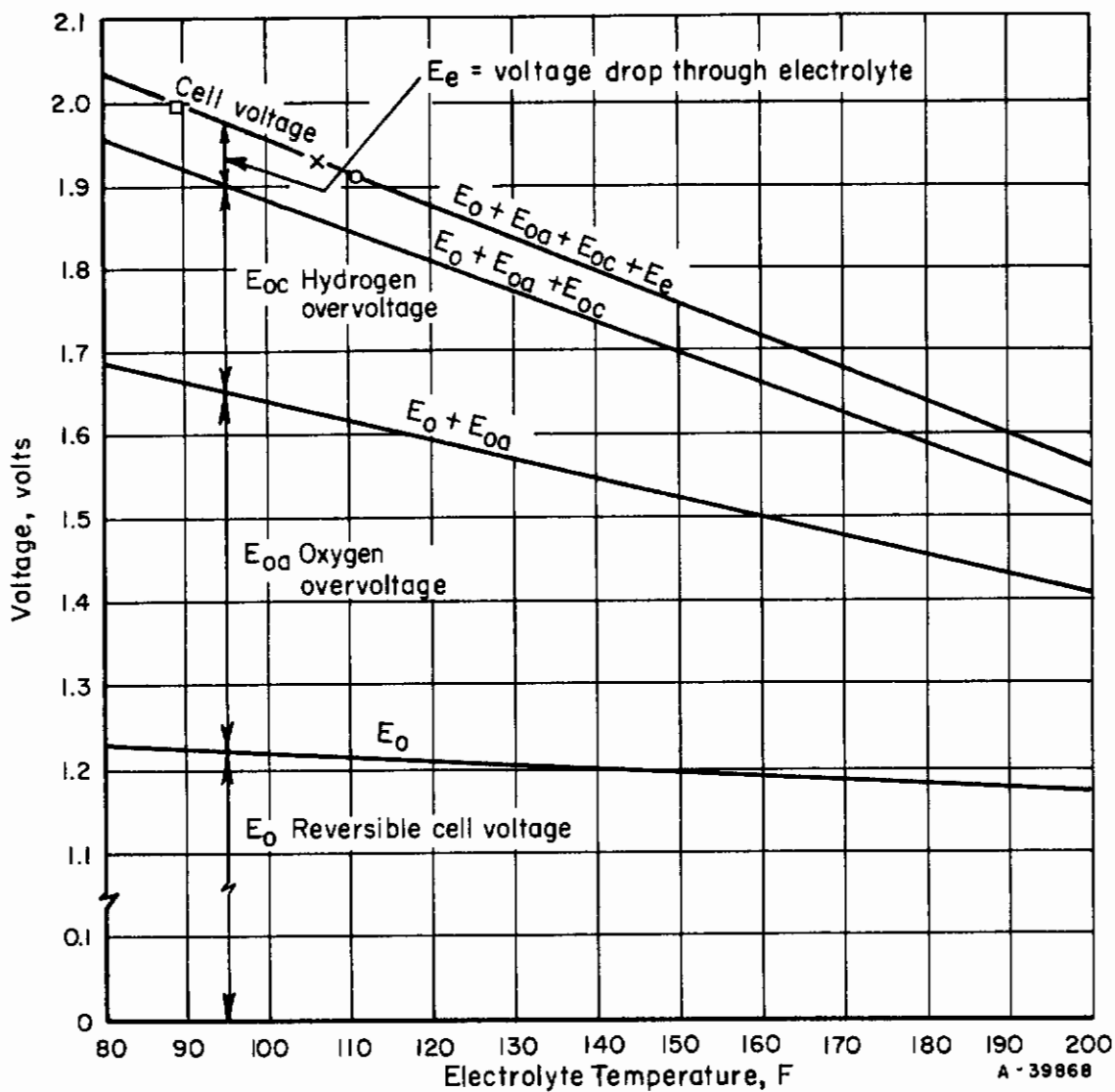


FIGURE 22. ESTIMATED EFFECT OF ELECTROLYTE TEMPERATURE ON ELECTROLYSIS VOLTAGE FOR OPERATION OF LABORATORY MODEL AT 254 AMPERES (TWO-MAN CELL)

temperature coefficient of cell voltage based on the three evaluation runs (or Run 3 Figure 19) is about 0.0046 volt/F. The latter value is about the same as obtained from the sum of the individual temperature coefficients:

$$\frac{\Delta E_o}{\Delta t} + \frac{\Delta E_{oA}}{\Delta t} + \frac{\Delta E_{oC}}{\Delta t} + \frac{\Delta E_e}{\Delta t} = \frac{\Delta E_{cell}}{\Delta t}$$

$$0.00083 + 0.001805 + 0.00139 + 0.00055 = 0.0046 \text{ volt/F.}$$

As mentioned previously, a temperature equilibrium at about 150 F might be expected at which temperature a cell voltage less than 1.8 volts might be obtained based on Figure 22. Many industrial cells operate at temperatures of 150 F \pm 20 F; some operate at temperatures up to 200 F. While there are prospects for significant reduction in cell voltage and electrolysis power by operation at high temperature, the possible adverse effect on cell life and reliability must be considered because of the greater importance of reliability in space applications.

System Optimization

Of the four principal system criteria - reliability, power, weight, and volume - only the last three are readily subject to mathematical analysis. In earlier sections of this report, an estimate was given that the present laboratory model might be redesigned, as a prototype model with reduction of the weight to 200 pounds and the volume to 2.2 ft³ without affecting the power. Further optimization of the electrolysis system design requires a consideration of weight/power ratios.

The electrolytic method of providing oxygen is versatile. A wide range of current densities are technically feasible, which can provide a wide range of weight/power ratios for the electrolysis cell. However, the optimization of the electrolysis cell requires a consideration of the integrated system; principally the weight of the source of the power for electrolysis. While the power source was not a direct concern of this project, a consideration of the power source allows a better appraisal of the present laboratory-model design.

The important consideration here appears to be attaining minimum weight for the total system which includes the electrolysis system weight plus the power source weight (technically an energy-conversion device rather than a power source) plus the weight of the radiation system for dissipation of excess heat that can be charged to the electrolysis system. Calculations indicate that heat dissipation from the electrolysis operation would be a minor factor in the system weight. Thus, the power consumed by the electrolysis system is mainly of concern in defining the power source weight. The important factor in electrolysis cell design is the weight/power ratio of the power source and the latter is not known accurately at the present time.

For satellite power supplies based on solar cells values reported range from 2 lb/watt to 7 lb/watt depending on orbit and provisions for orientation and energy storage. Considerable research effort is being devoted to decreasing the weight/power ratio for space vehicles of the future. Certain thermal-cycle systems have prospects of providing a ratio of 0.2 lb/watt.

The results of the evaluation of the laboratory model indicate that the present design current density would be optimum for combination with a power supply having a weight/power ratio of about 1-1/2 lb/watt to achieve the lowest combined weight of power supply and electrolysis cell. The system optimization can be illustrated by a simple example based on the present 16-cell design of the laboratory model. Table 3 indicates that to add or subtract one cell would change the total laboratory-model weight by 6-3/4 lb. The change of current density resulting from adding or subtracting one cell would change the power consumption by 4 watts (by the change in cell voltage with current density shown in Figure 17.

Thus, with a power supply of 2 lb/watt, it would be advantageous to use 17 cells and add 6-3/4 lb to the electrolysis cell weight to reduce the power supply by 8 lb. However, with a power supply of 1 lb/watt, it would be advantageous to use 15 cells and reduce the electrolysis cell weight by 6-3/4 lb while adding only 4 lb to the power-supply weight.

The important point is that while the electrolysis cell can be designed to operate at various current densities depending on whether power saving or weight saving is more important, the direction to go cannot be decided until there is a defined weight/power ratio for the power supply to be used on the space vehicle.

REFERENCES

1. Howat, D. D., "Electrolytic Hydrogen Production", The Chemical Age, Vol 51, pp 173-178, 197-202, 221-225, 1944.
2. Bowen, C. E., "The Production of Hydrogen and Oxygen by the Electrolysis of Water", Inst. Elec. Engrs., Vol 90, Pt 1, pp 474-485, 1943.
3. Mantell, C. L., Industrial Electrochemistry, 3rd Edition, "Hydrogen and Oxygen", Chap 18, McGraw-Hill Book Co., Inc., pp 455-470, 1950.
4. Sutherland, B. P., "Electrolytic Hydrogen Cells of Trail Design", Tran. Electrochem. Soc., Vol 85, pp 183-191, 1944.
5. The Stuart Cell, The Electrolyzer Corporation, Ltd., 901 Yonge Street, Toronto 5, Canada, 4 pp.

Contrails

6. "Pressure Lowers Electrolytic H₂ Cost", Chem. Eng. , Vol 66, p 68, March 7, 1960.
7. Chemical Engineers' Handbook, Edited by John H. Perry, Third Edition, McGraw-Hill Book Co. , New York, p 475.
8. Ibid, p 1782.
9. Ibid, p 182.

Contrails

APPENDIX I

DESIGN AND EXPLANATION OF AUTOMATIC CONTROL CIRCUIT FOR ZERO-GRAVITY ELECTROLYSIS MACHINE

Zero-Gravity Electrolysis-Machine Outline of Automatic Control Functions

(See Figure 23 and Table 6)

- (1) Before startup, Valves D and E for H₂ and O are open, and remain open till tank is filled with KOH.
- (2) Push "Start" button.
 - (a) All timers or logic elements are reset to initial conditions.
 - (b) Centrifugal unit drive motor starts.
 - (c) Unit rotation indicator light comes on.
- (3) After unit is rotating.
 - (a) Sensor circuit is energized.
 - (b) Pump starts, indicator light comes on, and KOH electrolyte is pumped into the electrolysis machine.
 - (c) When KOH electrolyte reaches the 2-inch radius, the pump shuts off, indicator light goes off. (KOH solution will not be called for again.)
 - (d) Valves D and E close and stay closed.
 - (e) Current to cells can be turned on, on external command (250 amp at 2).
- (4) At 2-1/4-inch radius, cells call for more liquid.
 - (a) Pump starts and light comes on. Water is now pumped into the electrolysis machine.
 - (b) When water reaches the 2-inch radius, pump shuts off and light goes out.
- (5) Step (4) is repeated at intervals, on command of sensor.
- (6) On stopping (emergency or otherwise)
 - (a) Valves D and E open
 - (b) Cell current shuts off.

(7) On "Stop" command

- (a) Machine is evacuated (see circuit drawing for automatic control).
- (b) Pump and rotational motors are shut off.

Zero-Gravity Electrolysis-Machine Summary Explanation of Automatic Control Circuit

A. Push "Start Motor" Button S1

- (1) Relay K1 is energized, and locks in through its own contact.
- (2) Power is applied to unit drive motor through N. O. K1 contact.

B. Push "Start Pump" Button S2

- (1) Relay K2 is energized through a N. O. K1, a N. C. K10, and holds in through its own contact.
- (2) Power is applied to the sensor circuits through a N. O. K2.
- (3) Relay K3 is energized and holds in through its own contact and a N. C. K7.
- (4) Valve A is energized through a N. O. K3.
- (5) Power is applied to coil of K4 through a N. O. K2, a N. C. K6, and a N. C. K5. K4 holds in through its own contact.
- (6) Pump starts through a N. O. K4.
- (7) Pump continues to run.
- (8) Electrolyte reaches a 2-1/4-inch-diameter sensor, and K5 is energized.
- (9) Electrolyte reaches 2-inch-diameter sensor, and K6 is energized.
 - (a) K3 is de-energized, dropping out Valve A which will then stay de-energized.
 - (b) K4 is de-energized and pump stops.
 - (c) K7 is energized through a N. O. K2, a N. O. K6, and holds in through its own contact.
 - (d) Valves D and E are energized through a N. O. K7.

C. Push "Cell Current on" Button S3

- (1) Relay K8 is energized through a N. O. K7, and holds in through its own contacts.
- (2) High current relay K9 is energized through a N. O. K8.
- (3) As electrolyte level drops, K6 becomes de-energized.
- (4) As electrolyte drops below 2-1/4-inch level, K5 becomes de-energized.
- (5) K4 is energized through N. C. K6 and N. C. K5, and pump cycle starts again.

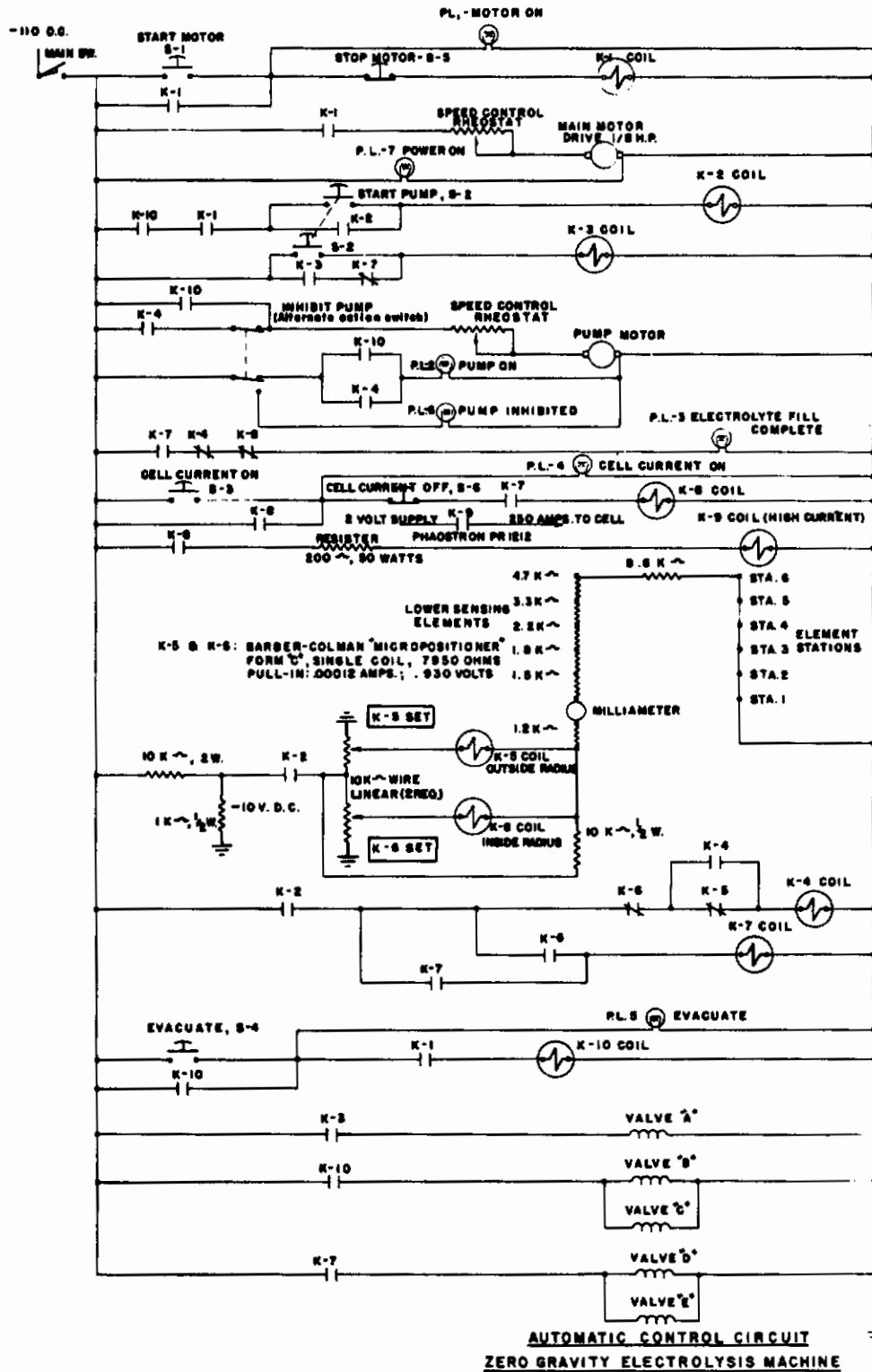


FIGURE 23. AUTOMATIC CONTROL CIRCUIT FOR ZERO-GRAVITY ELECTROLYSIS MACHINE

TABLE 6. ZERO-GRAVITY ELECTROLYSIS-MACHINE SUMMARY TABLE OF AUTOMATIC CONTROL FUNCTIONS

Controlled Functions	Unit												
	Valve A	Valve B	Valve C	Valve D	Valve E	Drive Motor	Pump	Cell Current	2-1/4-inch Sensor	2-inch Sensor			
(1) Off	De-energized	De-energized	De-energized	De-energized	De-energized	Off	Off	Off	Off	Off			
(2) Start unit drive motor	De-energized	De-energized	De-energized	De-energized	De-energized	On	Off	Off	Off	Off			
(3) Start pump (pump KOH)	Energized	De-energized	De-energized	De-energized	De-energized	On	On	Off	On (no output)	On (no output)			
(4) KOH reaches 2-1/4-inch radius	Energized	De-energized	De-energized	De-energized	De-energized	On	On	Off	On (output)	On (no output)			
(5) KOH reaches 2-inch radius	De-energized	De-energized	De-energized	Energized	Energized	On	Off	Off	On (output)	On (output)			
(6) Cell current on	De-energized	De-energized	De-energized	Energized	Energized	On	Off	On	On (output)	On (output)			
(7) KOH electrolyte between 2 and 2-1/4-inch radii	De-energized	De-energized	De-energized	Energized	Energized	On	Off	On	On (output)	On (no output)			
(8) KOH electrolyte drops below 2-1/4-inch radius	De-energized	De-energized	De-energized	Energized	Energized	On	On	On	On (no output)	On (no output)			
(9) Water pumped into 2-inch radius	De-energized	De-energized	De-energized	Energized	Energized	On	Off	On	On (output)	On (output)			
(10) Electrolyte drops below 2-1/4-inch radius	De-energized	De-energized	De-energized	Energized	Energized	On	On	On	On (no output)	On (no output)			
(11) Water pumped into 2-inch radius	De-energized	De-energized	De-energized	Energized	Energized	On	Off	On	On (output)	On (output)			
(12) Evacuate electrolyte	De-energized	Energized	Energized	De-energized	De-energized	On	On	Off	Off	Off			
(13) Stop	De-energized	De-energized	De-energized	De-energized	De-energized	Off	Off	Off	Off	Off			

Contrails

D. Push "Evacuate" Button S4

- (1) Relay K10 is energized through a N. O. K1, and holds in through its own contacts.
- (2) K2 is de-energized, removing all sensor control and cell current, and dropping out Valves D and E.
- (3) Pump continues to run through a N. O. K10.
- (4) Valves B and C are energized through a N. O. K10.

E. Push "Stop Motor" Button S5

- (1) All circuits de-energized.

Contrails

FEASIBILITY STUDY REPORT ON METHODS FOR ELECTROLYSIS
OF WATER UNDER ZERO-GRAVITY CONDITIONS

The following criteria provided the necessary framework to select and evaluate available data:

- (1) The system should be designed to provide oxygen for two men and should be capable of electrolyzing water at rates from 0.7 to 2.25 lb/man/day. Maximum capacity of the electrolyzer is, therefore, 4.5 lb of water per day and 254 amperes for one cell. Voltage will depend on the cell design. Series connection of cells will decrease the amperage but increase the voltage in direct proportion to the number of cells so connected.
- (2) Weight, space, and power requirements will be severely limited in all aerospace equipment. Accordingly, cells having the least weight, smallest size, and lowest power requirement are desired. But these criteria must be balanced against the availability of cell components and the reliability of the cell's operation.
- (3) The principle of design should inherently permit zero-gravity operation. The equipment should be designed to operate in a range from 0 to 1-G force with the equipment being capable of withstanding 15 G without damage.
- (4) Electrical and thermal power will be available. Hence, power sources are outside the scope of this study. The heat generated by the electrolytic cell should be considered as an overall advantage or disadvantage, but the inclusion of the heat exchanger which may be required to dissipate the heat overboard should not be integral to the selected electrolysis principle. In other words, the amount of heat should be listed but the exchanger weight should not be estimated for an individual cell. The equipment is expected to operate within an environmental temperature range of from 60 F to 75 F. For flexibility of systems, a temperature range of 32 F to 100 F is desirable.
- (5) Mission duration will vary from 2 days to 2 years. This requirement is interpreted to mean that the cell may have up to two years of continuous operation with no planned maintenance.
- (6) The oxygen evolved should be hydrogen free. For example, if a catalyst bed is necessary then it should be considered.

Contracts

a part of the over-all electrolysis system. The oxygen may be saturated with moisture and it can be assumed that the cabin clean-up system will remove this moisture.

- (7) No requirement will be established for the optimum pressure. The cylinders or storage facilities will not constitute a part of the system unless the principle of operation for the cell dictates this requirement.
- (8) The water will be supplied as a liquid within the temperature range of 60 F to 75 F. Purity of the water will be approximately the same as the drinking-water standards of the Public Health Service.

The above framework for study includes all requirements from the statement of work in the original contract plus comments from a letter dated 12 September 1960 from Omer M. McGlone, Contracting Officer, to Battelle Memorial Institute.

METHODS STUDIED

Rotating Cells

Principle of Operation

Centrifugal force produced by rotation of the electrolytic cell can be used to establish an artificial gravity field as shown in Figure 24. Then operation of the cell is similar in principle to many well known industrial-cell designs with regard to arrangement of electrodes and use of diaphragms to keep hydrogen and oxygen separate. A radial cross section of the cylindrical cell is similar to the conventional rectangular cells used under normal gravity conditions. Using the rotation principle, several variations of commercial cells were considered, each being representative of design variations involving mainly electrolytic-gas pressure and electrode arrangements.

High-Pressure Cell. Several types of high-pressure cells are in use for industrial production of hydrogen and oxygen. Advantages over low-pressure (or atmospheric) cells relate to direct charging of gas-storage tanks and lower power consumption. While there are differences of opinion as to the magnitude of the effect of pressure on decreasing cell voltage, there seem to be two effects: (1) the cell overvoltage is decreased by increased pressure (the effect is small, less than 0.1 volt for 100 atmospheres) and (2) increased pressure decreases the size of the gas bubbles produced, which effectively decreases the resistance of the electrolyte

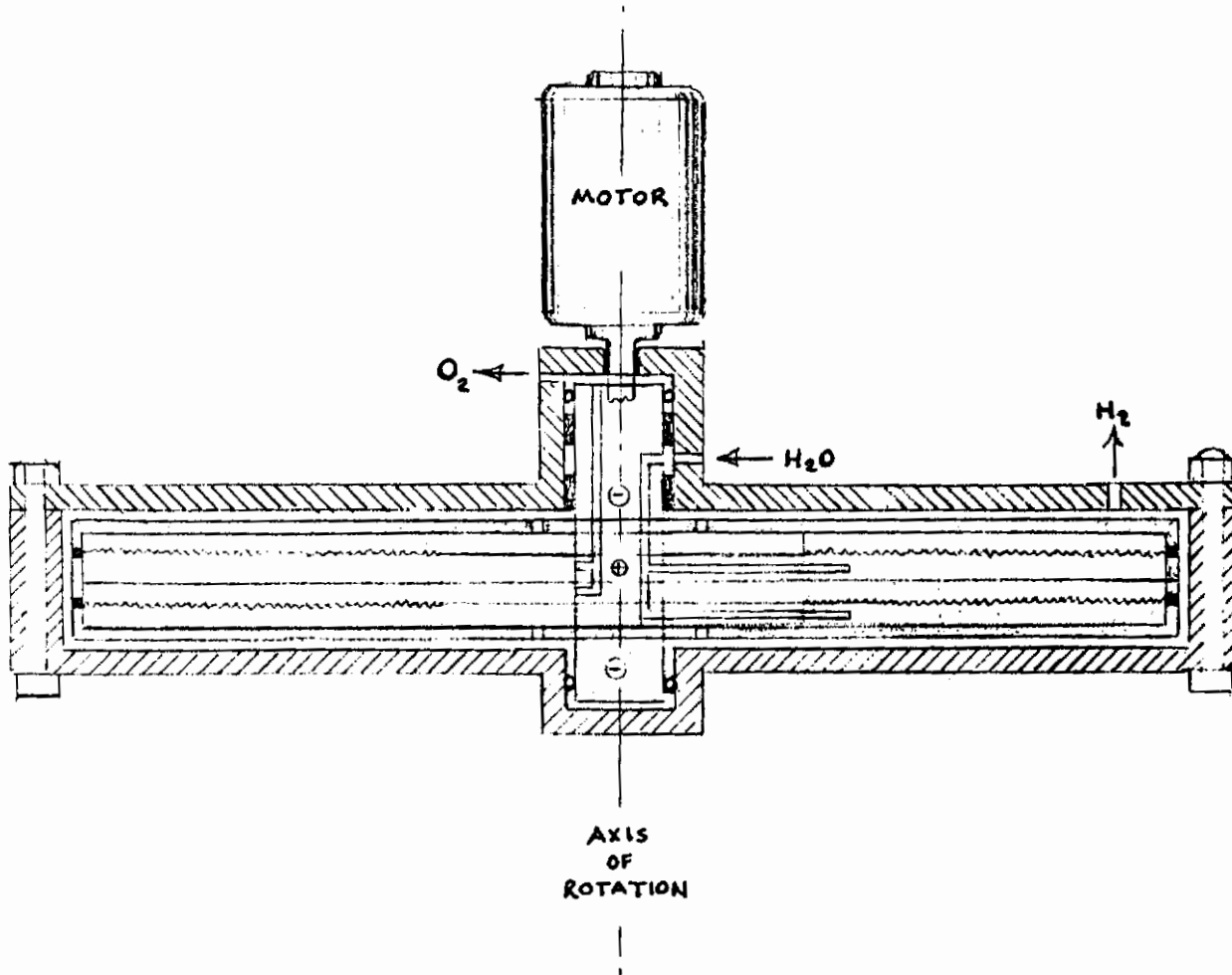


FIGURE 24. HIGH-PRESSURE CELL

Contrails

between the electrodes. Thus, relatively high current densities are practical in high-pressure cells. The disadvantages of high-pressure cells relate to the problems of sealing, differential-gas-pressure control across the diaphragm, and the need for more sturdy construction. An example of a high-pressure cell pertinent to this project is the unit built by the Treadwell Company for use on submarines. (1)* In the design of this unit, which operates at 3000 psi, the differential-gas-pressure regulating system and numerous safety devices have been worked out.

Operating design data of 1.5 amp/in.² (216 amp/ft²) at 3 volts and 3000 psi were used in arriving at tentative specifications for a rotating cell to operate at zero gravity.

The additional problems for a rotating cell are the high-pressure rotary seals and associated friction, which would influence the power required to maintain the cell in continuous rotation. Opinions of people familiar with high-pressure rotary seals were as follows: at 3000 psi, 2 years of reliability not likely; at 1500 psi, 1-2 years possibly; at 500 psi, 2 years of reliable operation definitely possible. A possible arrangement of rotary seals is shown in Figure 24, with the water to be injected between the hydrogen and oxygen. With both gas and water at the same pressure, the negligible differential pressure across the rotary seal would minimize leakage of gas or liquid. The seal for the motor shaft could have a differential pressure to the atmosphere of 500 to 3000 psi. Any small leakage of oxygen to the atmosphere would not be as serious as a hydrogen leak. The energy contained in the high-pressure oxygen might be dissipated through a turbine to provide part or all of the power to maintain cell rotation.

In addition to the electrolysis power, electrical power is assumed to be needed to maintain rotation of the cell. The amount of this power is dependent on the bearing friction, air drag, and speed of rotation. Because of high current densities used, the high-pressure cell is relatively small. The cell design assumed has an outer radius of 6 in., the liquid surface at a radius of 3 in., and a shaft radius of 2-in. For a minimum centrifugal acceleration of 1 G at the liquid surface the rotational speed has to be at least 100 rpm. At the outer radius, the acceleration would be 2 G. Thus, the mean artificial gravity field causing gas bubbles to move to the liquid surface would be slightly greater than normally encountered in industrial operations and might increase the current density/cell voltage ratio.

In starting up the apparatus, the available power of about 540 watts (3/4 hp) could be directed to the direct-current drive motor. After the cell is rotating at speed, the majority of the available power (97%) could be directed to electrolysis. To maintain rotation, power is needed to overcome rotation friction, bearing friction, and high-pressure-seal friction. The latter is not a large factor if the cell is designed for small differential pressure across the seal, even though the pressure is high. Rotation in a

*References are at the end of the report.

Contrails

hydrogen atmosphere should result in drag less than normal air drag. The following estimates were made for some of the auxiliary cell equipment.

	<u>Dimensions,</u> <u>inch</u>	<u>Total</u> <u>Volume,</u> <u>in. ³</u>	<u>Weight,</u> <u>lb</u>	<u>Power,</u> <u>hp</u>	<u>Watts</u>
(2) Seals	1 OD x 1-1/4	2	0.5	--	--
(1) Water pump (3000 psi)	3 OD x 6	42	1.5	0.01	7
(1) Cell rotation motor	2.8 OD x 5	30	1.3	0.01	7

Commercially available seals and motors were assumed. The water pump would probably be of special design, because of the very low flow (0.025 gal/hr) required at high pressure, but feasible to design and build.

Low-Pressure Cell. The design of a cell to operate at normal atmospheric pressure could be patterned after several commercial electrolyzers. As distinguished from the high-pressure cell, low-pressure cells operate at lower current densities of 25 to 75 amperes per square foot depending on electrode design. The lower current density means a larger cell. To establish an upper limit on size, the Levin cell design⁽²⁾ was assumed with a current density of 25 amperes per square foot, which results in a 31-inch-diameter cell. In other respects, the cell would be similar to the high-pressure cell except for the absence of a pressurized container around the cell.

Bipolar or Tank Type Cell. The low-pressure cell design might occupy too much space with one large-diameter thin section unless current densities much higher than 25 amp/ft² could be used. A more compact cell, as shown in Figure 25, could be made by clamping together several cells of the approximate unit-cell dimensions of the high-pressure cell. To replace the two unit cells in the high-pressure design at 225 amp/ft² would require about 18 cells at 25 amp/ft² (actually 15 cells by a permissible decrease in the gas "free space" per cell). By alternating anodes and cathodes within a single cell a savings in weight and size can be achieved. Two variations are possible with the "filter-press" type of construction. In a bipolar design, the electrodes are electrically connected in series, which requires a high-voltage low-amperage direct-current power source. In a tank-type design, the electrodes are connected in parallel, which requires a low-voltage, high-amperage direct-current power source. Both bipolar and tank-type designs are used commercially.

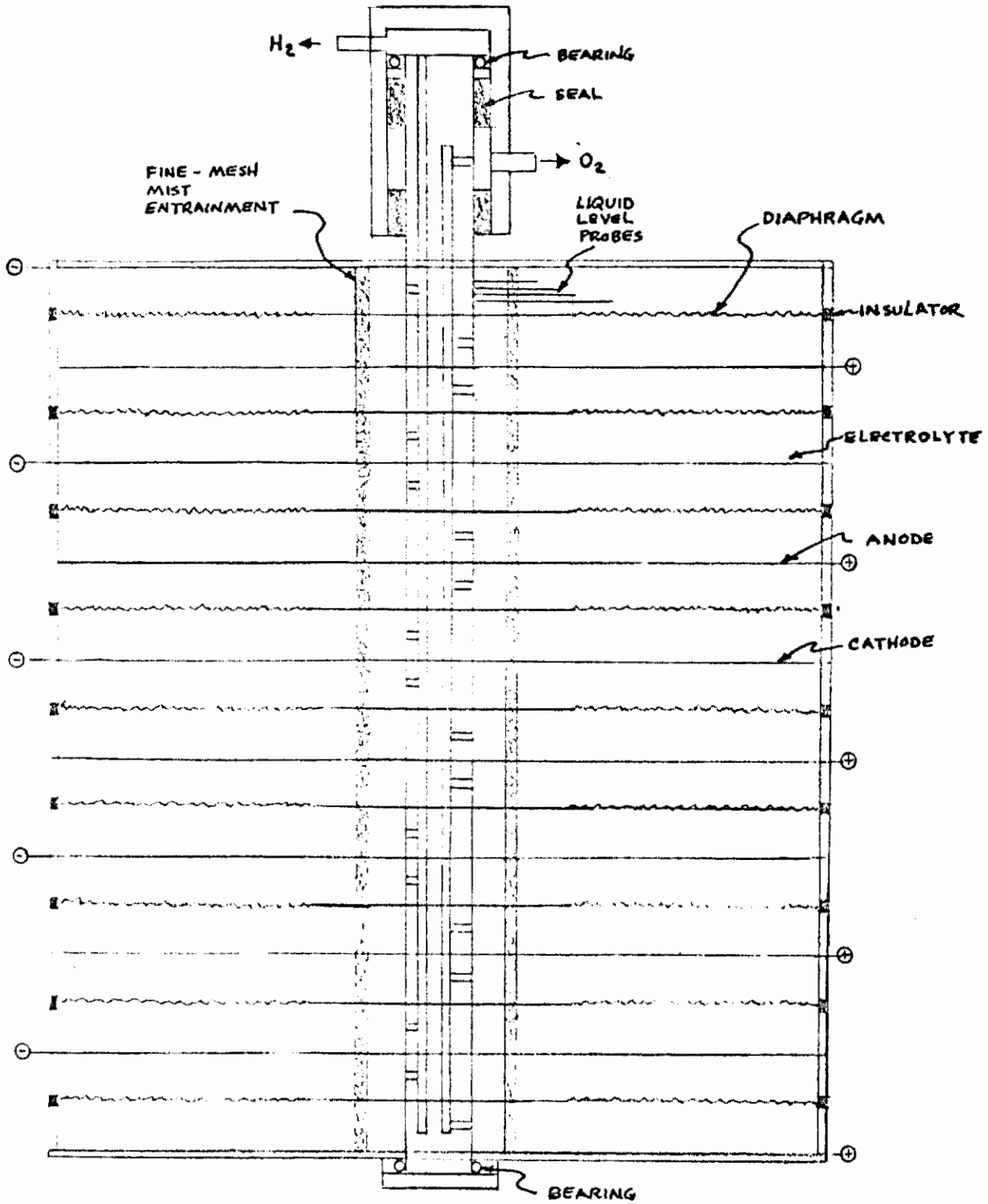


FIGURE 25. BIPOLAR (SERIES) OR TANK (PARALLEL) TYPE CELL (PARALLEL CONNECTION SHOWN)

Tentative Specifications

High-Pressure Cell.

Pressure	3000 psi
Current density	216 amp/ft ²
Current	254 amp
Voltage	3 v
Watts	762 w
Rotation	100 rpm
Gravity at liquid level	1 G
Gravity at periphery	2 G
Cell construction	
Diameter	12 in.
Width	1-1/4 in.
Electrode spacing	1/2 in.
Metal thickness (anode end plates)	1/8 in.
(cathode)	1/16 in.
Shaft	1-in. diameter x 3-1/2 in.
Volume	44 in. ³
Weight	3.6 lb
Pressure container	
Diameter	13-1/2 in.
Width	2 in.
Metal thickness	1/4 in.
Width at axis	4-3/8 in.

Contrails

Volume	106 in. ³
Weight	32 lb
Electrolyte	28% KOH at 75 C
Volume	80 in. ³
Weight	3.6 lb
Seals (2), water pump, cell motor	
Volume	74 in. ³
Weight	3.3 lb
Power	14 w
Total cell volume	0.2 ft ³
Total cell weight	52 lb
Total power	776 w

Low-Pressure Cell.

Pressure	less than 15 psig
Current density	25 amp/ft ²
Voltage	2.1 v
Power	533 w
Rotation	132 rpm
Gravity at liquid level	1 G
Gravity at periphery	5 G
Diameter	31 in.
Width	2 in.
Electrode spacing	1 in.
Total cell volume	0.85 ft ³

Contrails

Total cell weight 138 lb

Total power 547 w

Bipolar or Tank Type Cell.

Pressure less than 15 psig

Current density 25 amp/ft²

Number of unit cells 15

Volt-amperes (series) 31.5 v, 16.3 amp
(parallel) 2.1 v, 254 amp } 533 w

Rotation 132 rpm

Gravity at liquid level 1 G

Gravity at periphery 3 G

Cell Construction

Diameter 12 in.

Width 7-1/2 in.

Electrode spacing 1/2 in.

Metal thickness (outer plates) 1/8 in.

(internal
electrodes) 1/16 in.

Shaft 1-in. diameter x 9 in.

Volume 0.52 ft³

Weight 47 lb

Electrolyte 28% KOH at 75 C

Volume 653 in.³

Weight 29.4 lb

Contrails

Seals (2), water pump, cell motor

Volume	74 in. ³
Weight	3.3 lb
Power	14 w
Total cell volume	0.52 ft ³
Total cell weight	80 lb
Total power	547 w

Reliability.

Should be relatively high since practically all of the individual components of the cell have been tested for many years.

Stability to G Forces.

Should be good because of the relatively sturdy construction. Rotating parts of the cell can be ground-tested at high G forces by increasing the speed of rotation. It is assumed that during brief periods of high acceleration the cell would be drained of electrolyte and locked in a fixed position. Electrolyte would be admitted to the cell only after the cell is at the desired rotational speed.

The different designs of rotating cells should be considered as one method and as having a common principle of operation. The various designs have several important features in common. Each design involves a cylindrical cell. For ease of assembly as well as providing for disassembly for emergency repair, the cylinder must be made in at least two parts that are electrically insulated from each other. This presents a sealing problem which all designs have in common with industrial cells based on a filter-press construction and commonly referred to as "bipolar cells". Thus, all of the disadvantages of this type of construction will be present in addition to the special requirement of rotary seals and bearings and rotary electrical contacts.

As a method to be studied, the range of combinations of pressure, current density, and constructional features which have been proven in industrial practice must be considered an advantage which would favor a successful outcome of Phase III of the program. The several specific examples of rotating cells can be considered together as defining a range of tentative specifications as summarized on the following page:

Contrails

	<u>High Pressure</u>	<u>Bipolar</u>		<u>Low Pressure</u>
		<u>Series</u>	<u>Parallel</u>	
Weight, lb	52	80	80	138
Volume, ft ³	0.2	0.52	0.52	0.85
Power, w	776	547	547	547
Diameter, in.	13-1/2	12	12	31
Length, in.	2	7-1/2	7-1/2	2
Current, amp	254	16.3	254	254
Voltage, v	3	31.5	2.1	2.1
Pressure, psi	3000	15	15	15

Advantages of Rotating Cells

- (a) Cell design features have been proven in industrial use.
- (b) Materials of construction have a proven minimum 2-year life.
- (c) A liquid heat-transfer fluid is available.
- (d) Operation at higher-than-design output for short periods would not be detrimental.
- (e) Artificial gravity force is available to act as separator of any liquid entrained in the evolved gases.
- (f) Within the rotating-cell concept, many design features can be considered (i. e. , high or low pressure, high or low temperature, high voltage/low amperage or low voltage/high amperage).

Disadvantages of Rotating Cells

- (a) The mechanical features of a rotating cell have not been tested.
- (b) A rotating cell will act like a gyroscope and influence vehicle guidance.

Contrails

- (c) Requires CO₂-free water for proposed use of alkaline electrolyte.

As suggested in Exhibit WCLDEE 60-33 of the contract for this project, consideration was given to the "Bipolar Electric Cell as constructed for the Navy by Applied Science Laboratories, Inc. , State College of Pennsylvania, and to the method involving utilization of a low speed rotating cell where centrifugal force keeps the gas and water separate". The latter principle is discussed briefly in a study by the Martin Company, Denver, Colorado as part of an environmental conditioning system for use in a manned satellite designed to stay aloft for 60 days. The present section of this report on "Rotating Cells" covers this principle in greater detail.

A copy of the patent application for an "Electrolytic Cell Apparatus" containing substantially all of the information which was reported to the Bureau of Ships (Contract NObs-72399) was obtained from Mr. Hoover and reviewed on this project. The cell is claimed to be an improvement on present industrial-bipolar-cell construction, but is not intended for zero-gravity operation. Various constructional features might be considered in Phase III of the program if a rotating bipolar cell is to be designed.

Vortex Separator

Principle of Operation

If a liquid is made to move in a circular path, an artificial gravity field is established by centrifugal force. The strength of the gravitational field accelerating the gas toward the axis depends on the tangential velocity and the radius of curvature. A vortex is formed so that gas can be withdrawn from the central core.

Several methods of achieving gas-liquid separation were considered that depend on a vortex or similar principle. All require pumping of electrolyte, as differentiated from rotating the cell. Thus, these methods were considered as separate units to be used in conjunction with proven industrial-electrolysis-cell designs. Several of the methods will be discussed briefly before presenting estimates based on a study by the Pratt & Whitney Company on a vortex separator.

Pipe Bends. Figure 26a shows a simple 180-degree bend to illustrate how the gas would be removed. No specific information was found for this method and experiments would be needed to determine vortex stability. In practice, a spiral coil of pipe might be needed to allow sufficient time for gas separation. There might not be an advantage in size over a true vortex formed in a cylindrical container to be discussed later.

Centrifuge. Figure 26b illustrates the centrifuge principle. The only apparent advantage of centrifuging the electrolyte over rotating the complete cell is that smaller masses must be rotated. This would decrease the effective gyroscope reactions and, probably, require less power.

In-Line Vortex Separator. Figure 26c shows a gas-liquid separator developed by the AEC for use with homogeneous reactors⁽³⁾. Curved vanes at an angle of about 45 degrees twist the electrolyte and cause a tangential velocity component in addition to the axial velocity component. Gas is removed from the vortex. Restoring vanes are used downstream to recover some of the vortex energy.

Stable flow and good gas separation is reported when the Froude number is greater than 4 in the following equation:

$$Fr = \frac{(V_o)^2}{Rg}$$

where

V_o = tangential velocity at R, ft/sec

R = inside radius of pipe, ft

g = gravitational acceleration.

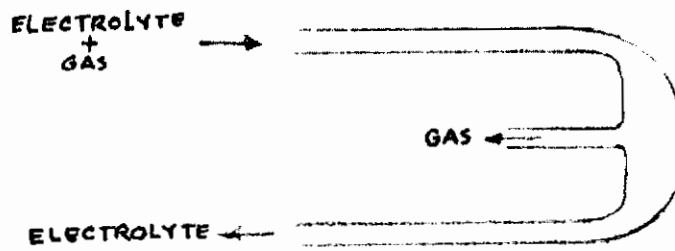
Gas separation efficiency depends on:

- (a) Physical properties of liquid and gas
- (b) Size distribution of bubbles
- (c) Thickness of annulus of rotating fluid
- (d) Axial and rotational velocities
- (e) Length of separator.

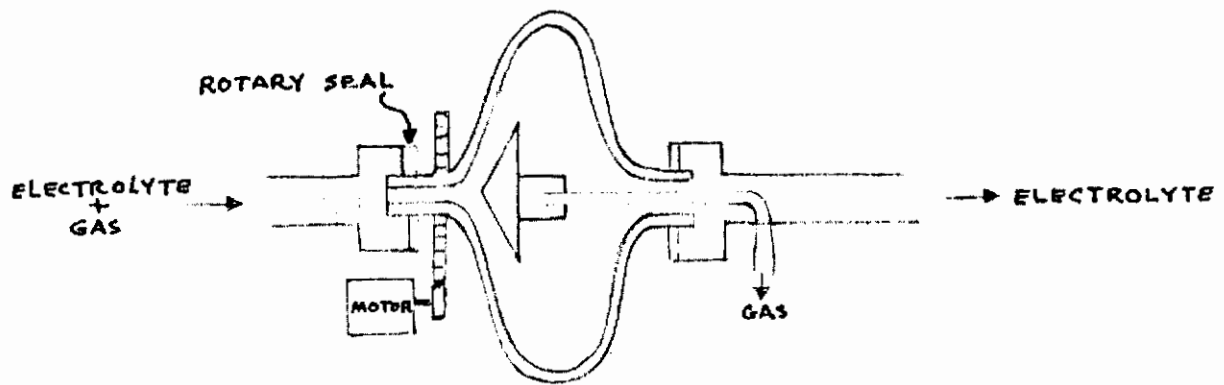
The lengths of separator required for better than 90 per cent efficiency in gas separation are usually in the range of three to eight pipe diameters.

Pratt & Whitney Design. Pratt & Whitney Company is developing a 500-w regenerative power system.⁽⁴⁾ The fuel cell is the Bacon type operated at 232 C and 800 psi. For their requirements, heat rejection and circulation of electrolyte from a common reservoir is required. The zero-gravity electrolysis and gas-separation system consists of a pair of vortex

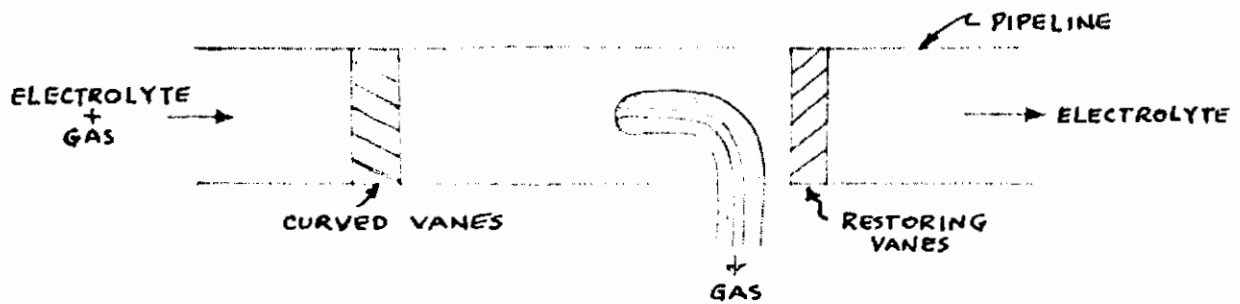
Contrails



a. PIPE BEND



b. CENTRIFUGE



c. IN-LINE VORTEX SEPARATOR

FIGURE 26. VORTEX SEPARATORS

Contrails

separators mounted axially on either side of a semipermeable membrane. Electrolysis is to be carried out across the membrane.

The initial work reported includes derivations of theoretical equations of gas-bubble motion in a vortex separator. This theoretical work was helpful in analyzing systems based on establishing an artificial gravity field. Subsequent reports are not yet available.

Figure 27 shows the system that can be estimated at this time for the needs of this project. It is proposed to design the electrolysis cell along the lines of present industrial cells except that the electrolyte would be pumped past the electrodes to remove the gas bubbles. The electrolyte containing entrained gas bubbles would then be passed through a separate vortex separator to separate the gas and liquid. The normal bubble size in electrolysis is about 0.001 in. to 0.010 in., permitting easy removal in the vortex separator. The velocity of flow through the electrolysis unit should not be so high that small-size bubbles form. The forced electrolyte circulation will tend to minimize gas polarization so that an expected current density of 50 amp/ft² at 2.1 v seems reasonable.

The apparatus shown in Figure 27 includes a vortex separator similar to the experimental design used by Pratt & Whitney except that the central semipermeable membrane for electrolysis has been replaced by a solid disk to separate two vortex separators mounted axially. A separate pump is used for each vortex separator to keep the electrolyte containing hydrogen separate from the electrolyte containing oxygen. It is assumed that the pump can be on the discharge side of the separator. This would be advantageous because it would avoid breaking up the large gas bubbles, which are easier to separate. If the bubbles are sufficiently large (greater than 0.001-in. diameter for the separator design assumed), the separator efficiency theoretically should be 100 per cent. Under this condition, the pump would only handle gas-free electrolyte and one pump (at twice the flow rate) would be sufficient for both feeds to the electrolytic cell. With suitable piping between the two pumps, the system could be arranged to work on only one pump in an emergency, thus increasing the reliability of the system.

A surge tank is provided in each line to handle the electrolyte displaced when the gaseous core is formed in the vortex.

Formula and data developed by Pratt & Whitney were used to design the vortex separator. The artificial gravity field developed is determined from the following formula:

$$G = \frac{1.04 \times 10^{-7} (W)^2}{R_o (d_i)^4}$$

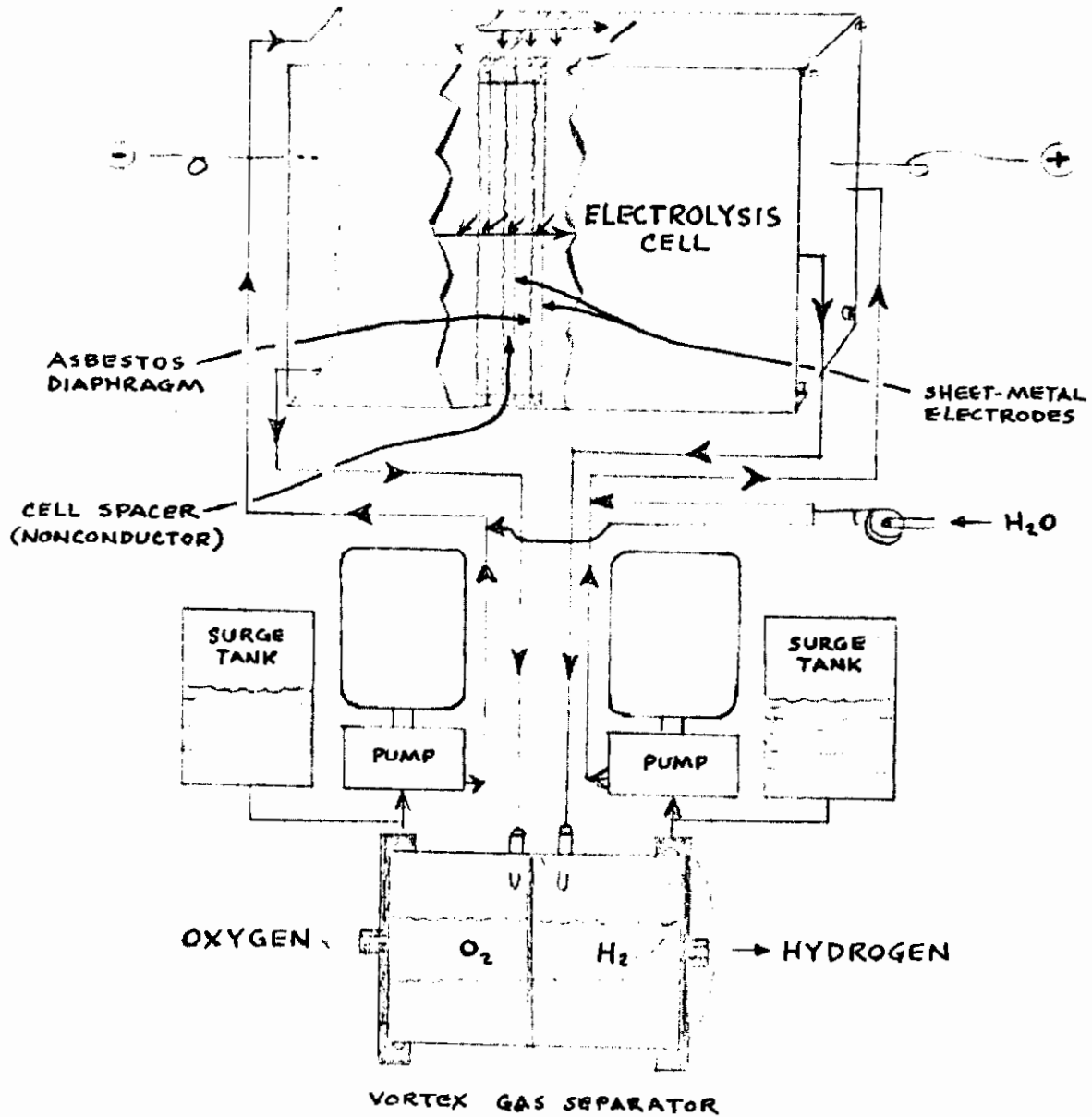


FIGURE 27. VORTEX GAS SEPARATOR (PRATT & WHITNEY DESIGN) AND SEPARATE ELECTROLYSIS CELL (CONVENTIONAL BIPOLAR DESIGN)

Contrails

where

G = artificial gravity field in G units

W = flow rate in lb/hr

R_o = outer radius of separator

d_i = diameter of inlet hole to separator.

Assuming $W = 1200$ lb/hr, $R_o = 4.5$ in., and $d_i = 3/16$ in., the gravity field is 56 G. At this flow rate, the pumping power required was 0.2 hp (15 w).

Theoretical curves relating bubble diameter to the time required to migrate from the outer diameter to the gas core were derived for various values of G based on the following formula for a forced vortex:

$$t = \frac{216 \mu R_o}{d^2 \rho_l \left(\frac{R_o W^2}{g} \right)} \ln \frac{R_o}{R}$$

where

$$\frac{R_o W^2}{g} = G = \text{artificial gravity field at outer diameter}$$

R = radius of gas core, in.

d = bubble diameter, in.

μ = viscosity, lb-sec/ft²

ρ_l = density of liquid, lb/ft³

For 28% KOH at 75 C, $\mu = 0.95$ centipoise and $\rho_l = 1.26$ g/cm³. Where $R = 0.688$ and $G = 56$, $t = 6$ sec for a bubble diameter of 0.0013 in.

The length of separator can now be calculated to be 3.3 in. for $t = 6$ sec by the following formula:

$$L = \frac{0.0021 Wt}{R_o^2 - R^2}$$

Tentative Specifications

Bipolar electrolytic cell

Pressure	~20 psi
Current density	50 amp/ft ²
Number of unit cells	20
Volt-amperes (series)	42 v x 12.7 amp (533 w)
Electrode size	6 x 6 x 1/16 in.
Electrode spacing	1/2 in.
Outer cell thickness	1/8 in.
Over-all cell dimensions	8-1/8 x 8-1/8 x 11-3/4 in.
Cell volume	775 in. ³
Cell weight	42 lb

Electrolyte

Volume in cell	500 in. ³
Weight in cell	22.5 lb
Volume in separator	105 in. ³
Weight in separator	4.7 lb
Velocity between electrodes	1.3 ft/min

Vortex separator

Over-all dimensions	4-3/4 OD x 7 in.
Metal thickness	1/8 in.
Separator volume	124 in. ³
Separator weight	8 lb

Contrails

Flow rate	1200 lb/hr (~2 gal/min)
Inlet diameter	3/16 in.

Surge tanks

Over-all dimensions	3 OD x 4 in.
Metal thickness	1/8 in.
Tank volume (2)	57 in. ³
Tank weight (2)	3.6 lb

Pumps

Over-all dimensions	3 OD x 6 in.
Volume (2)	85 in. ³
Weight (2)	3 lb
Power (2)	30 w
Total system volume	0.6 ft ³
Total system weight	84 lb
Total system power	563 w

Reliability.

Should be fairly good for such a system. Good reliability can be expected for the electrolysis cell since the problems normally associated with gas-liquid separation within a cell in a normal gravity field are eliminated. The main question relates to stability of the vortex and bubble size for which there are insufficient operating data available.

Stability to G Forces.

Should be good because of the rugged construction. During high acceleration periods all of the system except the surge tank would be completely filled with electrolyte, which should

be advantageous. Possibly, a vortex could be maintained during accelerations of 25 to 50 G if the artificial gravity field in the separator has comparable values. Any temporary reduction in separator efficiency (even to zero) during these periods would not be serious, since the hydrogen and oxygen lines are separate, and electrolysis could continue.

Advantages of Vortex Separation

- (a) Permits use of conventional industrial electrolysis cells with minor modifications that may be beneficial.
- (b) Electrolysis-cell design features have been proven in industrial use, and materials of construction are available with at least 2-year life.
- (c) Pumped electrolyte could be bypassed through a heat exchanger if heat rejection is necessary.
- (d) Use of two pumps and separate gas lines might allow maintenance of pumps without interrupting operation.
- (e) In-line vortex separator (Figure 26c) is similar in principle and might offer advantages.
- (f) Continued successful development of combination electrolyzer and separator in one unit might reduce volume and weight; a practical system operating on Bacon-cell electrolyte at 200 C and 800 psi would allow higher current densities at reduced power and smaller size and weight.

Disadvantages of Vortex Separation

- (a) Insufficient data on stability of vortex core under varying conditions of temperature and pressure for continuous use.
- (b) Operation with pump on discharge side of vortex and use of surge tank as proposed are unknown factors.
- (c) Very small bubbles, less than 0.001-inch diameter, might not be removed in a small, low-power separator. This separator inefficiency would be cumulative and might eventually result in a fine foam.
- (d) Pumping of electrolyte decreases the reliability with regard to leakage at connections and pump packing.

- (e) Insufficient data on separator design and operating conditions are available at the present time, but continued experimental study by the Pratt & Whitney Company will provide additional information.

Membrane Cells

Principle of Operation

In this type of cell, electrolysis is carried out across a wetted and conductive membrane. The wet membrane separates the evolved gases. Surface-tension forces keep the membrane wet, and separate liquid from gas in the absence of gravity. The process is illustrated in Figure 28.

The porous membrane may, in principle, be any absorbent material, such as paper or asbestos. As long as the pores remained filled with water, there will be a liquid barrier between the hydrogen and oxygen. Considering only the membranes, ion-exchange membranes have an inherent advantage in that they have a low permeability rate for gases, even if dry.

Ion-Exchange Membrane Cell. The ion-exchange membrane fuel cell under development by General Electric Company has a structure and design similar to the proposed electrolysis cell. The G.E. cell has catalysts on the membrane to permit its operation for the production of power. Catalyst problems seriously limit the reliability and life of present fuel cells. However, as an electrolysis cell, the thin, film catalysts may not be needed. Hence, reported characteristics for G.E. cells may be used for conservative estimates of specifications for the proposed electrolysis cell.

By private conversations with specialists at G.E., the following numbers were agreed to be suitable for the purpose of estimating:

- (a) Membrane cells may be used to decompose water at 50 amp/ft², 2.0 v/cell, 2 ft³/kw, and 130 lb/kw.
- (b) Surface-tension forces were observed to be sufficient, in one cell, to wet a membrane 12 in. in diameter against 1 G.
- (c) G.E. fuel cells have successfully operated after a few minutes of acceleration at 50 to 60 G, and for over 1 year under ambient conditions.
- (d) Some G.E. fuel cells have been in continuous operation for more than 1 year.

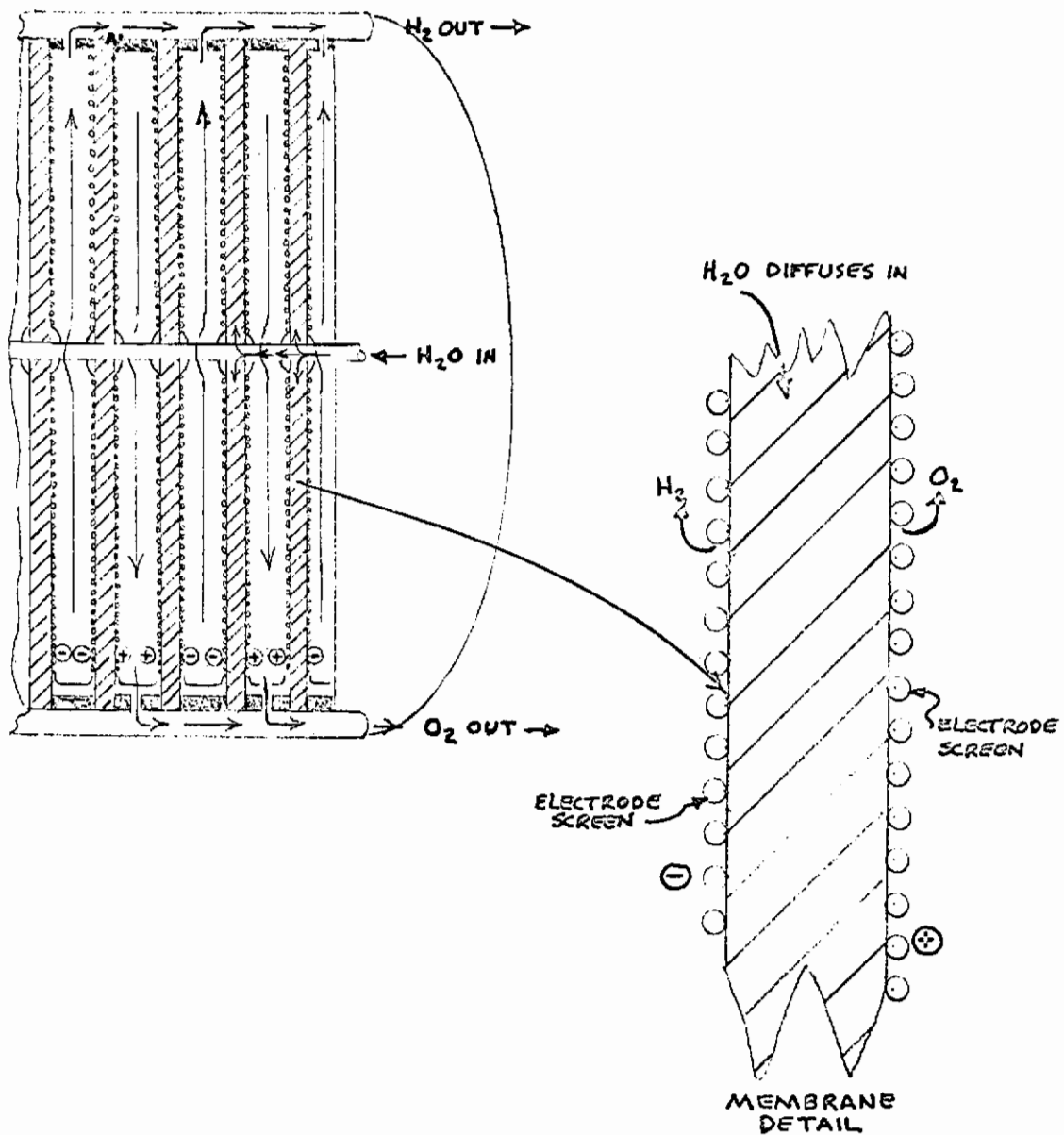


FIGURE 28. SECTION THROUGH MEMBRANE CELL

Tentative Specifications

Using the above numbers for the G. E. ion-exchange membrane cells, the proposed cell would have the following specifications:

Weight 65 lb
Size 1.0 ft³
Power 510 w

Reliability.

Uncertain, because life of membrane or catalysts in present fuel cells is uncertain. Electrolysis properties in absence of catalysts are unknown.

Stability to "G" Forces.

May withstand 50 "G"; strength will depend on direction of accelerating force. Electrolysis may not be possible at high G forces.

Tentative Description.

12-in.-OD cells; 9 cells in series; length = 12 in.; 18 v;
28 amp

Advantages of Membrane-Type Cells

- (a) No moving parts.
- (b) Additional engineering data may be available for more detailed studies and designs.
- (c) High strength to resist accelerating forces.
- (d) As an electrolysis cell, as opposed to a fuel cell, size may be reduced twofold or threefold.
- (e) Low power requirement.

Disadvantages of Membrane-Type Cells

- (a) Reliability and life are uncertain
- (b) Diffusion rates for moisture through membranes are unknown.
- (c) Operating data needed for cells without thin, film catalysts.

Vapor Cell

Principle of Operation

For this type of cell, a solid or viscous film of phosphorus pentoxide hydrate separates two screen electrodes. Electrolysis across the hydrate film decomposes water, "dehydrating" the film. The "dehydrated" film absorbs moisture added to the cell, maintaining electrolysis. The absorbent film separates the hydrogen from the oxygen, and electrolysis separates the gases from moisture. Diffusion gradients allow operation of the cell independently of gravity. The process is illustrated in Figure 29.

This vapor-cell principle is an adaptation of recently developed moisture indicators⁽⁵⁻⁸⁾. The investigators report that phosphorus pentoxide is the preferred dehydrating agent but that potassium carbonate or potassium hydroxide can be used. Carbon dioxide or inert gases have no effect on the cell operation.

Assumptions Made for Design of a Vapor Cell. Assume electrodes of nickel or stainless steel screens of 20 mil wires, screens with 50 per cent void space, and only 50 per cent of the remaining screen area is effective as electrode area for electrolysis at 50 amp/ft² and 3.0 v.

Assume further that the phosphorus pentoxide hydrate is formed within 5-mil bibulous paper, and that, after impregnation of the paper, gases will not diffuse through it. As long as the impregnated paper has some moisture, this seems to be a reasonable assumption. Assume still further that the cell operates normally with about 15 per cent moisture in the phosphorus pentoxide so that the film separating the electrodes has a resistivity of about 100 ohm-cm. Assume also that the case of each cell is a tube of 40-mil rigid plastic of specific gravity about 1.3 g/cm³, the inner (hydrogen) electrode is 250 mils' ID, and 40 mils of free space exists between the outer (oxygen) electrode and the case.

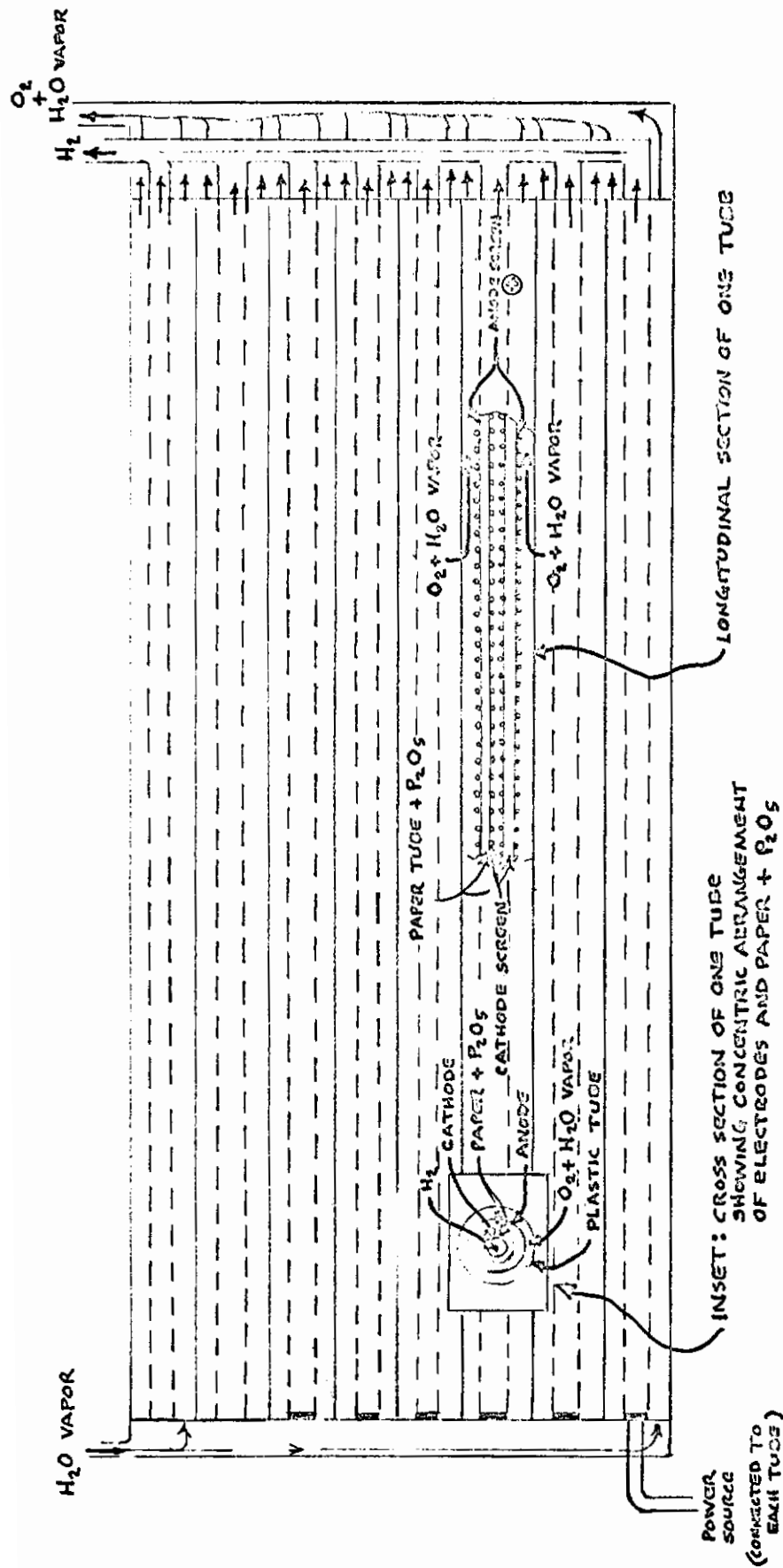


FIGURE 29. VAPOR-CELL TUBE BUNDLE

Tentative Specifications

Using the above assumptions, the following specifications were calculated:

Weight 30 lb
Size 0.32 ft³
Power -

Reliability.

Unknown. Life of phosphorus pentoxide hydrate film is probably limiting factor.

Stability to G Forces.

May withstand forces of several G. Mobility of phosphorus pentoxide hydrate under acceleration is probably the limiting (and unknown) factor.

Tentative Description.

Sixty 0.5-in. -OD tubes, 5.2 ft long; 180 v; 4.2 amp.

Advantages of Vapor Cell

- (a) No moving parts
- (b) Can use water vapor instead of liquid.
- (c) Insensitive to impurities in the input.
- (d) Might be used as part of the air conditioning system within a sealed cabin.

Disadvantages of Vapor Cell

- (a) Reliability and life unknown.
- (b) Stability to G forces unknown; data are unavailable to make a realistic estimate.
- (c) An experimental study is needed to obtain the necessary engineering data before an appropriate cell could be designed.

Porous-Electrode Cell

Principle of Operation

A porous electrode provides numerous interfaces of solid-liquid-gas for electrochemical reactions. Surface-tension forces retain electrolyte in the porous electrodes, thus making operation possible under zero-gravity conditions. Hydrogen-oxygen fuel cells have been observed to give off gases on the reverse side of their porous electrodes when the current is reversed. This fact suggests the feasibility of separating gas from liquid. The National Carbon fuel cell uses porous carbon electrodes which have been water-proofed, and it operates at relatively low temperatures and pressure. Higher current densities are obtained with the Bacon-type fuel cell⁽⁹⁾, which operates at high temperature and pressure. The Bacon cell uses porous nickel electrodes of different porosity on the electrolyte and gas sides as shown in Figure 30.

Bacon Cell

Patent applications on the Bacon cell are reported to cover use as an electrolyzer, but no operating data are available. It is reported that when used as an electrolyzer the hydrogen electrode operates satisfactorily but that oxygen tends to evolve on the electrolyte side of the oxygen electrode. For use solely as an electrolyzer, it might be preferable to make the fine pore layer adjacent to the electrolyte of a nonconducting material that is chemically resistant to the electrolyte.

The assumption made in estimating the cell voltage as an electrolyzer was that the deviation from the theoretical reversible cell voltage of 1.2 v was equal and opposite to operation as a fuel cell. Estimates of electrolyzer-cell voltages are shown below based on reported Bacon fuel-cell operating data:

Current Density, amp/ft ²	Fuel Cell		Electrolyzer Estimated Voltage, v
	Voltage, v	Power Density, kw/ft ³	
0	1.100		1.30
9.3	1.020	0.23	1.38
46.5	0.954	1.08	1.45
93.0	0.905	2.05	1.50
232.0	0.805	4.55	1.60
465.0	0.677	7.67	1.72
631.0	0.585	9.0	1.82

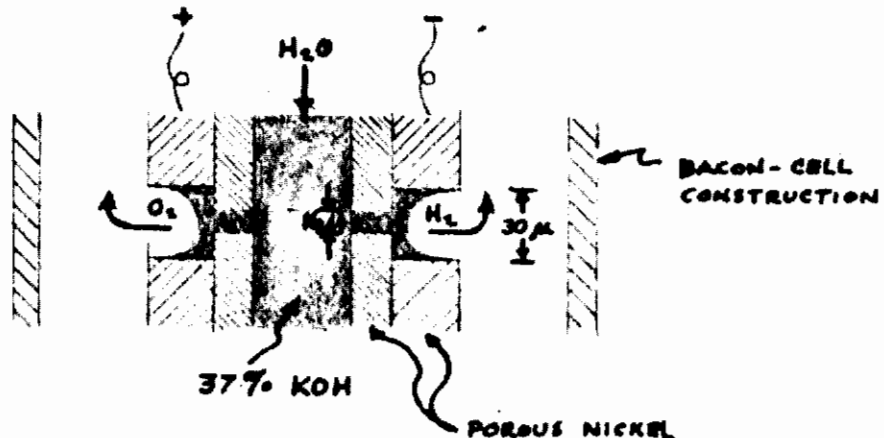
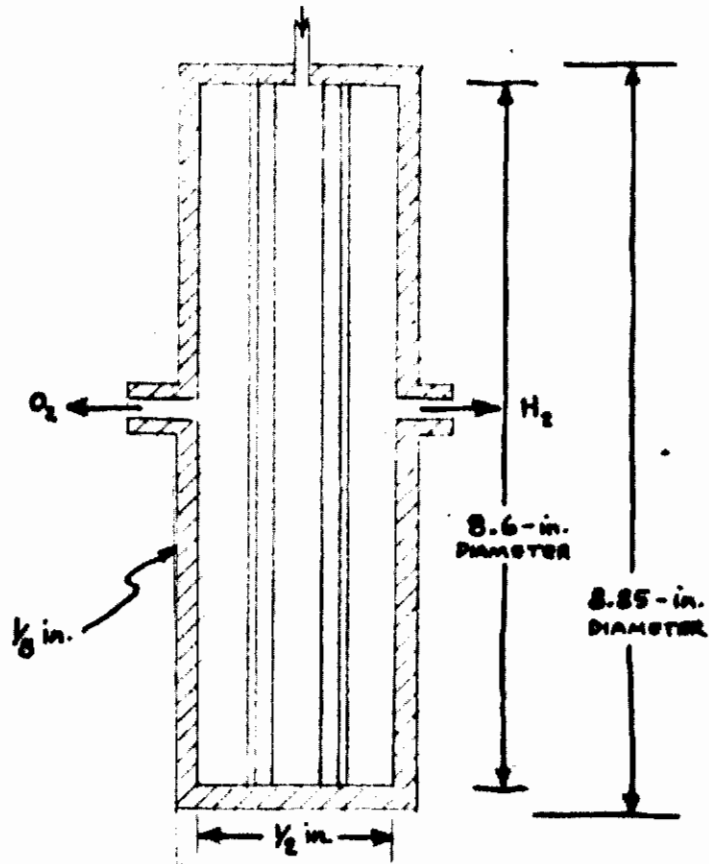


FIGURE 30. POROUS ELECTRODE CELL

Contrails

The Bacon cell operates at current densities up to 1000 amp/ft², which indicates a small volume and weight electrolyzer. At 631 amp/ft² and 0.585 v, the power output per unit of internal volume is reported to be 9 kw/ft³. From these figures, an internal cell width of 1/2 in. can be calculated. If 1/16-in. -wide electrodes spaced 1/8 in. apart are assumed, circular electrodes of 8.6-in. -diameter are sufficient for the designed current density of 631 amp/ft². Assuming 1/8-in. thickness for the cell walls for operation at 600 psi and an electrolyte of 37% KOH, which has a density of about 1.2 g/cm³ at the operating temperature of 200 C, the following component weights were calculated:

Walls	5.2 lb
Electrodes	0.5 lb
Electrolyte	<u>0.3 lb</u>
Total	6.0 lb

Over-all volume (8.9-in. -diameter x 3/4 in.) = 0.027 ft³. Reported power density values of 2000 w/ft³ and 17.5 w/lb indicate a Bacon-fuel-cell density of 114 lb/ft³. For a 0.27 ft³ cell, this would indicate a weight of only 3 lb. Thus, the estimated design weight of 6 lb appears conservative.

Water would be added at 200 C and 600 psi. Performance is not affected greatly by pressure, and operation at 300 psi has been suggested. Saturated steam feed could be considered at 300 psi and 215 C.

Tentative Specifications

Diameter	8.9 in.
Width	3/4 in.
Volume	0.027 ft ³
Weight	6 lb
Current density	631 amp/ft ²
Current	254 amp
Voltage	1.8 v
Power	460 w
Electrolyte	37% KOH
Temperature	200 C
Pressure	600 psi

Reliability.

For periods of operation greater than 2 to 6 months, reliability as a fuel cell is not known to have been demonstrated for the high-temperature Bacon cell. Reliable operation of the low-temperature National Carbon cell as a fuel cell is

not known to have been demonstrated for periods beyond 6 months to a year.

Stability to G Forces.

Does not appear likely for a cell containing electrolyte because of the delicate balance of gas pressure and capillary forces. Provision must be made for withdrawing electrolyte during periods of high G force. Optimum conditions appear to be at zero gravity with variations from 0 to 1 G permissible while operating. Greater variations in gravity could have a detrimental effect because of the small differential pressure between liquid and gas.

Advantages of Porous-Electrode Cell

- (a) Light weight.
- (b) Small volume.
- (c) Low power consumption.
- (d) Excess heat generated (about 150 watts) would maintain cell temperature and compensate cell radiant-heat losses and other heat loss in gases.
- (e) If excess heat must be removed, liquid electrolyte could be circulated to a radiant-heat exchanger of small size because of high temperature.
- (f) No moving parts.
- (g) With gas-storage tanks, the electrolyzer could serve as an auxiliary power supply, operating as a fuel cell.
- (h) Materials, piping, pumps, valves, and pressure controls are being improved. Bacon-type fuel cells are currently being investigated as a regenerative solar cell by Pratt & Whitney Aircraft Company.

Disadvantages of Porous-Electrode Cell

- (a) Operating life uncertain and possibly less than 1 year at the present state of development of porous electrode fuel cells because of corrosion, flooding, etc.

Contrails

- (b) Not suited to intermittent or nonsteady load because of heat balance, extra heat required for start up and expansion and contraction problems.
- (c) Requires CO₂-free water for proposed use of alkaline electrolyte.
- (d) Requires auxiliary pressure-control devices to maintain gas pressure about 2 psi greater than electrolyte pressure. (Such controls have been worked out for a porous-electrode fuel cell.)
- (e) Uncertainty regarding Bacon fuel cell as an electrolyzer. (Pratt & Whitney is developing a separate electrolyzer based on vortex separation of gas from liquid to be used in conjunction with Bacon fuel cell. The reasons for choice of a separate electrolyzer are not completely determined from available reports.)

Rotating Cell With Palladium Cathode

Principle of Operation

This method is a combination of several desirable features contained in other methods considered. As shown in Figure 31, electrolysis occurs near the periphery of a rapidly rotating cell. The cathode is a thin layer of palladium into which the atomic hydrogen formed at the cathode immediately diffuses. The anode is a nickel wire screen close to the cathode. Oxygen formed at the anode is forced towards the axis of rotation under the influence of the hydrostatic pressure gradient created by the artificial gravity field of rotation.

Close anode to cathode spacing is permissible (i. e. , 0.010 in.) because ideally there is no tendency of either gas to move toward the opposite electrode, thus no diaphragm is required. The voltage drop between the anode and cathode should be low because of the minimum electrolyte resistance (short current path, absence of gas in the gap and at cathode surface) and no added resistance as with a diaphragm.

High Temperature-Low Speed Cell. The electrolyte could be 37 per cent potassium hydroxide at a temperature of 200 C, as is used in the Bacon fuel cell. In the latter cell, high temperature allows increased current densities up to 1000 amp/ft² and reduced overvoltage. A porous nickel anode might be needed instead of a nickel screen. The partial pressure of water above 37% KOH at 200 C is about 200 psi. Assuming 200 C and 200 psi at a 0.0008-in.-thick palladium cathode, the diffusion rate of hydrogen is

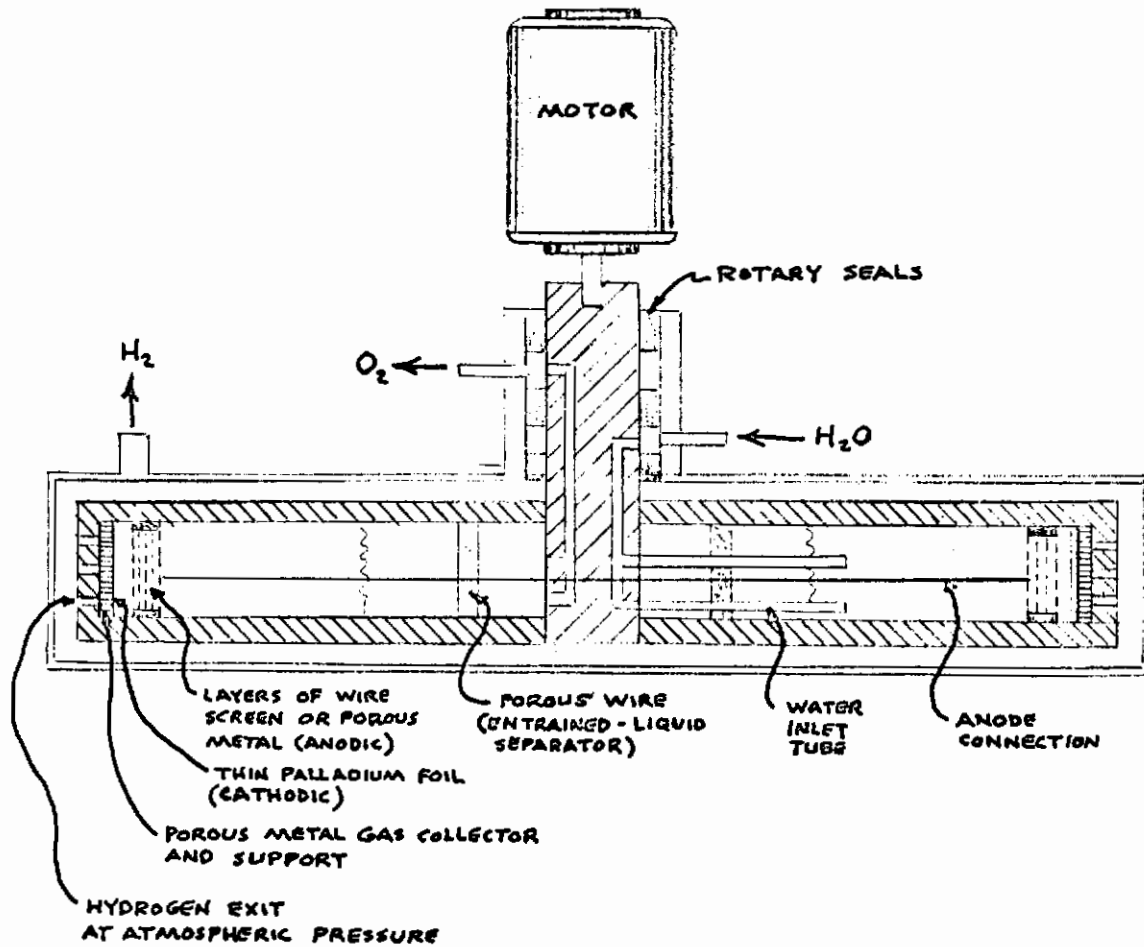


FIGURE 31. ROTATING CELL WITH PALLADIUM CATHODE

Contrails

55 ft³/hr/ft²(12-15). Molecular hydrogen dissociates to atomic hydrogen, which diffuses through the palladium. If the palladium is a cathode, some of the atomic hydrogen formed at the surface immediately diffuses through, so that for this portion of the hydrogen the step of dissociation of molecular hydrogen to atomic hydrogen is eliminated.

For a palladium cathode of 8-in. OD x 1/2 in. wide, the area of 0.087 ft² would pass 4.8 ft³ of hydrogen, which is more than adequate, since a maximum of 3.75 ft³ of hydrogen will be generated. The rotational speed of the cell would be sufficient to establish at least a 1-G field at the anode (close to the cathode), which would cause the oxygen formed at the anode to move towards the axis of rotation. Rotational speeds of 100 and 200 rpm would create an artificial gravity field of 1 G and 4 G, respectively, at the anode. The amount of electrolyte in the cell need only be sufficient to cover the anode. With the liquid level at a radius of 3-1/2 in. and the anode nearly at a 4-in. radius, the time for diffusion of oxygen bubbles across the 1/2-in. layer of electrolyte would be short. The oxygen removed from the core would be at 200 psi and 200 C and saturated with water vapor. Feed to the cell could be steam or water. Hydrogen could be removed from outside the rotating cell at about 200 C and atmospheric pressure (or some positive gage pressure up to 200 psi, depending on the driving force of the atomic hydrogen generated electrolytically at the palladium cathode). Rotary seals will handle a differential pressure of up to 500 psi.

An estimate of cell voltage was made as follows: Assuming a hydrogen overvoltage of 0.35 v at 30 amp/ft², a logarithmic increase of about 0.15 v for each tenfold rise in current density indicates 0.65 v at 3000 amp/ft². A negative temperature coefficient of overvoltage of 0.0025 v/C indicates a net hydrogen overvoltage of 0.15 v at 200 C. Similarly, for an oxygen overvoltage of 0.6 v at 30 amp/ft² and a negative temperature coefficient of 0.00325 v/C gives an oxygen overvoltage of 0.25 v at 3000 amp/ft² and 200 C. Assuming an electrolyte resistivity of 1 ohm-in. and a gap of 0.010 in., the voltage drop through the electrolyte is about 0.2 v. Assuming no gas formed at the cathode and another 0.1 v for the small effect of gas at the anode and polarization, the total cell voltage should be 0.7 v above the theoretical reversible voltage of 1.2 v, or 1.9 v.

Low Temperature-High Speed Cell. A reduction of the electrolyte temperature below 200 C would be desirable to increase the reliability of the unit with respect to corrosion. As the temperature is reduced, the pressure above the electrolyte can be decreased and thus the pressure of the discharged oxygen. For the same hydrogen diffusion rate, the temperature can be reduced if the pressure at the palladium cathode is increased. In a rapidly rotating cell, large G forces can be established at the palladium surface. The high G forces acting on the liquid create a hydrostatic pressure which increases as the head of liquid increases.

Contrails

For example, the palladium cathode at a radius of 4 in. rotating at 5000 rpm experiences 2830 G. With the liquid surface at a 2-in. radius, to give a 2-in. head of electrolyte of density 0.047 lb/in.³, the hydrostatic pressure at the palladium cathode surface would be 800 psi. At this pressure, the electrolyte temperature can be reduced to 100 C and the diffusion rate maintained at 4.8 ft³/hr, which is 25 per cent greater than needed. While the pressure in the electrolysis zone is 800 psi, the pressure at the liquid surface is practically atmospheric because of the negligible head of wet gas and the lower partial pressure of water over 37% KOH at 100 C.

Some industrial electrolysis cells operate at temperatures as high as 100 C. At 100 C, oxygen can be produced at atmospheric pressure, as can hydrogen, in the cell shown in Figure 31. Thus the pressure differential across the rotating seals will be small. Since the cell rotates in a hydrogen atmosphere, the resistance to rotation at high speed will be less than it would be in air. The actual power required for rotation is difficult to estimate. If the palladium width were increased from 1/2 in. to 1-1/2 in., the rotational speed could be reduced from 5000 rpm to 1700 rpm for the same hydrogen diffusion rates at 100 C. The increased width of electrode would also reduce the current density threefold to 1000 amp/ft². A lower current density might be needed to compensate the increase in cell voltage as temperature is decreased. The principal overvoltage at the anode should be low because of the increased pressure for electrolysis and rapid removal of oxygen bubbles under the influence of high G forces.

Tentative Specifications

Pressure	200 to 800 psi (for electrolysis)
Temperature	100 to 200 C
Current Density	1000 to 3000 amp/ft ²
Voltage	1.9 to 2.1 v
Electrolysis power	480 to 530 w
Rotation	100 to 5000 rpm
Gravity	1 to 2830 G
Cell construction	
Diameter	8-1/4 in.
Width	3/4 in.
Shaft	1/2 in. OD x 1-3/4 in

Contrails

Electrode spacing	0.010 in.
Metal thickness	1/8 in.
Volume	16 in. ³
Weight	4.8 lb
Container (thin wall)	8-1/2 in. OD x 1 in.
Volume	58 in. ³
Electrolyte	37% KOH at 100 C to 200 C
Level	2-in. radius
Volume	19 in. ³
Weight	0.8 lb
Seals (3), water pump, motor	
Volume	75 in. ³
Weight	3.5 lb
Power	75 w
Total cell volume	0.08 ft ³
Total cell weight	9 lb
Total power	550 to 600 w

Reliability.

Difficult to estimate because there is no comparable cell used for electrolysis. Increased reliability would be expected as the speed and temperature are reduced; particularly the latter. This could be determined only by experiment.

Stability to G Forces.

Inherent in successful design of a practical cell.

Advantages of Rotating Cell With Palladium Cathode

- (a) Lightweight.
- (b) Small volume.
- (c) Low electrolysis power.
- (d) Low rotating power anticipated in hydrogen atmosphere.
- (e) Delivers dry hydrogen gas at elevated temperature and atmospheric pressure.
- (f) Versatility, in that hydrostatic pressure at electrodes can be controlled by rotational speed as needed, depending on electrolysis rate.
- (g) Electrolysis at high pressure without need for differential pressure control of gases and electrolyte (as in "high pressure" cell or Bacon fuel cell).
- (h) Hydrogen and oxygen can be generated at different pressures, depending only on rotary seals (i. e. , up to 500-psi differential pressure).
- (i) Very little chance of oxygen getting into hydrogen line or vice versa if cell operates as predicted.

Disadvantages of Rotating Cell With Palladium Cathode

- (a) A system like this has never been tried before.
- (b) Use of a hydrogen diffusion cathode in a practical cell is new.
- (c) Electrolysis cell voltage and particularly the power for rotation cannot be estimated accurately.
- (d) If a temperature as high as 200 C is required, the reliability of materials of construction is less.

- (c) A high-speed rotating cell will act as a gyroscope and influence vehicle guidance (on the other hand this might be put to advantageous use).
- (f) The mechanical features of a rotating cell have not been tested.
- (g) Rotating part of cell must be designed in sections for assembly and maintenance, which indicates a sealing problem at the periphery for high hydrostatic pressure.

Electromagnetic Gravity Field

Principle of Operation

A current conductor such as an electrolyte in a magnetic field experiences a force perpendicular to the electric and magnetic field, as shown in Figure 32. In a closed system, the force on the electrolyte sets up a pressure gradient similar to the hydrostatic liquid pressure in a gravitational field. The differential hydrostatic pressure exerts a buoyancy force, causing acceleration of a gas bubble in a direction opposite to the force on the electrolyte. Thus, a magnetic field could be used to create an artificial gravity field.

A. Kolin⁽¹³⁾ has reported that a magnetic field of 10,000 oersteds crossed with a current density of 1 amp/cm² in acidulated water will prevent an air bubble from rising, i. e. , will counterbalance the buoyant effect on the bubble at a gravitational force of 1 G. Then this same field intensity and current density applied under zero-gravity conditions should just restore the force normally exerted by gravity.

For a coil, the magnetic intensity H (in oersteds) is given by $H = \frac{4NI}{10L}$

where $\left(\frac{NI}{L}\right)$ is the amp-turns/cm of coil length. To provide 10,000 oersteds requires 7950 amp-turns/cm. Even if the high current density of 930 amp/ft² (1 amp/cm²) could be obtained, the smallest cell would require a coil about 6 in. long. Thus over 120,000 amp-turns would be required. This does not appear feasible without a large voltage drop (50 to 100 v) through the coil.

Reliability should be relatively high if the method is feasible and stability to G forces should be good.

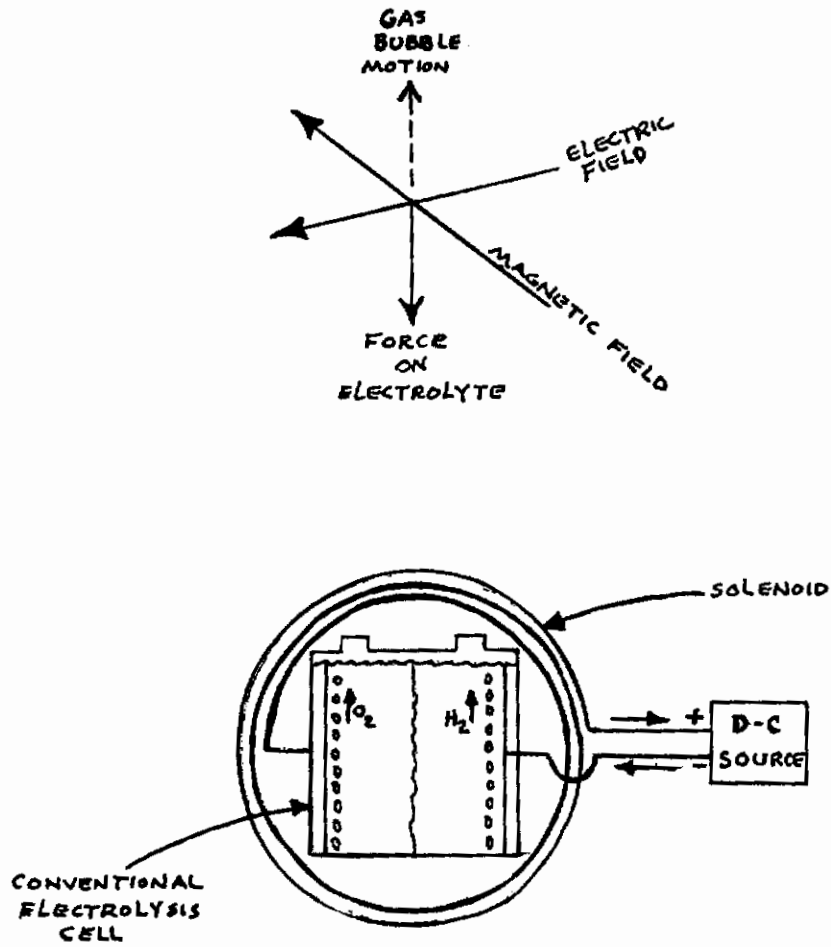


FIGURE 32. ELECTROMAGNETIC ARTIFICIAL GRAVITY FIELD

Advantages of Electromagnetic Gravity Field

- (a) No moving parts
- (b) Would utilize industrial-electrolysis-cell designs of proven reliability.

Disadvantages of Electromagnetic Gravity Field

- (a) Requires extremely high current densities.
- (b) Extremely large power consumption required to produce artificial gravity field of 1 G.
- (c) Would require uniform magnetic and electric fields.

Tentative Specifications

Does not appear practical.

SUMMARY

Essentially six different principles of electrolysis appear capable of operation under zero-gravity conditions. The various methods have been listed in the report in order of acceptability at the present time.

- (1) Rotating cells
- (2) Vortex separator
- (3) Ion-exchange membrane
- (4) Vapor cell
- (5) Porous-electrode cell
- (6) Rotating cell with palladium cathode.

In the final analysis, weight, volume, and power required were not the deciding criteria since specific values could not be listed. Operation for 2 years was specified. Thus the system recommended for continued investigation in Phase III has to be the one which is estimated to be the most feasible for continuous operation for 2 years. The only systems that meet this requirement at the present time are electrolysis cells patterned after

industrial electrolysis cells. With the choice narrowed to two systems, the rotating cell was favored over the separate vortex separator at the present time for having greater simplicity, reliability, and potentiality for size, weight, and power requirements.

Another factor to consider is that the principle of using a rotating cell is not known to be under active consideration at the present time. Methods 2 through 5 are being studied directly or indirectly by other organizations listed below:

Vortex cell

Pratt & Whitney, East Hartford, Connecticut
U. S. Army Signal Corps

Ion-exchange membrane fuel cell

General Electric Company, Philadelphia, Pennsylvania
U. S. Army Signal Corps

Porous-electrode fuel cell (regenerative hydrox type)

National Research Development Corp. , London, England
Patterson Moos Division of Leeson Inc. , Jamaica, New York
Pratt & Whitney, East Hartford, Connecticut
National Carbon Company, Cleveland, Ohio
Electro-Optical System Inc. , Pasadena, California

Vapor Cell

Consolidated Electrodynamics Corp. , Pasadena, California

Except for the vapor cell, the studies are directed toward regeneration of hydrogen and oxygen for power systems in space where zero gravity operation is a requirement. The continuing research of these companies should add to the knowledge of these systems with regard to operating life and reliability.

One principle that does not appear to be under consideration at the present time is the use of a gas-diffusion electrode to separate gas from liquid at zero gravity. The rotating cell with palladium cathode discussed in this report appears to have interesting potentialities. At the present time, this is only an idea which would require an experimental feasibility study on diffusion of hydrogen through palladium foil under the proposed conditions of electrolysis.

At this time, it is preferred not to choose a particular modification of the several rotating cells discussed. It is planned to design a "filter-press" arrangement of cells for connection in series or parallel for operation at atmospheric pressure. Experimental study of current density and voltage in relation to the power required for rotation will indicate the direction for improvement, which might include investigation of high-pressure and/or high-temperature electrolysis.

RECOMMENDATIONS

- (1) The principle of using a rotating cell to establish zero gravity electrolysis conditions should be studied in Phase III of this program.
- (2) Arrangements should be made to follow developments in other companies and agencies that could have a bearing on zero-gravity electrolysis by other schemes that will no longer be a concern of this project.
- (3) A separate contract should be considered to evaluate the feasibility of utilizing gas diffusion through metal as a method of gas/liquid separation at zero gravity, as suggested in this report.

REFERENCES FOR APPENDIX II

- (1) Bialecki, A. , "Submarine Air Revitalization", presented at the Semi-Annual Meeting of the American Rocket Society, Los Angeles, Calif. , May, 1960.
- (2) Mantell, C. L. , Industrial Electrochemistry, 3rd Edition, McGraw-Hill Book Co. , Inc. , p 456, 1950.
- (3) Etherington, Harold, Nuclear Engineering Handbook, McGraw-Hill Book Co. , Inc. , Section 13-66, 1958.
- (4) "Research on a 500-Watt Solar Regenerative H₂-O₂ Fuel Cell Power Supply System", Final Report, Pratt and Whitney Aircraft Division, United Aircraft Corp. , Hartford, Connecticut, (Contract DA36-039SC-85259), ASTIA Report Nr. AD 250721 (Unclassified), 1960.
- (5) Keidel, F. A. , "Determination of Water by Direct Amperometric Measurement", Analytical Chemistry, Vol 31, pp 2043-2048, 1959.
- (6) Cole, L. G. , Czuha, M. , Mosley, R. W. , and Sawyer, P. T. , "Continuous Coulometric Determination of Parts per Million of Moisture in Organic Liquids", Analytical Chemistry, Vol 31, pp 2048-2050, 1959.
- (7) Keidal, F. A. , "Coulometric Analyzer for Trace Quantities of Oxygen", Ind. and Eng. Chem. , Vol 52B, pp 490-493, 1960.
- (8) Friel, D. D. , "Continuous Process Control", Ind. and Eng. Chem. , Vol 523, pp 494-496, 1960.
- (9) "Observations on the Current Developments of the Bacon Hydrogen/Oxygen Fuel Cell", Electrical Power Branch, Electrical Engineering Department, U. S. Army Engineer Research and Development Laboratories, Corps of Engineers, Fort Belvoir, Virginia, ASTIA Report Nr. AD 220,062 (Unclassified), 1958.
- (10) DeRosset, A. J. , "Diffusion of Hydrogen Through Palladium Membranes", Ind. and Eng. Chem. , Vol 52, pp 525-528, June, 1960.
- (11) Smithells, C. J. , and Ransley, C. E. , "The Diffusion of Gases Through Metals", Proc. Roy. Soc. , Vol 150, pp 172-197, 1935.
- (12) Smithells, C. J. , Gases and Metals, Chapter II, John Wiley & Sons, Inc. , New York, 1937.
- (13) Kolin, A. , "An Electromagnetic Phenomenon Involving Migration of Neutral Particles", Science, Vol 117, No. 3032, pp 134-137, 1953.